THE EFFECT OF LOSSES UPON THE PROPAGATION OF SURFACE AND LEAKY WAVES OVER A GROUNDED DIELECTRIC SLAB

by

JERRY KENT SUTTON

B. S., Louisiana Polytechnic Institute, 1967

A THESIS

submitted in partial fulfillment of the

requirements for the degree

MASTER OF SCIENCE

Department of Electrical Engineering

KANSAS STATE UNIVERSITY
Manhattan, Kansas

1969

Approved by:

gary johnson
Major Professor

PREFACE

Surface waves have been found useful in many antenna applications and in some transmission line applications for the past seventy years. The surface wave transmission line is exceptionally efficient. This very fact makes the surface wave a nuisance when it is not the desired mode. Undesired coupling between components of a system, particularly at microwave frequencies and above, may occur via surface waves. Unpublished research by Dr. Gary L. Johnson into the attenuation of surface waves guided by electrically thin lossy dielectric slabs showed that the attenuation does not increase monotonically with increasing dielectric loss. This thesis extends those results to electrically thick slabs. It is found that the same effect appears for relatively thick slabs but not for extremely thick slabs, an abrupt change from decreasing to increasing attenuation occurring at some thickness. Furthermore, the existence of an extraordinary mode has been discovered.

I wish to express my gratitude to Dr. Gary L. Johnson, my thesis advisor; to the National Aeronautics and Space Administration for financial support in the form of a NASA traineeship which made this research possible; to Dr. W. W. Koepsel and Dr. F. W. Harris of my advisory committee for their assistance; to Mr. J. H. Peterson for his valuable programming assistance; and to the Collins Radio Company and Mr. G. W. Deen for the programming experience which was invaluable to me during my research.

TABLE OF CONTENTS

LIST OF TABLES

LIST OF FIGURES

Figure | Page

CHAPTER I

INTRODUCTION

1.1 Statement of the problem. During the past seventy years, considerable interest has been exhibited in surface and leaky waves. Antennas utilizing surface waves and leaky waves have narrow beamwidth and can easily be scanned electronically; a large quantity of literature has appeared concerning the design and characteristics of such antennas. A rather extensive bibliography of articles published prior to 1961 is given by Zucker [1961]. There are cases of interest in which surface waves may be present but are not desirable. For example, radio frequency interference (RFI) is propagated along electric power lines by a surface wave; at microwave frequencies and above, the use of dielectric substrates with dimensions comparable to a wavelength makes the excitation of surface waves very likely. It appears that the introduction of losses should produce attenuation and thus help to eliminate such waves. Little information appears, however, concerning the lossy case for a thick dielectric coating. Goubau [1950] and Collin [1960] treat low loss cylindrical conductor cases; Barlow and Cullen [1953] and Johnson [1966] treat the thin planar slab lossy case.

It is the purpose of this research to present data from a computer aided numerical analysis to demonstrate the effect of lossy materials upon the propagation of surface waves over thick dielectric slabs. An ideal planar case is treated in which it is assumed that the structure considered is infinitely wide, that the source and other discontinuities are sufficiently removed from the region under consideration that no reflected waves are present, and that the system is in the steady state, the source having an $\exp(j\omega t)$ time dependence. Only TM modes having no field variation along the width of the structure are considered. The materials are allowed to be lossy, but are assumed to be linear, homogeneous, isotropic, and time-invariant.

The dielectric slab is coated onto the surface of a perfect conductor. It can be shown that the use of a good but not perfect conductor has a negligible effect. If it is desired to consider the conductor losses a perturbational analysis should be entirely satisfactory. The assumption that there is no reflection in the lengthwise or axial direction is taken merely for convenience since the case having reflection can be handled with the reflectionless fields and the usual transmission-reflection techniques. The least realistic assumption is likely to be the assumption that the slab is of infinite width, which is equivalent to the assumption of no reflection from discontinuities at the edges of a finite slab or that the region under consideration is sufficiently removed from the discontinuities that losses eliminate the reflected wave. Techniques for reducing the reflection at the edges of a finite slab are described by Zucker [1961]. The consideration of a finite slab width would make the problem a rather formidable boundary value problem.

<u>1.2 Discussion of the terms "Surface Wave" and "Leaky Wave."</u> It is convenient to first describe surface and leaky waves for the lossless case. At a boundary between two different media there must result reflection and transmission of any electromagnetic wave which is present. The surface wave in this lossless case is totally reflected at the boundary so that the field in the less dense medium is an evanescent field and the field in the more

dense medium exhibits a standing wave behavior. The direction of propagation is parallel to the interface. There is no energy propagating into the less dense medium from the more dense medium or vice-versa. The wave is unattenuated in the direction of propagation but decays exponentially with increasing distance from the interface in the less dense medium.

The leaky wave is one having no real critical angle so that the wave cannot be totally reflected at the interface. Instead energy now passes from the more dense medium to the less dense medium, and as a result the amplitude of the wave decreases along the interface. The wave in the less dense medium is still an evanescent wave although the direction of propagation is tilted into the less dense medium. The amplitude of the wave increases without bound as the distance into the less dense medium increases; though this is not a physically meaningful wave in this ideal case, the increasing amplitude is caused by an energy source infinitely removed from the region under consideration. Such a source is not present in physically real situations; the resulting fields from the physically real source are known to be described reasonably well by the ideal model at reasonable distances from the interface.

Qualitatively speaking, the presence of losses modifies the direction of propagation in such a direction as to support the losses. If the less dense region is lossy the wave in that region will not be evanescent. The wave will not be totally reflected at the interface except possibly for certain relations between the complex permittivities and permeabilities of the two media. In any lossy case, both the surface wave and the leaky wave must diminish in amplitude as the wave propagates along the interface. The distinction between a surface wave and a leaky wave in a lossy case is in the direction of attenuation.

CHAPTER II

THE CHARACTERISTIC EQUATION

2.1 Derivation of Equations. Consider the geometry of Figure 1, showing the dielectric slab and the perfect conductor to which the slab is attached, and the orientation of the cartesian coordinate axes. The y-axis is directed out of the page; the slab and conductor are infinite in extent in the y-direction and in the z-direction. The slab thickness is t, with the conductor-slab interface in the y-z plane. Both the dielectric slab

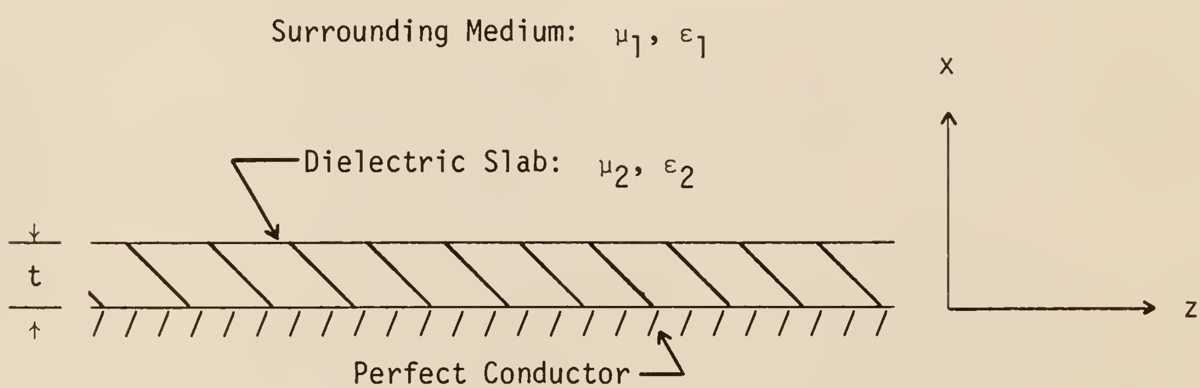

Figure 1. Geometry of the Problem.

and the surrounding medium are linear, homogeneous, isotropic and time-invariant; thus μ_1, μ_2, ϵ_1, and ϵ_2 are scalar complex constants. It is assumed that $\mu_2\epsilon_2 > \mu_1\epsilon_1$ and $\epsilon_2 > \epsilon_1$.

The losses appear in the permittivity and permeability with the following notation:

$$\varepsilon = \varepsilon_r \varepsilon_0 = \varepsilon_0(\varepsilon_r' - j\varepsilon_r'')$$

$$\mu = \mu_r \mu_0 = \mu_0(\mu_r' - j\mu_r'').$$

In these expressions ε and μ are the permittivity and permeability of the material while the zero subscripts denote the free space values. ε_r' is the relative AC capacitivity or dielectric constant while ε_r'' is the relative dielectric loss factor. Similarly μ_r' is the relative AC inductivity and μ_r'' is the relative magnetic loss factor.

In writing the field quantities the conventions employed by Harrington [1961] will be used. The time variation $e^{j\omega t}$ is suppressed. Since only the sinusoidal steady state is considered, there is no requirement to consider the actual instantaneous values. As used in this thesis the vector magnetic potential $\vec{A}$ will be defined by the relations

$$\vec{H} = \nabla \times \vec{A} \qquad [2.1.1]$$

$$-j\omega\varepsilon\Phi = \nabla \cdot \vec{A} \qquad [2.1.2]$$

where Φ is a scalar electrical potential. This choice causes $\vec{A}$ to satisfy the well-known Helmholtz equation. Subscripts 1 and 2 will be used to identify the field quantities in the surrounding medium and in the dielectric slab respectively.

Before beginning the derivation of the characteristic equation, an outline of the procedure used will be presented. An elementary plane wave function for each of the two homogeneous regions $0 \leq x \leq t$, $t \leq x$ will be assumed. These functions will be used for the vector magnetic potential.

The resulting field components will be calculated from Maxwell's equations, and boundary conditions will be matched at $x = t$. Finally, two additional necessary relations will be obtained from the separation equation.

It is assumed that the vector magnetic potential is given by the expressions

$$\vec{A}_2 = C_2 \sin(ux)\, e^{-jk_z z}\,\vec{a}_z \qquad 0 \le x \le t \qquad [2.1.3]$$

$$\vec{A}_1 = C_1\, e^{-vx}\, e^{-jk_z z}\,\vec{a}_z \qquad t \le x \qquad [2.1.4]$$

$$\vec{A} = 0 \qquad x \le 0 \qquad [2.1.5]$$

where C_1 and C_2 are undetermined coefficients. Thus in the dielectric the x-component of the propagation constant is u, while in the surrounding medium it is jv. The z-component of the propagation constant is k_z in both regions as is required by Snell's Law. The fields are zero beneath the surface of the perfect conductor; it is immaterial how thick this conductor is or what lies below it, as any -x traveling wave is totally reflected at the surface in this ideal case. $\vec{H}$ is calculated from equation 2.1.1:

$$\vec{H}_2 = \nabla x\vec{A}_2 = -uC_2 \cos(ux)\, e^{-jk_z z}\,\vec{a}_y \qquad [2.1.6]$$

$$\vec{H}_1 = \nabla x\vec{A}_1 = vC_1 e^{-vx}\, e^{-jk_z z}\,\vec{a}_y. \qquad [2.1.7]$$

$\vec{E}$ is calculated from Maxwell's equations for this source-free case:

$$\vec{E}_2 = \frac{1}{y_2}\nabla x\vec{H}_2 = -\frac{uk_z}{\omega\varepsilon_2} C_2\cos(ux)e^{-jk_z z}\,\vec{a}_x + \frac{u^2}{j\omega\varepsilon_2} C_2\sin(ux)e^{-jk_z z}\,\vec{a}_z \qquad [2.1.8]$$

$$\vec{E}_1 = \frac{1}{y_1} \nabla x \vec{H}_1 = \frac{vk_z}{\omega\varepsilon_1} C_1 e^{-vx} e^{-jk_z z} \vec{a}_x - \frac{v^2}{j\omega\varepsilon_1} C_1 e^{-vx} e^{-jk_z z} \vec{a}_z. \qquad [2.1.9]$$

At $x = t$, the tangential components of both $\vec{E}$ and $\vec{H}$ must be continuous; continuity of E_z requires that

$$\frac{C_2}{\varepsilon_2} u^2 \sin(ut) = - \frac{C_1}{\varepsilon_1} v^2 e^{-vt} \qquad [2.1.10]$$

while continuity of H_y requires that

$$-C_2 u \cos(ut) = C_1 v e^{-vt}. \qquad [2.1.11]$$

The continuity of normal electric flux leads to 2.1.11 also, so it imposes no additional constraints. The necessary boundary condition of zero tangential component of $\vec{E}$ at the conductor surface is satisfied by E_{z2}. Taking the ratio of 2.1.10 to 2.1.11 to eliminate C_1 and C_2, we have

$$\frac{u}{\varepsilon_2} \tan(ut) = \frac{v}{\varepsilon_1} ;$$

it is convenient to rearrange this to yield

$$vt = \frac{1}{\varepsilon_r} ut \tan(ut). \qquad [2.1.12]$$

In equation 2.1.12 the relative permittivity between the two media has been defined as

$$\varepsilon_r = \varepsilon_2/\varepsilon_1.$$

Equation 2.1.12 is the characteristic equation relating u and v.

Another equation relating u and v is necessary in order to obtain a solution. The Helmholtz equation is a direct consequence of Maxwell's equations, and it has been separated in the cartesian coordinate system, yielding the separation equation

$$k_x^2 + k_y^2 + k_z^2 = k^2 \qquad [2.1.13]$$

where k is the propagation constant or wave number of the medium and k_x, k_y, and k_z are the components of the vector propagation constant of the wave. In the case considered here, k_y is zero in both regions, k_z is the z-component in both regions, jv is the x-component in the surrounding medium, and u is the x-component in the dielectric. Therefore the application of 2.1.13 to each medium yields the two equations

$$u^2 + k_z^2 = k_2^2 = \omega^2\mu_2\varepsilon_2 \qquad [2.1.14]$$

$$(jv)^2 + k_z^2 = k_1^2 = \omega^2\mu_1\varepsilon_1 \qquad [2.1.15]$$

containing the three unknowns u, v, and k_z. k_z can be eliminated by subtraction of 2.1.15 from 2.1.14 to yield

$$u^2 + v^2 = \omega^2(\mu_2\varepsilon_2 - \mu_1\varepsilon_1). \qquad [2.1.16]$$

It is convenient to re-write this as

$$(ut)^2 + (vt)^2 = (2\pi[\frac{t}{\lambda o}] \sqrt{\mu_{r2}\varepsilon_{r2} - \mu_{r1}\varepsilon_{r1}})^2 \qquad [2.1.17]$$

where λo is the free-space wavelength of the wave, and μ_{r1}, μ_{r2}, ε_{r1}, ε_{r2} are the various permeabilities and permittivities normalized to the free space values. The unknown v may be eliminated from equations 2.1.12 and 2.1.17 to yield

$$(ut)^2 + \frac{1}{\varepsilon_r^2}(ut)^2 \tan^2(ut) = (2\pi[\frac{t}{\lambda o}]\sqrt{\mu_{r2}\varepsilon_{r2} - \mu_{r1}\varepsilon_{r1}})^2. \qquad [2.1.18]$$

This is a non-linear, transcendental equation with coefficients which are in general complex. This is the equation which will be solved to obtain u.

2.2 Graphical Analysis of Real Roots in the Lossless Case. For the lossless case, the parameters of the surface wave modes can be obtained from a graphical solution. Since ε_{r1}, ε_{r2}, μ_{r1}, and μ_{r2} are real for the lossless case, and k_z and v must be real for a surface wave mode in the lossless case, u is also real. This is shown by considering Equations 2.1.14 and 2.1.15. When u and v are real they represent only two unknowns whereas they would represent four unknowns in the complex case. Two simultaneous equations in two unknowns can be solved by graphing the two relationships and finding the points of intersection as is commonly known. Equations 2.1.12 and 2.1.17 are well-suited for this purpose; Equation 2.1.17 is recognized as a circle in the ut-vt plane, while Equation 2.1.12 has the general features of a tangent function.

Figure 2 demonstrates the graphical solution for $\varepsilon_{r2} = 2.0$, $\varepsilon_{r1} = 1.0$, $\mu_{r2} = \mu_{r1} = 1.0$, and several values of $t/\lambda o$. The radius of the circle is $2(t/\lambda o)\pi$ for this set of parameters. Modes (solutions to 2.1.18) are numbered in order of increasing ut for the lossless case. The same mode number is retained as losses are added. The TM_o mode refers to the real intersection of the circle and the quasi-tangent function in the interval $0 \leq ut < \pi/2$. This mode always propagates as a surface wave regardless of how thin the slab is. Higher order modes may represent surface waves, leaky

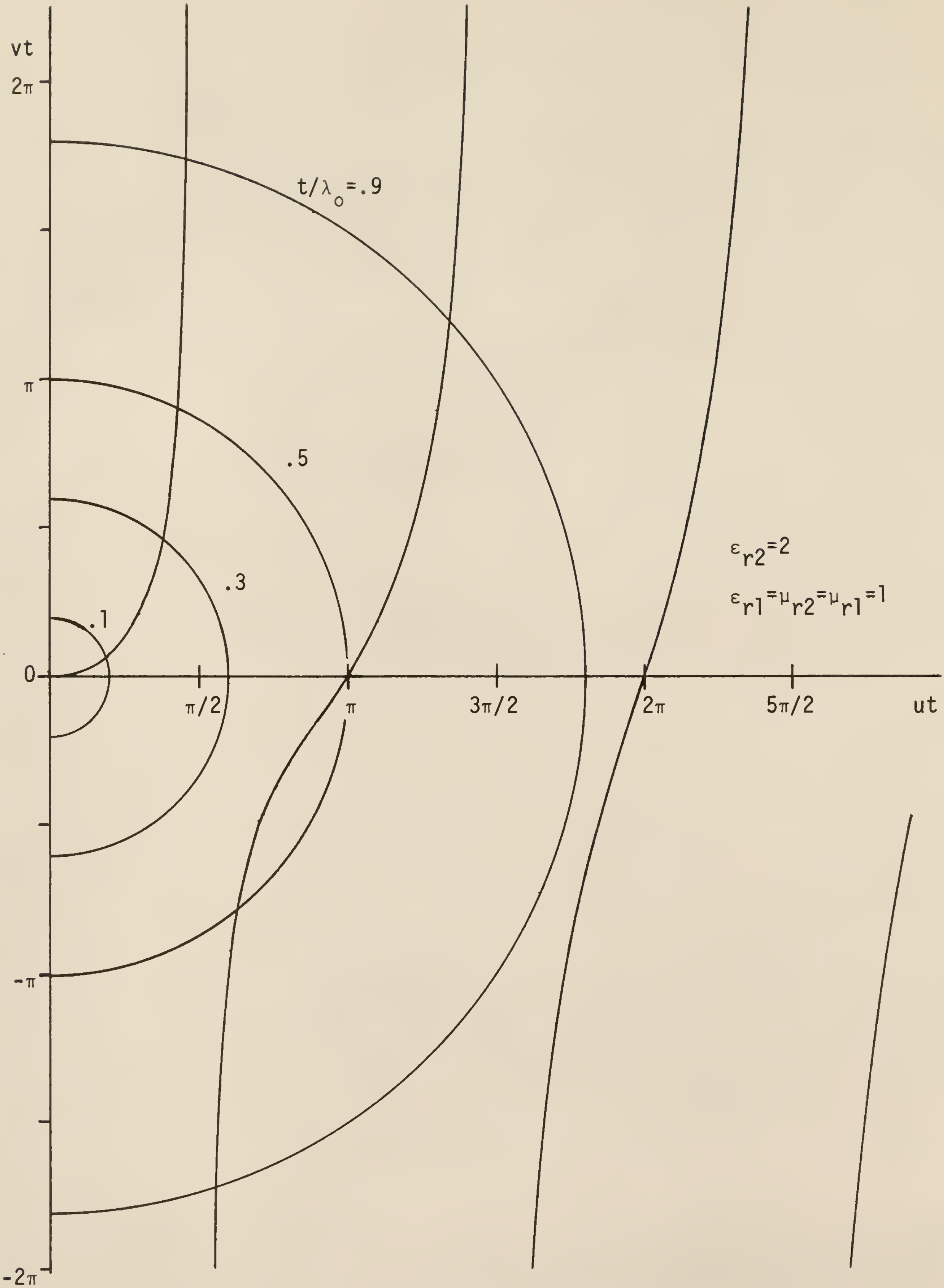

Figure 2. Graphical Solution for the Lossless Case.

waves, or non physical waves depending upon the radius of the circle and losses.

It is clear that there is either one or no real intersection of the two curves between any two successive integral multiples of $\pi/2$ on the ut axis. In general, there will be exactly one real intersection, and hence one surface wave mode, having a value of ut between $k\pi/2$ and $(k+1)\pi/2$, where k, the mode number, is an even integer, provided that the circle radius is greater than or equal to $k\pi/2$. All higher ordered surface wave modes have a definite cutoff frequency below which they become leaky wave modes. Cutoff for the k^{th} mode occurs when the circle radius is equal to $k\pi/2$.

Obviously there may also be intersections in the intervals $m\pi/2 \leq ut \leq (m+1)\pi/2$ where m is an odd integer if the radius of the circle is at least $m\pi/2$. There may be either two distinct intersections or a point of tangency in an interval in which the radius of the circle lies; for the intervals such that $m\pi/2 \leq ut \leq (m+1)\pi/2$ and the circle radius is at least $(m+1)\pi/2$ there will be exactly one distinct intersection. The value of v which results in these intervals is negative, so that the fields would increase in magnitude with increasing distance from the slab. There would not be any radiation from the slab. This describes neither a surface wave nor a leaky wave, so such modes will be regarded as non-physical.

Negative values of ut are not shown in Figure 2. It is apparent from Equations 2.1.12 through 2.1.18 that if u_1 is a solution, $-u_1$ is also a solution resulting in the exact same values of v and k_z. Inspection of Equations 2.1.6 through 2.1.11 shows that if u changes sign but v remains unchanged then either C_1 or C_2 must change sign. If C_2 changes sign there is no difference between the fields resulting from u_1 and $-u_1$. If C_1 changes sign, all field components are reversed in direction; this corresponds to the original field pattern viewed half a guide wavelength in either direction from the original point. Therefore, the consideration of negative values of u adds no new information and is unnecessary.

Considerable insight into the behavior of the propagation constants can be obtained with this graphical technique. In order to determine the behavior of k_z, Equations 2.1.14 and 2.1.15 are also necessary. These two equations are easily rearranged to show that $k_1 \leq k_z < k_2$ for the cases discussed in this section, that is, cases in which u, v, and k_z are real.

Consider cases in which λ_o, the free space wavelength, is the only parameter allowed to vary in Figure 2. As λ_o is changed, only the radius of the circle changes. As λ_o decreases, t/λ_o increases and ut and vt increase. Therefore, u, v, and k_z all increase since t is fixed. For very large λ_o, so that the radius is small compared to $\pi/2$, ut is approximately equal to the radius and vt is small. k_z tends toward its lower bound k_1. Relatively speaking, the wave will be loosely bound, and the wavelength close to λ_1. For very small λ_o, so that the circle radius is much greater than $\pi/2$, ut is approximately $\pi/2$ for the first mode, and the corresponding vt is approximately the radius of the circle. k_z tends toward its upper bound k_2. Again, relatively speaking, the wave will be tightly bound, and the wavelength close to λ_2.

The behavior of any higher propagating modes is obviously similar, ut being approximately the radius and vt being small for a case slightly away from the cutoff region, ut being near (slightly less than) an odd multiple of $\pi/2$ and vt being somewhat less than the radius for a very large value of radius.

2.3 Some Notes Concerning Solutions in More General Cases. No closed form solution of Equation 2.1.18 is known. The graphical technique of section 2.2 is not useful when the solutions are complex since there are four unknowns rather than two. An iterative numerical procedure appears to be the most straightforward method of solution. In order to use this technique it is necessary to have a reasonable estimate of the solution to use as a starting value. In particular, it would be appropriate to be able to place bounds upon the value of u for a given mode.

As a first step in examining the complex case it is convenient to introduce the substitution z = ut; note that this variable z is not the coordinate value z, but another distinct variable. Equation 2.1.18 then becomes

$$z^2\left(1 + \frac{1}{\varepsilon_r^{\,2}} \tan^2(z)\right) = \left(2\pi\left[\frac{t}{\lambda o}\right] \sqrt{\mu_{r2}\varepsilon_{r2} - \mu_{r1}\varepsilon_{r1}}\right)^2 \qquad [2.3.1]$$

or

$$z - 2\pi\varepsilon_r\left[\frac{t}{\lambda o}\right] \sqrt{\frac{\mu_{r2}\varepsilon_{r2} - \mu_{r1}\varepsilon_{r1}}{\varepsilon_r^{\,2} + \tan^2(z)}} = 0. \qquad [2.3.2]$$

If $f_1(z)$ is defined as

$$f_1(z) = z - 2\pi\varepsilon_r\left[\frac{t}{\lambda o}\right] \sqrt{\frac{\mu_{r2}\varepsilon_{r2} - \mu_{r1}\varepsilon_{r1}}{\varepsilon_r^{\,2} + \tan^2(z)}} \qquad [2.3.3]$$

the solutions desired are the zeros of $f_1(z)$. For convenient reference, equations 2.1.12, 2.1.14, and 2.1.15 are also repeated here:

$$vt = \frac{1}{\varepsilon_r} z \tan(z) \qquad [2.3.4]$$

$$u^2 + k_z^2 = k_2^2 = \omega^2\mu_2\varepsilon_2 \qquad [2.3.5]$$

$$-v^2 + k_z^2 = k_1^2 = \omega^2\mu_1\varepsilon_1. \qquad [2.3.6]$$

In obtaining equation 2.3.2 from equation 2.3.1 at least one root has been ignored as a consequence of the convention that the radical sign indicates the root with the non-negative real part, or the root with the positive imaginary part if both roots are purely imaginary. This does not detract from the generality of the resulting solution as has been discussed in section 2.2; i.e., while solutions with negative real parts are distinct mathematical solutions, they are not distinct physical solutions. Having restricted the choice of z (and hence u) a single unique value of v is thus determined by equation 2.3.4; therefore one of the values which results from equation 2.3.6 is extraneous. k_z, however, is not so restricted mathematically; the two values $k_z = \pm\sqrt{k_2^2 - u^2}$ are both valid physically. Clearly, the significance of the existence of two values is that propagation may occur in either the +z or the -z direction, or both (when there is reflection, say). Since the features of the two waves are identical except for the direction of propagation it will be sufficient to examine only the +z propagating solution in this research; if the more general case must be considered the appropriate change of signs may be used to describe the oppositely traveling wave.

Consider now the meaning of the signs of the three propagation constants u, v, and k_z. As the wave inside the dielectric slab is a standing wave, the signs of the real and imaginary parts of u (and z = ut) do not have any physical significance. The signs of the real and imaginary parts of v and k_z determine the direction of propagation and the direction of attenuation as indicated in table 1. For a surface wave traveling in the +z direction, it is required that k_z lie in the fourth quadrant of the complex k_z plane, and that v lie in the right half of the complex v plane. For a leaky wave mode

k_z must still lie in the fourth quadrant, but v must lie in the left half of the complex v plane.

TABLE 1

SIGNIFICANCE OF ALGEBRAIC SIGNS OF v AND k_z.

		positive	negative
phase travel	$Re[k_z]$	in +z direction	in -z direction
attenuation	$Im[k_z]$	in -z direction	in +z direction
attenuation	Re[v]	in +x direction	in -x direction
phase travel	Im[v]	in +x direction	in -x direction

It is now informative to consider the vector propagation constant. As defined by Harrington [1961] the vector propagation constant $\vec{\gamma} = \vec{\alpha} + j\vec{\beta}$ represents a wave having equiphase surfaces normal to $\vec{\beta}$ and equiamplitude surfaces normal to $\vec{\alpha}$. In this research $\vec{\alpha}$ and $\vec{\beta}$ in region 1 are given by the expressions

$$\vec{\alpha} = v'\vec{a}_x - k_z''\vec{a}_z \qquad [2.3.7]$$

$$\vec{\beta} = v''\vec{a}_x + k_z'\vec{a}_z . \qquad [2.3.8]$$

Since these vectors are independent of the coordinates (x,y,z) the wave in region 1 is a plane wave traveling in the $\vec{\beta}$ direction and attenuating in the $\vec{\alpha}$ direction. The wave in region 2 is a standing wave composed of two plane waves which are totally reflected at the perfect conductor and are reflected also at the interface between the two media. For a lossless surface wave total reflection occurs at the dielectric interface so that the wave in region 1 is an evanescent wave. Examination of the behavior of $\vec{\alpha}$ and $\vec{\beta}$ is of some interest, particularly their directions. The angle θ_β between the $\vec{\beta}$ and $\vec{a}_z$ directions and the angle θ_α between the $\vec{\alpha}$ and $\vec{a}_z$ directions are given by the expressions

$$\theta_\beta = \tan^{-1}(v''/k_z') \qquad [2.3.9]$$

$$\theta_\alpha = \tan^{-1}(v'/(-k_z'')), \qquad [2.3.10]$$

where the notation $\tan^{-1}$ denotes the arctangent function. Figure 3 shows $\vec{\alpha}$, $\vec{\beta}$, θ_α, and θ_β for surface waves over lossy slabs and leaky waves. As mentioned earlier, the surface wave propagates into the lossy dielectric in the $\vec{\beta}$ direction to account for the losses. Since $\vec{\alpha}$ and $\vec{\beta}$ are orthogonal for region 1 lossless, and $\vec{\alpha}$ must be in or on the boundary of quadrant 1, then $\vec{\beta}$ will be in quadrant 4. A similar analysis for leaky waves shows that $\vec{\alpha}$ must lie in the fourth quadrant and $\vec{\beta}$ in the first quadrant.

The surface wave modes of the lossless case, i.e., the real solutions, have already been considered. The leaky wave modes of the lossless case will now be considered. If, for a given even mode number, there is no real intersection of the circle and the quasi-tangent function, the corresponding root of 2.1.18 will be complex and describe a leaky wave mode. A straight-forward examination of equations 2.3.5 and 2.3.7-10 shows for this case, that u and z lie in the first quadrant, k_z lies in the fourth quadrant, and v lies in the second quadrant (of their respective complex planes). Although the restriction of u to the first quadrant is informative, an entire quadrant is still a rather large region to scan for a particular root. It seems intuitively obvious that a given leaky wave mode solution must lie in a relatively small region as in the case of a given surface wave mode; however,

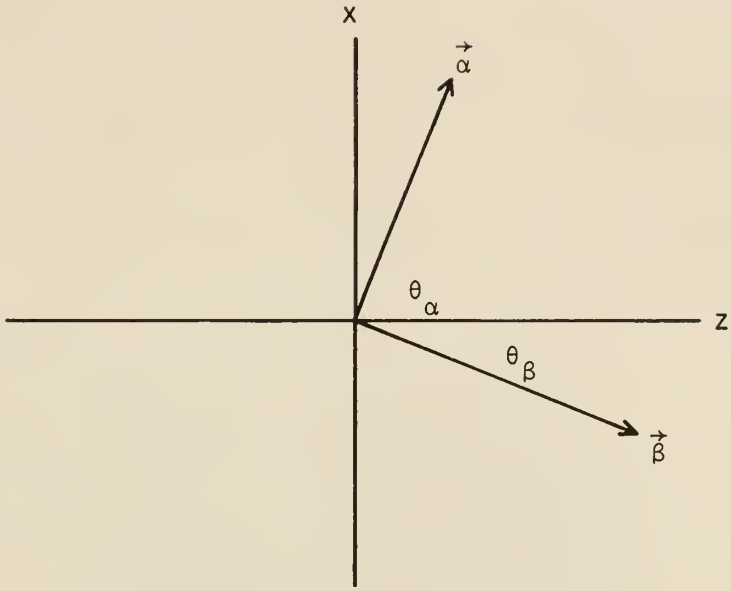

Surface Wave Over Lossy Dielectric

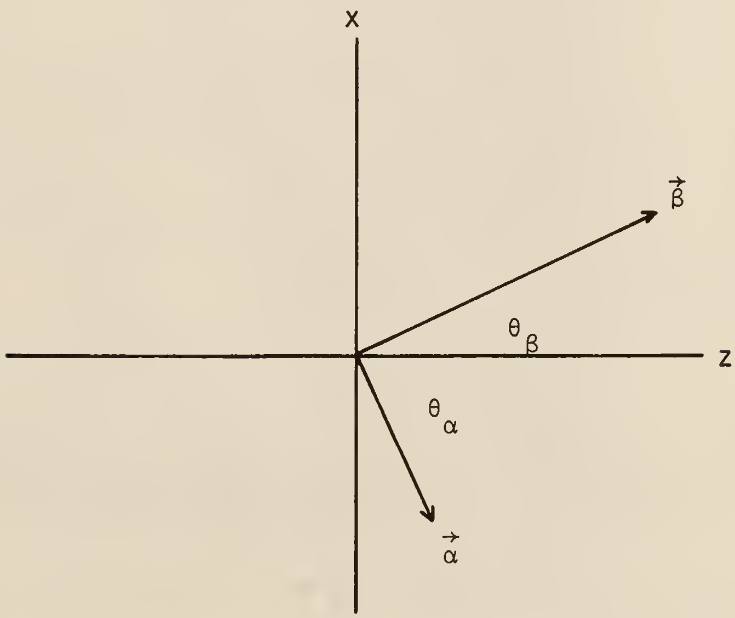

Leaky Wave

Figure 3. Typical Directions of Components of the Vector Propagation Constant.

no mathematical description of such a region has been determined by the author. This region is obviously a subset of the set $[z|\mathrm{Re}(z\tan(z))<0]$.

Similarly, it is extremely difficult to define the permissible region for the lossy surface wave case and the lossy leaky wave case, as the complex relative permeability between the two materials also enters into the determination of the sign of Re[v].

It is interesting to note that, in the lossless leaky wave case, if z, v, and k_z satisfy the equations 2.3.3 to 2.3.6, then their conjugate values z*, v*, and k_z^* also satisfy those equations, though the conjugate values describe a wave which is not physically meaningful. Using the first term of the Taylor series expansion of tan(z) in Equation 2.3.1, it is apparent that the lossless surface wave mode solutions are at least double roots, and one might expect the two roots to diverge and proceed along approximately conjugate paths as losses are added.

Another interesting and relevant matter is the behavior of tan(z) for arguments even moderately removed from the real axis. For $b=\pi$, $\tanh(b) \simeq 0.99595$; for $b=2\pi$, $\tanh(b) \simeq 0.99999$; $\tanh(b) \to 1$ monotonically as b increases from 0. Also, tanh(b) is an odd function. For $z=a+jb$,

$$\tan(z) = \frac{\tan(a) + j\tanh(b)}{1 - j\tan(a)\tanh(b)} ,$$

so that for $\tanh(b) \simeq \pm 1$, $\tan(z) \simeq \pm j1$. Under these conditions, $f_1(z)$ takes on the value

$$f_1(z) \simeq z - 2\pi\varepsilon_r[t/\lambda o] \sqrt{\frac{\mu_{r2}\varepsilon_{r2} - \mu_{r1}\varepsilon_{r1}}{\varepsilon_r^2 - 1}} .$$

For the lossless case, then, the roots must clearly be "close" to the real axis, as $|f_1(z)|>c \simeq |\mathrm{Im}[z]|$ for z sufficiently removed from the real axis.

This is significant information for use with a numerical technique, as the region of search can be restricted to the vicinity of the real axis.

CHAPTER III

THE COMPUTER PROGRAM AND NUMERICAL TECHNIQUES

3.1 Development of the Program. The early efforts employed in this research utilized various rearrangements of Equation 2.1.18. Some of these mathematically equivalent rearrangements are:

$$z^2 + \frac{1}{\varepsilon_r^2} z^2 \tan^2 (z) - (2\pi[t/\lambda o] \sqrt{\mu_{r2}\varepsilon_{r2} - \mu_{r1}\varepsilon_{r1}})^2 = 0; \qquad [3.1.1]$$

$$z - \sqrt{4\pi^2[t/\lambda o]^2 (\varepsilon_{r2}\mu_{r2} - \varepsilon_{r1}\mu_{r1}) - \frac{z^2}{\varepsilon_r^2} \tan^2 (z)} = 0; \qquad [3.1.2]$$

$$z \tan (z) - \varepsilon_r \sqrt{4\pi^2[t/\lambda o]^2 (\mu_{r2}\varepsilon_{r2} - \mu_{r1}\varepsilon_{r1}) - z^2} = 0. \qquad [3.1.3]$$

Unfortunately, such rearrangements are not equally useful with numerical techniques; whether or not a given iterative procedure converges to a valid result depends upon the expression iterated upon as well as the starting guess provided. The mathematical determination of whether or not a given expression is usuable in, say, linear iteration, is a problem of the same magnitude as the analytical solution of the original problem. It has been found to be more practical to experimentally rather than analytically test whether or not an expression is satisfactory.

Newton's method was the first technique attempted. In the earliest version the complex quantity was considered as a single variable, even though it was realized that Newton's method is not generally valid for complex variables. Later efforts considered the problem in terms of two real variables. The algorithms used did not yield convergent solutions, so Newton's method was discarded.

The second technique attempted was linear iteration; the most satisfactory expression found for the iteration is

$$z = 2\pi\varepsilon_r[t/\lambda o]\sqrt{\frac{\mu_{r2}\varepsilon_{r2} - \mu_{r1}\varepsilon_{r1}}{\varepsilon_r^2 + \tan^2(z)}}\ . \qquad [3.1.4]$$

The basic problem with this technique is that it is not self-starting, i.e., the starting value must be quite close to the root or the procedure diverges. Also, it appears that the starting value must be in a certain direction in the complex z plane from the root, and this direction depends on all of the parameters of the case under consideration. Linear iteration was not completely abandoned, but temporarily put aside to allow investigation of other techniques.

A simple-minded form of steepest descent was next tried. In this approach, termed the "garbage can lid" approach, the error, or magnitude of the left hand side of an expression $f(z) = 0$, is calculated at 24 points on a circle about some starting point z. The new point is the point on this circle having the smallest error associated with it. Once a minimum has been isolated, the circle radius is shortened and the procedure repeated until the minimum is located accurately. Hopefully, the minimum will be zero. This technique is very simple-minded, very reliable, and requires a relatively large number of iterations. It is not true steepest descent, and the ultimate accuracy is more limited by the number of points taken on the circle than by machine precision.

Steepest descent is, in general, a very attractive procedure, at least in theory. The method is widely known and documented in many texts, such as Kunz [1957]. A factor which is strongly in its favor is that it is simple to visualize. The unknowns must be real, as must the expression to be minimized. If the objective is the location of zeros, the error expression must be positive semidefinite; this requirement is easily met by using the magnitude or the square of the expression. As steepest descent is a minimizing procedure, extraneous results can be obtained if non-zero minima exist, and, possibly, if saddle points exist.

For true steepest descent it is necessary to proceed in the direction opposite the gradient; it is necessary, then, to calculate the partial derivatives of the error with respect to the unknowns, which unknowns are in this case the real and imaginary parts of z. In this particular case, the generation of analytic expressions for the derivatives is almost out of the question. The hand calculation of them is so tedious and lengthy as to be virtually impossible. An attempt to generate such expressions using PL/1 FORMAC resulted in expending two hours of System 360 computer time and obtaining expressions for both derivatives, each of which required approximately 350 cards. Therefore it was necessary to use central difference approximations for the derivatives. It is intuitively obvious that, provided the signs of the derivatives are calculated correctly, the procedure will converge, although the convergence rate may be very slow if there is a large error in the magnitude of the derivative approximations. Far from the root, or the minimum, the derivatives may be determined reasonably accurately. However, if the error is not smooth and well behaved in the vicinity of the minimum, the numerical calculation may result in an incorrect sign as indicated in Figure 4. When finite difference derivative approximations are used, steps must be taken to deal with such cases as pictured in Figure 4, and with the possibility that the approximations may result in zero values when the gradient is not truly zero.

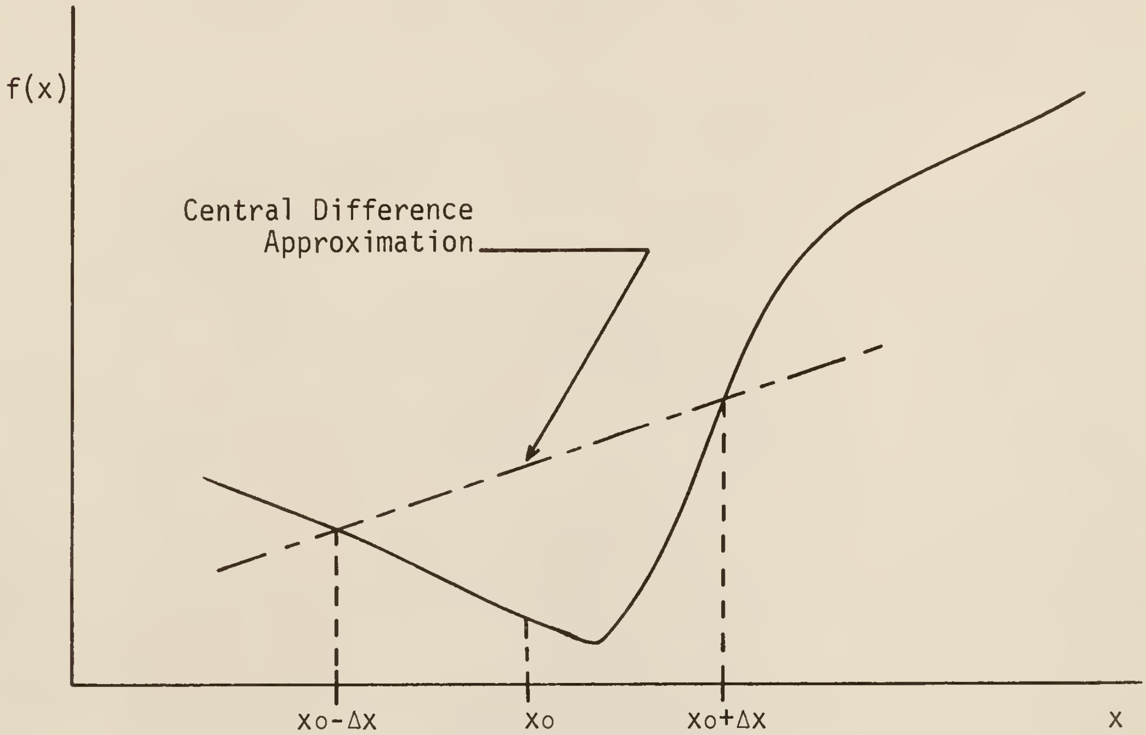

Figure 4. Illustration of the Possibility of an Erroneous Derivative Approximation Sign.

3.2 Final Version of the Basic Program. Linear iteration, steepest descent, and the garbage can lid procedure are all used in the final version of the program. The control section of the program, which performs such tasks as reading the input, choosing the starting guess for the unknown, and writing the output, is described in Section 3.3.

The basic program, an iteration loop, determines the value of the unknown Z, which is U*T as defined in Chapter 2. A flowchart of this iteration loop is included in Appendix A. The DO statement is indexed to allow a maximum of 100 iterations through this main loop. Using linear iteration, a value ZCK (the left hand side of 3.1.4) is obtained from the present value of Z (the starting value on the first pass), used in the right hand side of 3.1.4. The error expression is evaluated from Z and ZCK to obtain FERR and FCKERR respectively. If ZCK results in a smaller error than Z and ZCK is suitably close to Z so that the same root is being approached, Z and ZCK are interchanged so that the better approximation to the root is used in the remainder of the pass.

The error is tested next; if it is small enough that the true root has been satisfactorily approximated, the iteration loop is exited. Otherwise, the central difference approximations to the partial derivatives, FPX and FPY, are calculated, the gradient DELF is constructed, and the magnitude of the gradient, DELMAG, is tested to be certain it is non-zero. If DELMAG is zero, control is passed to the garbage can lid section, since steepest descent will not improve the value of the unknown. If not, DELMAG is tested to be certain it is less than or equal to one, and DELF is scaled down to yield a magnitude of no more than unity if necessary. This is done to limit the maximum change in Z to a value which will prevent crossing the "ridge" between two minima. A new estimate of Z is obtained from an expression of the form

$$Z = ZO - DELTA*DELF$$

where ZO is the present value of Z and DELTA is a small number which also limits the maximum change in Z.

If this steepest descent step reduces the error, the pass through the iteration loop is complete, and the next pass is begun. If the error is not reduced, the step distance DELTA is halved, the steepest descent step repeated, and the error checked again. The step distance may be halved twenty-six times before steepest descent is abandoned. This results in a minimum step distance which is lost due to machine precision when DELTA and Z are within the usual limits of the program. Since it is possible that failure to find a smaller error may be due to an incorrect derivative approximation sign rather than to having located a minimum, the garbage can lid section is entered after steepest descent fails.

After calculating the error at each of twenty-four points on a circle about the present value of Z, the garbage can lid procedure obtains the minimum error of the set along with the corresponding value of Z and tests to see whether or not the error has been improved. If the error is reduced, the pass through the iteration loop is complete. If not, the circle radius is halved and so on as in the steepest descent portion of the loop. If this fails to find a smaller error, the iteration loop is exited.

Thus, there are three ways to leave the iteration loop: negligible error, inability to find a smaller error, and one hundred iterations completed without finding a minimum.

The IBM System 360 FORTRAN IV-G language does not accept complex arguments in the tangent function, so the function ZTAN was written to provide this feature. Another problem arises when the real part of the argument passed to ZTAN is too near an odd multiple of $\pi/2$; the built in TAN function will terminate the job. To avoid this, ZTAN tests the real part and generates a large number within the range of the machine to use in place of the actual TAN value if the real part of the argument is near enough to result in job termination.

There are a number of statements in the basic program which are not described in the preceding description or in the flowchart of Appendix A since they are not essential to the algorithm. The variable IERR is used to indicate whether or not the argument proximity to $\pi/2$ problem occurred in ZTAN. FLAG is used to trace the flow through the loop; if FLAG is even, linear iteration did not improve the error, if odd, linear iteration did improve the error. If 0 or 1, steepest descent was used and the garbage can lid section was not; if 2 or 3, the garbage can lid section was used and steepest descent was not; if 4 or 5, both were used. IFORM determines the type of output format used; this will be described in Section 3.3.

3.3 The Monitor and Control Section of the Program. A flowchart of the monitor and control section is given in Appendix A. The program begins with a number of comment cards describing its purpose and use, followed by the non-executable statements. After the non-executable statements, the error function is defined by an arithmetic statement function. The expression used is

F(Z) = Z - ER*RAT*TWOPI*CSQRT((K2SQ-K1SQ)/(ER**2+ZTAN(Z)**2)).

In this expression, ER is the relative permittivity of region 2 relative to region 1, RAT is the ratio of the slab thickness to the free space wavelength, TWOPI = 2.*3.1415927, and K2SQ and K1SQ are symbols standing for the product of the relative permittivity and relative permeability of regions 2 and 1, respectively. Following this there are several replacement statements which initialize various switches and variables. A page of Hollerith output describing the output of the program is produced next. The entire set of data cards is read in next, each card being written on the printer for an echo check and on a disk file for re-reading. When end-of-file on the card read unit is encountered, the disk working unit is rewound; the data reading loop is then begun.

In this data reading loop, a record is read from the disk working unit. The format of this READ statement calls for two 4-character alphameric fields and three 10 character floating point numeric fields. The two alphameric fields are received by the variable INVARI, which is compared with alphameric character strings stored in the array LABEL. When a match is found, the values in the numeric fields are assigned to the appropriate variables. For example, if the title on the data card is 'FREQ   ', the variable FGHZ is assigned the value of VALUEA, the number in the first of the three numeric fields on the data card. After such a match is found and the appropriate value or values assigned to the appropriate variable or variables, another card is read from the disk working unit. The last card of the deck (the last FORTRAN data card) should be a card containing the character string 'STOP   '; this card causes subroutine EXIT to be executed. If no match is found, the erroneous character string is printed out, followed by a description of the allowable card types and formats; then execution is terminated by the statement STOP.

The appearance of a card 'RUN   ' causes the remainder of the program to be executed using the parameters in effect at that time; after such execution, another card is read.

Thus, the program may produce several sets of output with a minimum of input; if all that is to be changed between two sets of parameters during the same job is the relative permittivity of the dielectric (region 2), the data cards following the first run card (that is, the data cards for the second set of parameters) need only be 1) a card containing the title 'ER2P   ' and the new value in the first numeric field, and 2) the second 'RUN   ' card (followed by more data sets or the 'STOP   ' card). For a reasonably detailed description of the allowable data cards, refer to the comment cards in the program listing which is contained in Appendix B. Some of the cards, which serve only control functions such as do the 'RUN ' and 'STOP ' cards, contain only a title; others contain one or two numeric values. A notable exception is $DATA, the array used to set the value of the loss component of permittivity or permeability during loss parameter sweeps: the cards to determine the values of the elements of $DATA and the number of active elements are 1) a card containing the title '$DATA ' and the number of active elements in the first numeric field, and 2) cards containing the values of the elements in 10F8.4 format. For the mode numbers, the integers should be even since the program is valid only for even mode numbers. Note that all the numeric values on the data cards are floating point, and that some are converted to integer values. The statement "GO TO 900" preceding statement 924 is the last statement of the data reading loop.

The appearance of a 'RUN ' card causes control to be passed to statement 924. The parameters ER, K1SQ, and K2SQ are calculated. Next the mode loop is entered; this is simply a DO loop having index parameters related to the lowest and highest mode numbers requested. The variable IM contains the present mode number throughout the mode loop.

Next the starting value of Z is determined. If a starting value has been given as input data, as indicated by the variable IZSW having a value of 1, Z is set equal to the given value; control is passed to statement 925, bypassing the remainder of the starting value calculations. If IZSW is zero, the program calculates a starting value for Z by the following procedure: the radius of the circle (with reference to Figure 2) is calculated using the real parts of the relative permittivities and permeabilities. If the radius is greater than or equal to IM*PI/2, the mode is assumed to be a surface wave (propagating) mode and control is passed to statement 955. If this radius condition is not met, the mode is assumed to be a leaky wave (cutoff) mode and Z is calculated according to the statement

Z = (IM - 1 + 0.1)*PI/2 + J*0.5

where J stands for the imaginary unit and PI = 3.1415927; control is passed to statement 925. At statement 955, the radius is tested to determine whether or not it is greater than or equal to (IM+1)*PI/2. If not, then it must be between IM*PI/2 and (IM+1)*PI/2, so a starting value in this range is determined from the statement

Z = 0.9*RADIUS + 0.1*IM*PI/2;

control is transferred to statement 925. If the test expression is true, control is transferred to statement 960 where Z is calculated from the expression

Z = (IM+0.9)*PI/2.

Statement 925 follows statement 960.

NPASS is a variable indicating the number of times the iteration loop has been executed. IELEC and IMAG are, respectively, indices which determine which element of $DATA is used during electric and magnetic sweeps for ER2PP or MUR2PP, the loss components of the relative permittivity and relative permeability of region 2. IESW determines whether or not an electric sweep is requested, while IMSW performs the same function for magnetic sweeps. If both sweeps are requested, the electric sweep will be performed first. After the appropriate parameters have been modified, the iteration loop is entered. The value of Z having thus been determined, U, V, KZ, LRAT, ATTX, and ATTZ are calculated. U is the x-directed component of the propagation constant in region 2, V is the x-directed component of the propagation in region 1, KZ is the z-directed component of the propagation constant in both regions, ATTX is the attenuation in the x-direction in region 1, and ATTZ is the attenuation in the z-direction; all these parameters are in nepers per free-space wavelength except ATTX and ATTZ, which are in decibels per free-space wavelength. LRAT is the ratio of the free-space wavelength to the guide wavelength. The output is written next. The format of the output is determined by the variable IFORM. IFORM = 0 produces an output tracing the value of Z, the error, and the derivatives through the iterations and allows messages warning of the use of the approximation within ZTAN to be printed. This output is suitable for checking the proper operation of the program. IFORM = 1 produces a tabular output of the results only, giving no indication of the magnitude of the error, the number of iterations, or other such information. After producing the output for a pass, NPASS is checked; on the first pass, Z is stored in ZSTART for use in the magnetic sweep, should one be requested. IELEC and IMAG are checked next; if one of the sweeps is finished, the appropriate parameter ER2PP or MUR2PP is reset to zero. If an electric sweep is in progress but incomplete, IELEC is incremented and the next pass performed; similarly for a magnetic sweep IMAG is incremented. After completing the sweeps or the single pass if no sweeps are requested, the process is repeated for the next mode. When the mode loop is satisfied, control is passed to the READ statement number 900 to begin the input reading loop again.

3.4 Comments on Programming. The emphasis in this program has been placed strictly upon convenience to the programmer, with no attention paid to the execution time. For this reason, the symbol J was defined to be the complex constant (0., 1.); complex expressions were then written in the form A + J*B. This requires the conversion of A and B to complex mode, a complex multiplication, and a complex addition. The same result can be obtained by the use of the in-line built-in function CMPLX(A,B) with a very considerable reduction in execution time. Should the program be used for further research into a large number of cases, it would be highly appropriate to replace the statements using J with statements referencing CMPLX(A,B).

There are several peculiarities in the program which deserve discussion. The most important of these is the starting value used for Z and its relation to the mode number to which the result corresponds. For the lossless surface wave case, the value of Z is real and clearly bounded between IM*PI/2 and (IM+1)*PI/2. Thus, a starting value between these bounds is virtually certain to yield the desired result. For the other cases, the root cannot easily be bounded, so that a simple expression for a suitable starting value has not been determined. It is quite possible that, from a given starting value, the algorithm may converge to a root corresponding to a different mode than that which the programmer specified. It is necessary for the programmer to determine whether or not the root does correspond, and if necessary, to insert an appropriate starting value by means of a data card.

The Cutoff modes are particularly troublesome in this respect. Since, in the lossless case, the error is an even function of the imaginary part of Z, a real starting value must not be used, as the algorithm in this event will converge to a non-zero minimum on the real Z axis. For severely cutoff modes (RADIUS << IM*PI/2), the root may be so near an odd multiple of $\pi/2$ that it is necessary to specify a small value of DELTA0 to prevent the algorithm from allowing Z to jump over a "wall" in the error space.

When the sweep feature is used and the first case is a lossless surface wave case, the mode uncertainty problem is not likely to occur. That is, the expressions used to calculate a starting value of Z generate a value in the proper interval. The program keeps the last root value as the starting value for the following case during a sweep, so appealing to some notion of continuity, the correct roots should be obtained as the losses are increased if the increments of the swept variable are not too large. For lossless cutoff cases in which the degree of cutoff is not too severe, the built-in determination of the starting value should be satisfactory.

The garbage can lid section was included in order to cope with the problem of a calculated gradient of zero when in fact the value of Z was not sufficiently close to a zero of the error. It was necessary to iterate until the root was accurate to 7+ significant digits in order to obtain suitably accurate values of KZ and V. This may in part be due to the calculation of KZ from the expression

```
KZ = CSQRT(4.*PI*PI*(MUR2P-J*MUR2PP)*(ER2P-J*ER2PP)-U**2)
```

which results in taking the difference of nearly equal imaginary parts for lossy cases. Later versions of the program used the expression

```
KZ = CSQRT(4.*PI*PI*(MUR1P-J*MUR1PP)*(ER1P-J*ER1PP)+V**2)
```

which gives improved accuracy particularly when region 1 is lossless. It is still necessary to obtain the maximum single precision accuracy in the root for large relative permittivity cases.

CHAPTER IV

INTERPRETATION OF DATA

4.1 Behavior of TM_0 Surface Wave Modes. The TM_0 mode always propagates as a surface wave and is the dominant mode. It is probably the most interesting mode for practical purposes.

The results from the computer analysis for the TM_0 mode are presented in graphical form in Figures 5 through 18; reproductions of the computer output are contained in Appendix C. Figures 5 and 6 show the z-direction attenuation as a function of ε_{r2}'' for $\varepsilon_{r2}' = 2$ and values of (t/λ_0) from .005 to .50.

The same results may be obtained in closed form for $t/\lambda_0 < .05$ or so by approximating tan (ut) by (ut) in Equation 2.1.18 and solving the resulting quartic for u. This has been done for the low loss case by Barlow and Cullen [1953] and Johnson [1966]. As might be expected, this approximation gives a significant error at $t/\lambda_0 = .10$ and does not predict the interesting results which occur between $t/\lambda_0 = .10$ and $t/\lambda_0 = .20$.

In general, the attenuation tends to increase as t/λ_0 increases up to $t/\lambda_0 = .10$. For $t/\lambda_0 = .18$ and below the curves exhibit a tendency to turn downward at high losses while for $t/\lambda_0 = .19$ and above the curves exhibit a tendency to turn upward. In this transition region the curves break sharply, with the actual switch occurring between $t/\lambda_0 = .18$ and $t/\lambda_0 = .19$, and at an ε_{r2}'' of approximately 2. As the ratio increases from .10 to .75 the curves indicate that for small ε_{r2}'' the attenuation increases as t/λ_0 increases but

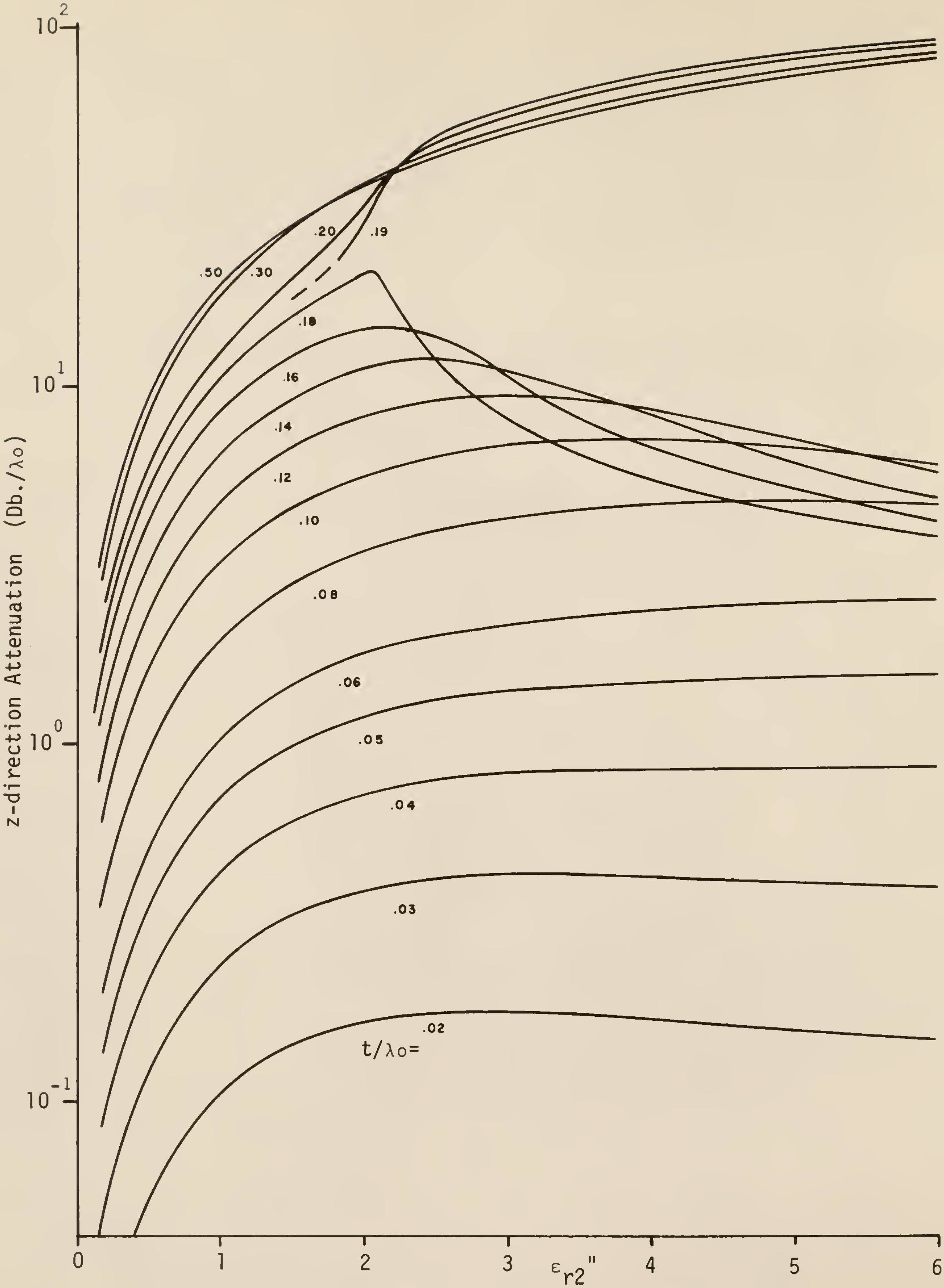

Figure 5. z-direction Attenuation for the TMo Mode and $\varepsilon_{r2}'=2$.

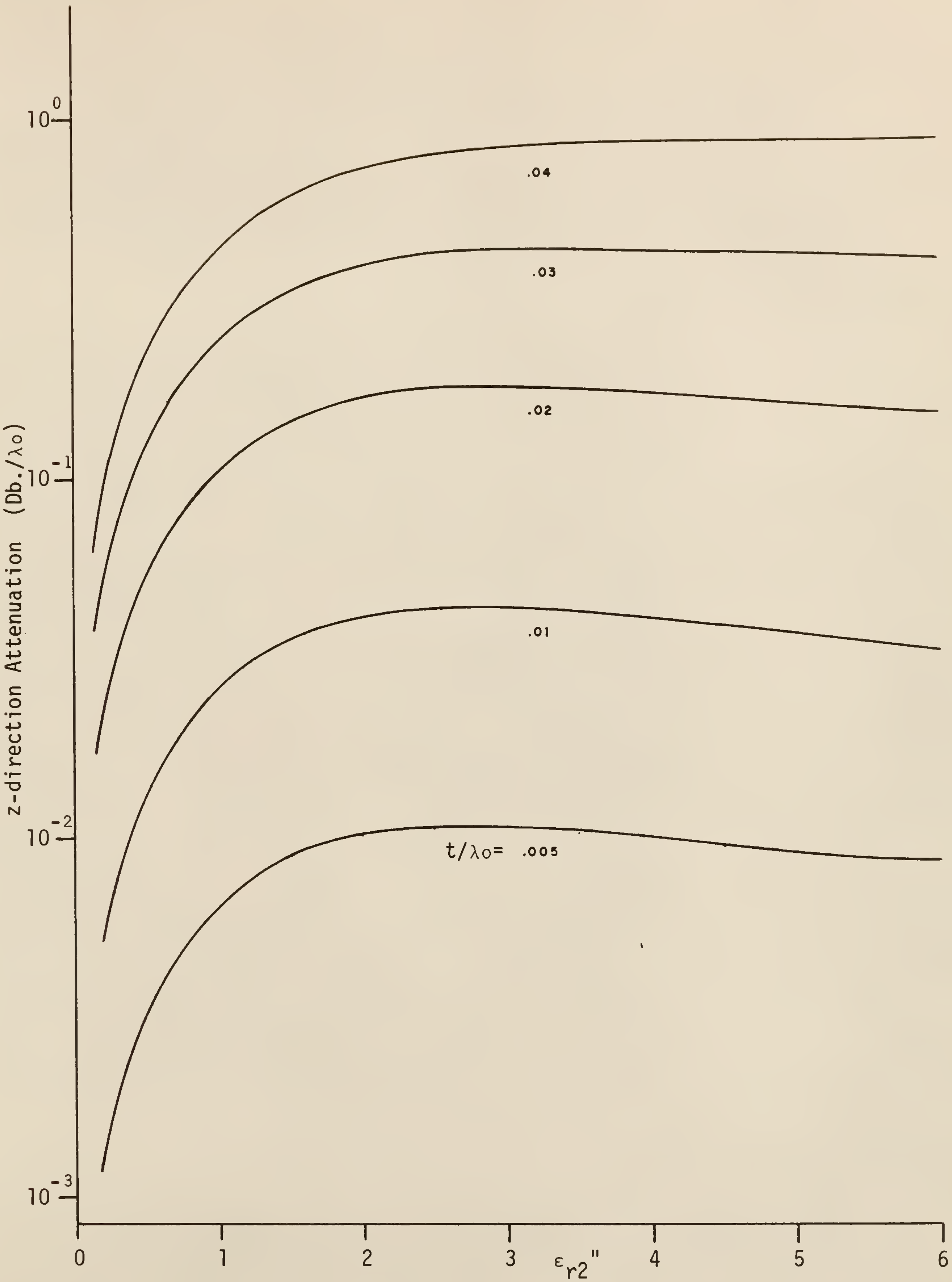

Figure 6. z-direction Attenuation for the TM_o Mode and $\varepsilon_{r2}'=2$ (Continued).

for large ε_{r2}'' the attenuation decreases as $t/\lambda o$ increases. That is, comparing two curves, the curve for the larger ratio will be above the curve for the smaller ratio when ε_{r2}'' is small but the curves will cross at some value of ε_{r2}'' (in the vicinity of $\varepsilon_{r2}'' = 2$ for $t/\lambda o \geq .19$) and reverse relative positions for larger ε_{r2}'' values. Obviously this is not true for a comparison of ratios of .18 and .19, but it is true if the two values under consideration are both between .10 and .18 or both greater than .19. For ratios greater than .50, at which value the second mode becomes feasible as a surface wave, there is little change in the z-direction attenuation as $t/\lambda o$ is increased.

Figure 7 shows the x-direction attenuation for the same cases as in Figure 5. There is a great deal of similarity between these curves and the curves of z-direction attenuation; they are related through Equation 2.1.15, the separation equation in region 1. Since the attenuation involves the real part of v and the imaginary part of k_z, the relation is not easy to visualize from the formula. Some curves representative of the guide wavelength along the z axis are shown in Figure 8. In the lossless case, the guide wavelength is always shorter than the free space wavelength and hence the phase velocity is less than the speed of light in free space. As losses are inserted, the guide wavelength decreases slightly for very small $t/\lambda o$ but for $t/\lambda o$ values in the transition range initially increases in a very pronounced fashion, peaks for ε_{r2}'' near 2 as do the attenuation curves, and drops off for further increase in ε_{r2}''. In some cases the guide wavelength and phase velocity rise above their free-space values.

Figures 9, 10, and 11 for $\varepsilon_{r2}' = 4.24$ correspond to Figures 5, 7, and 8 respectively; similarly the case for $\varepsilon_{r2}' = 8.28$ is presented in Figures

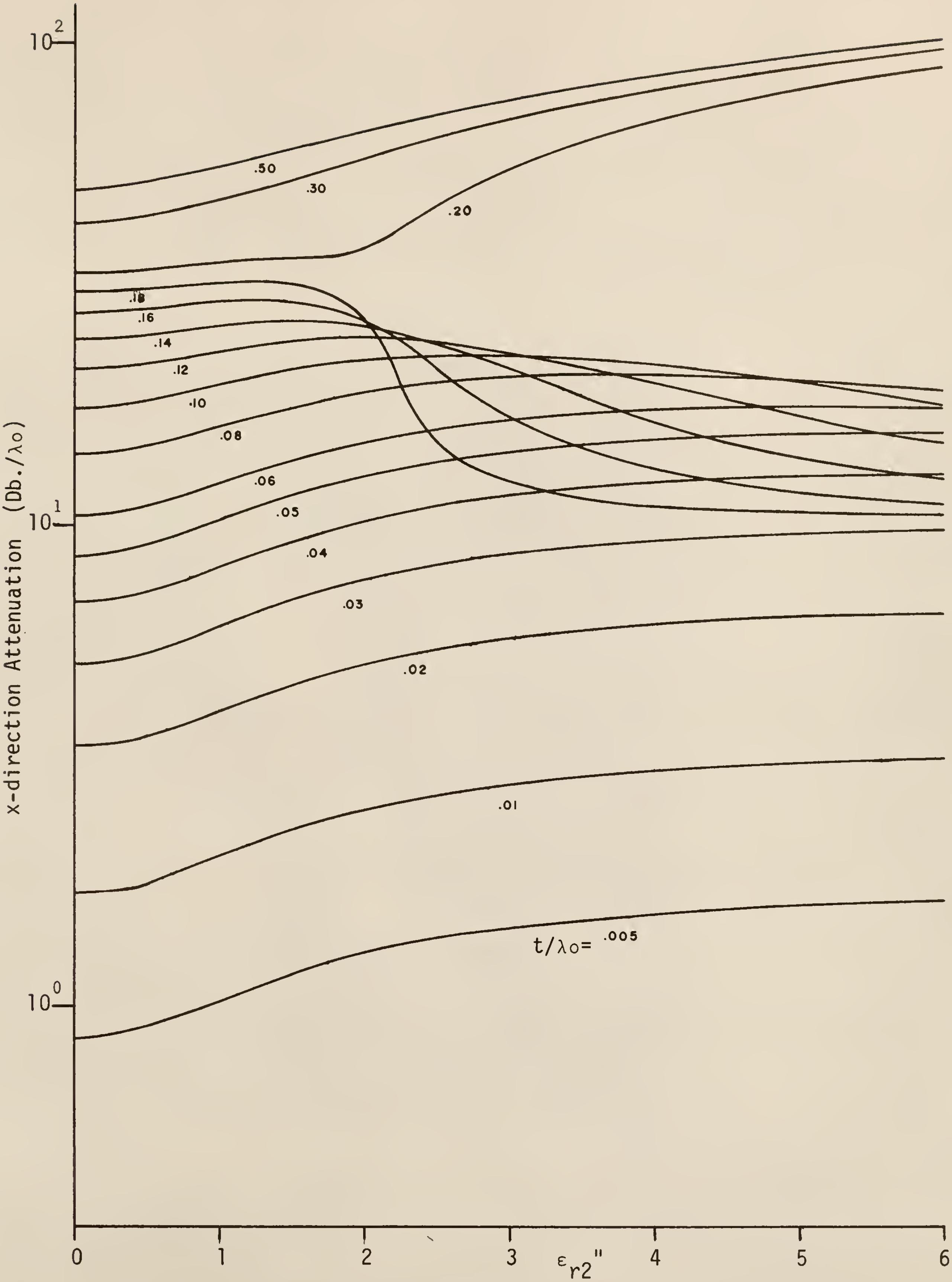

Figure 7. x-direction Attenuation for the TMo Mode and $\varepsilon_{r2}'=2$.

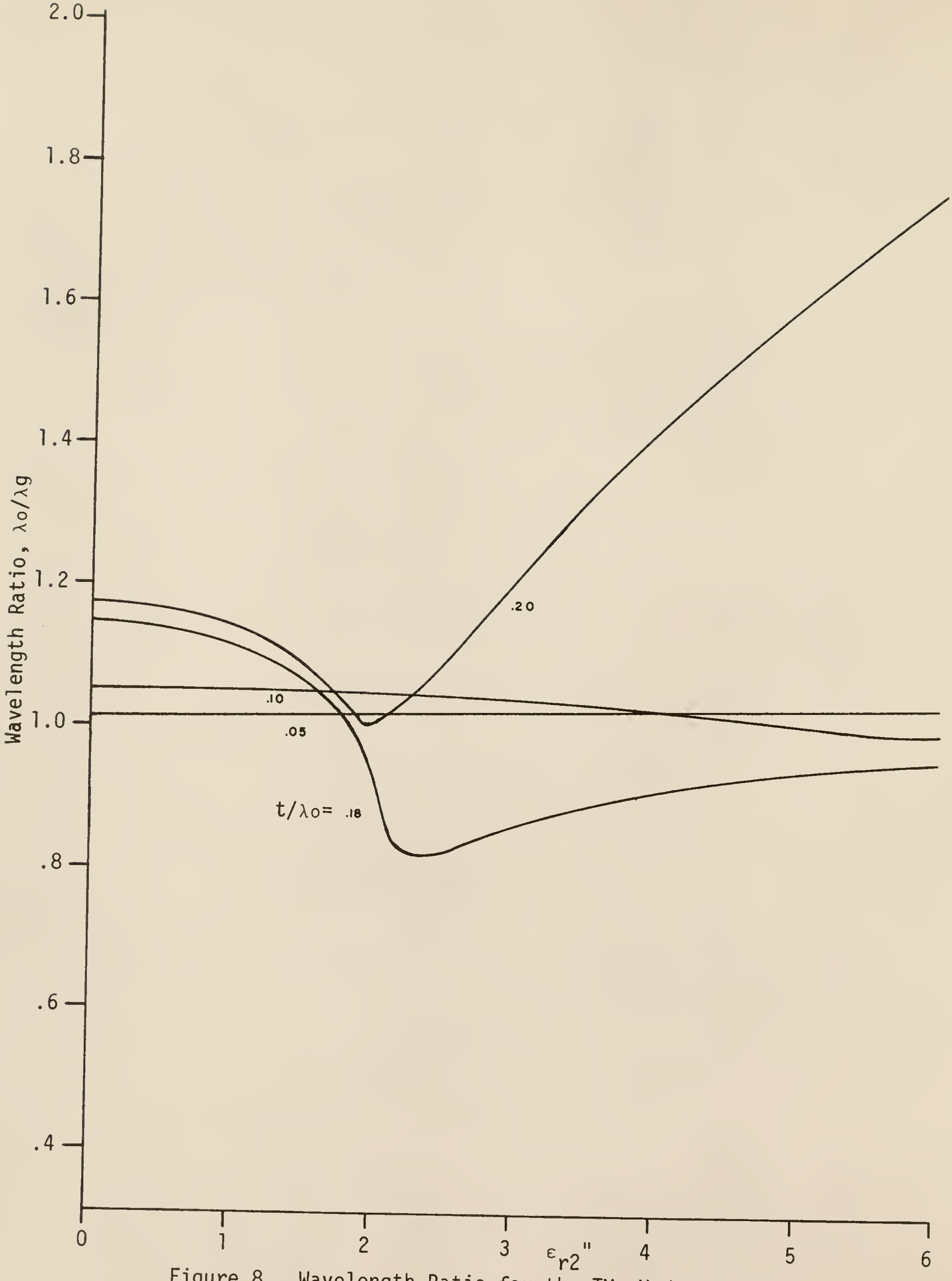

Figure 8. Wavelength Ratio for the TMo Mode and $\varepsilon_{r2}'=2$.

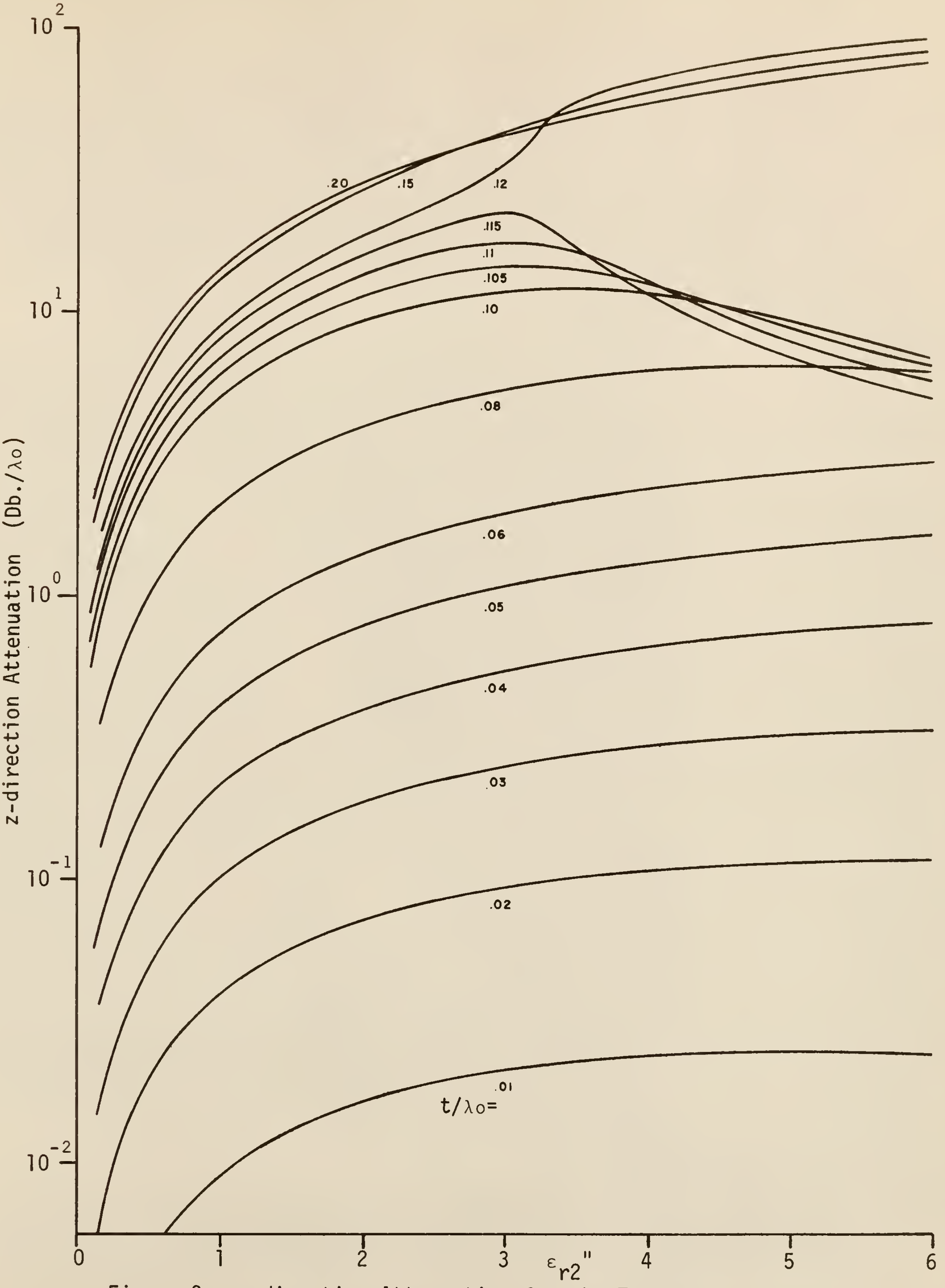

Figure 9. z-direction Attenuation for the TMo Mode and $\varepsilon_{r2}'=4.24$.

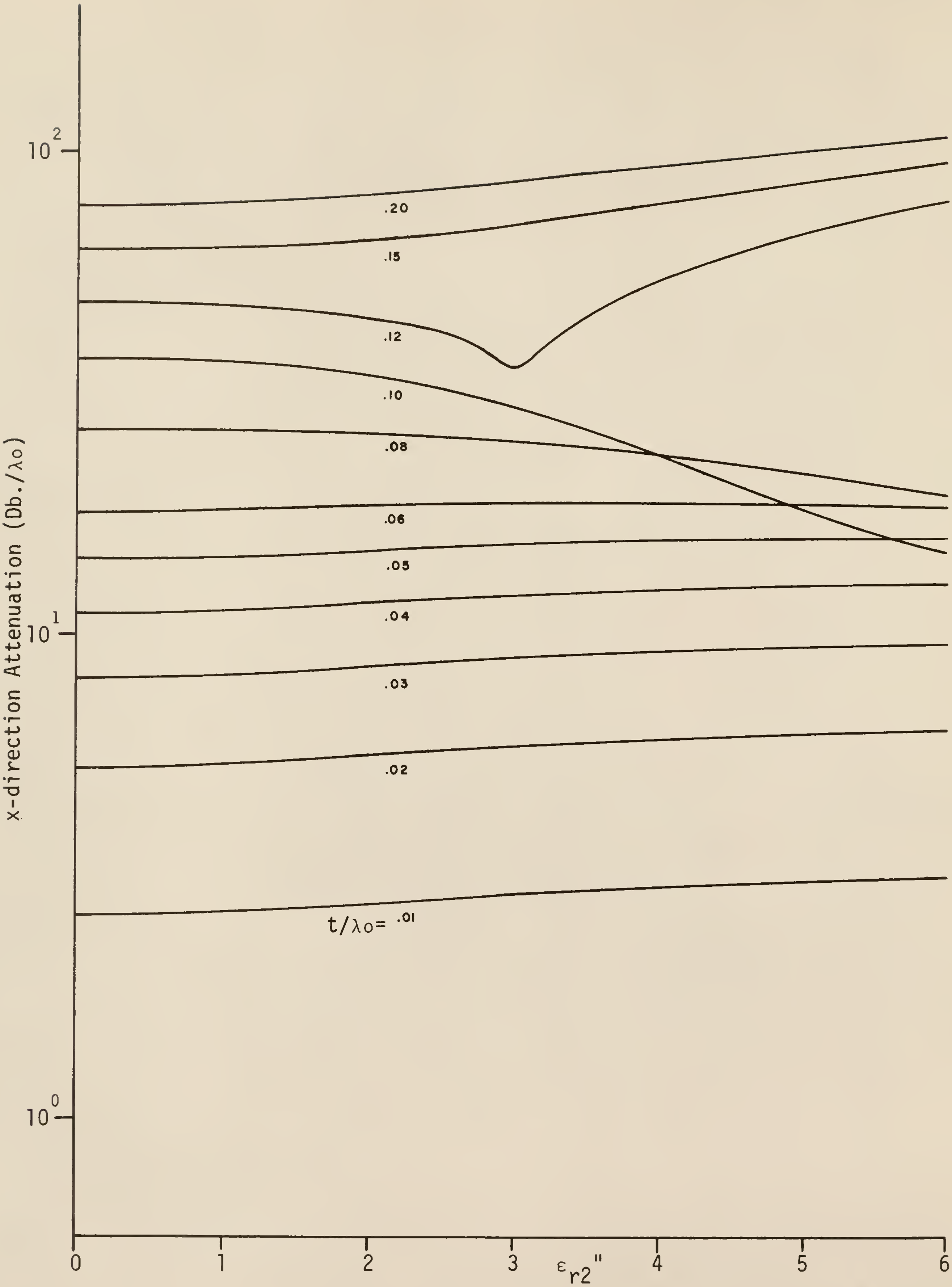

Figure 10. x-direction Attenuation for the TMo Mode and $\epsilon_{r2}'=4.24$.

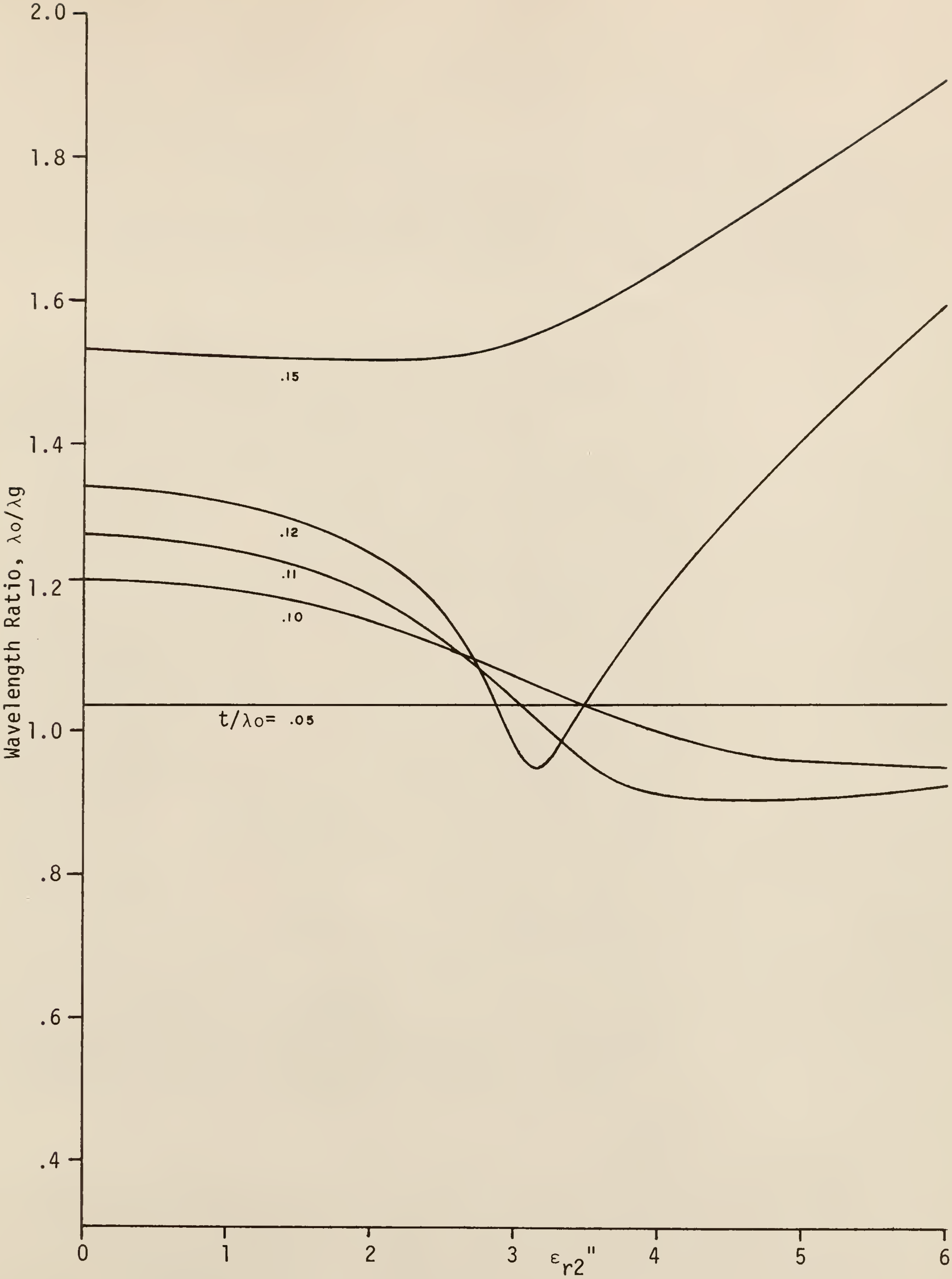

Figure 11. Wavelength Ratio for the TM_0 Mode and $\varepsilon_{r2}'=4.24$.

12, 13, and 14, while the case for $\varepsilon_{r2}' = 165$ is presented in Figures 15, 16, 17, and 18. The features of these families of curves are essentially identical to those for $\varepsilon_{r2}' = 2$. Table 2 shows the approximate values of ε_{r2}'' and $t/\lambda o$ at which the transition occurs for each value of ε_{r2}'.

TABLE 2

APPROXIMATE ε_{r2}'' AND $t/\lambda o$ TRANSITION VALUES

ε_{r2}'	2	4.24	8.28	165
ε_{r2}''	2	3	4.1	18
$t/\lambda o$	.18	.115	.083	.018

Roughly speaking, the following empirical relations among the transition values hold:

$$\varepsilon_{r2}'' \approx \sqrt{2\varepsilon_{r2}'} \qquad [4.1.1]$$

$$t/\lambda o \approx .24/\sqrt{\varepsilon_{r2}'} \ . \qquad [4.1.2]$$

Mathematically, it appears that the transition phenomenon is due to behavior of tan (z) for Re(z) near $\pi/2$; at the transition, the value of Re(z) is between $.43\pi$ and $.48\pi$. Some further physical and mathematical insight as to the mechanism of transition will be gained in later paragraphs.

In section 2.3 it was noted that conjugate pair solutions occur for the lossless leaky wave case, and it was conjectured that approximately conjugate roots might exist in the lossy surface wave case. Such roots have been encountered. For cases in which region 1 is lossy, such roots may have physical significance; they have not been examined in this research.

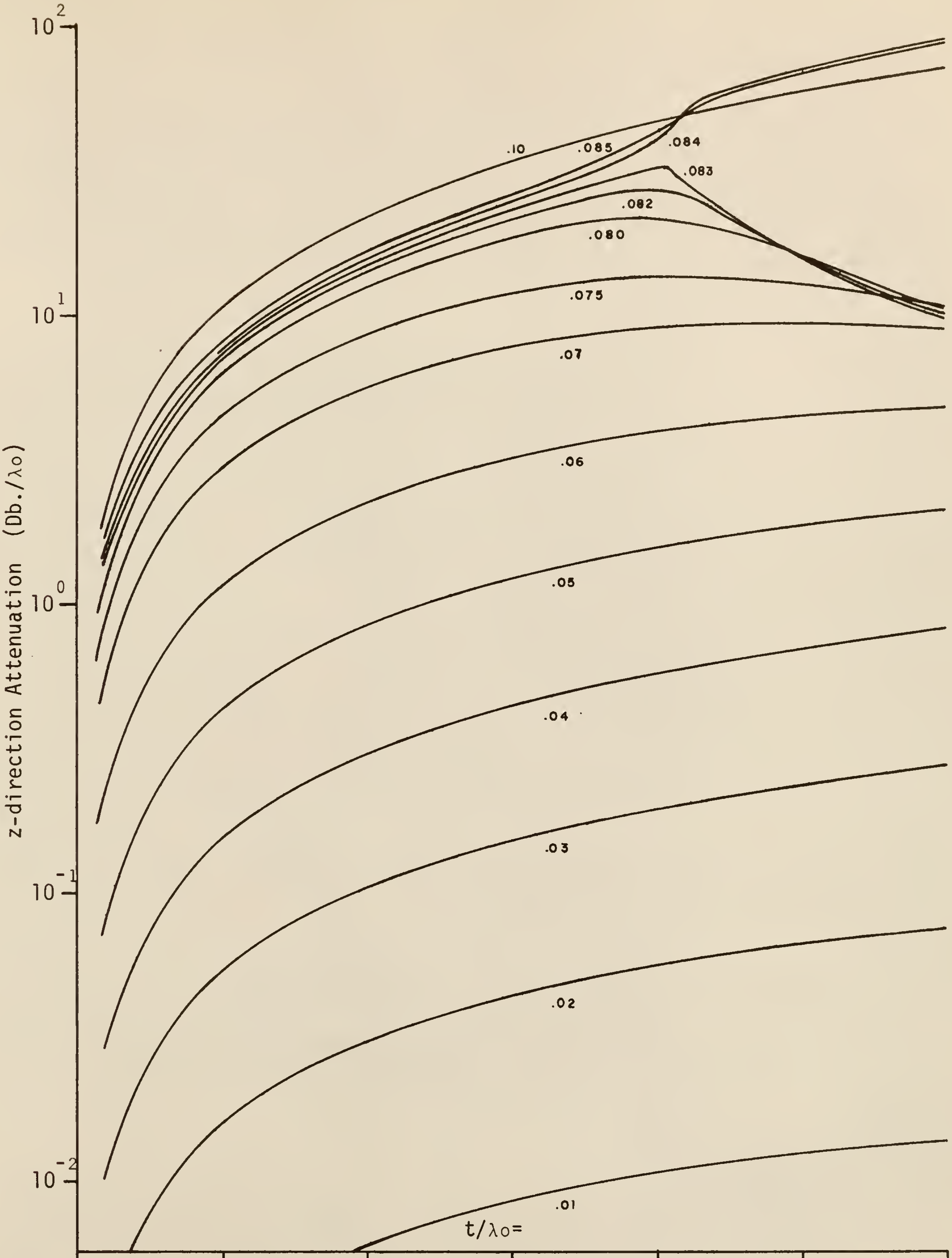

Figure 12. z-direction Attenuation for the TMo Mode and ε_{r2}'=8.28.

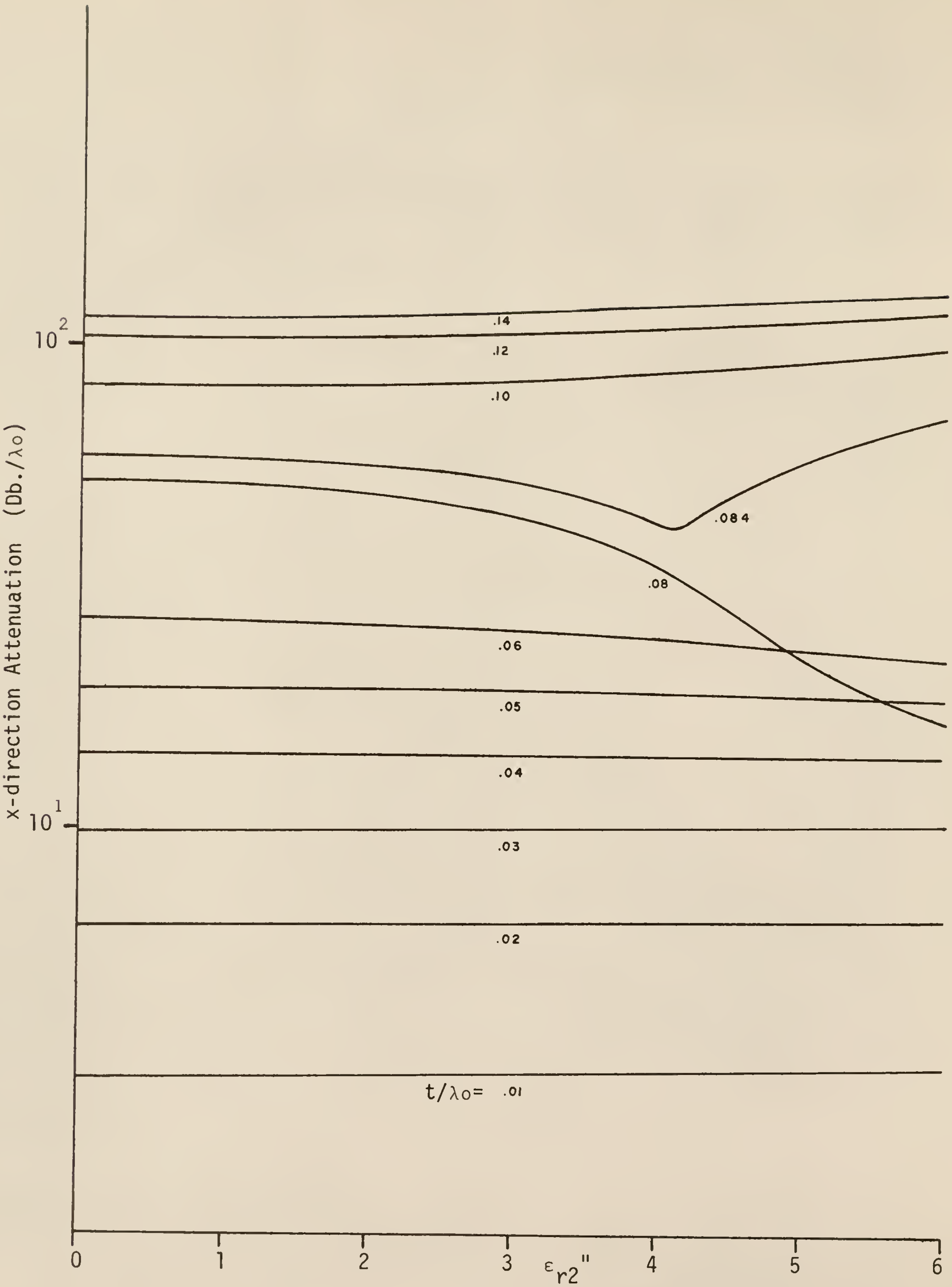

Figure 13. x-direction Attenuation for the TMo Mode and ε_{r2}'=8.28.

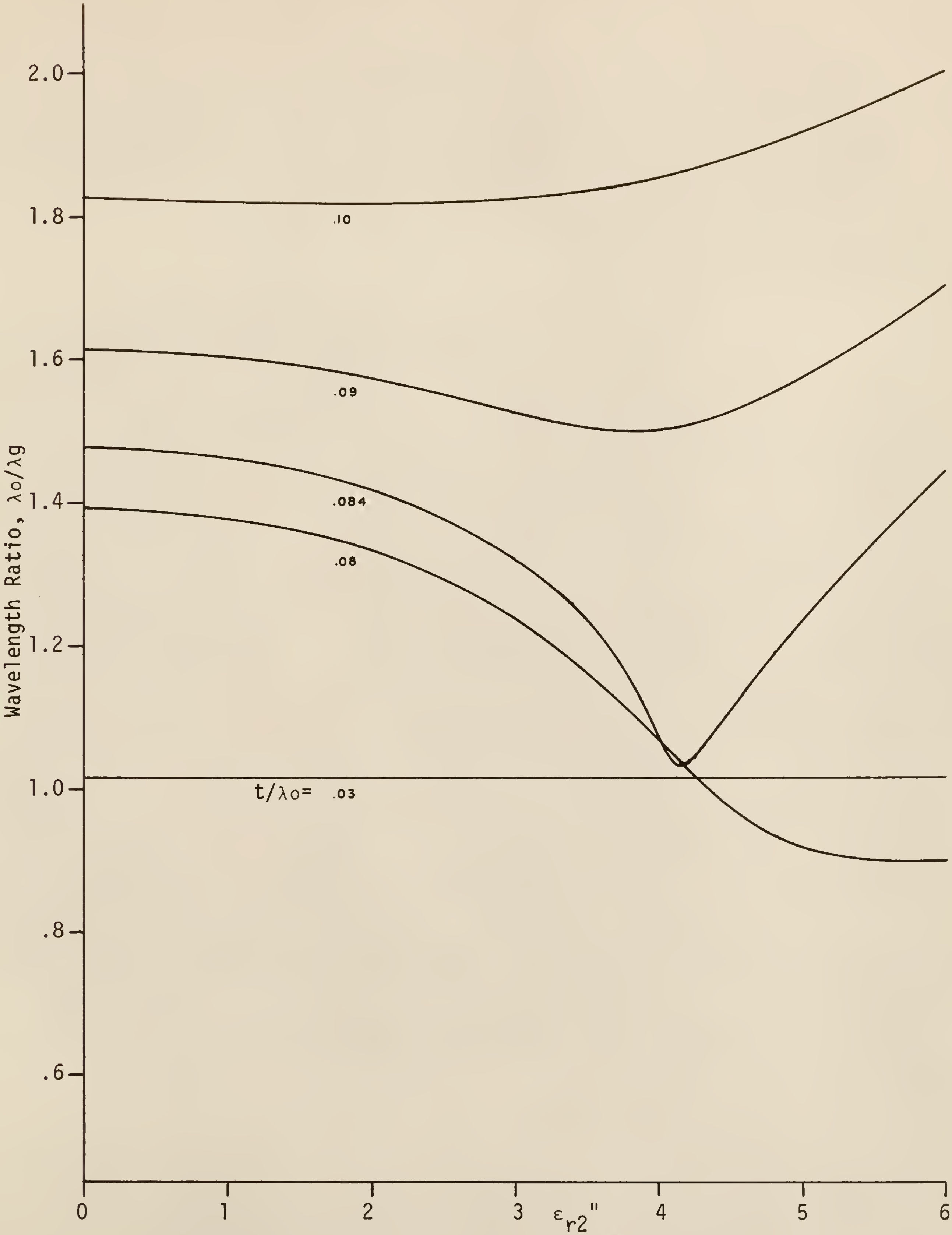

Figure 14. Wavelength Ratio for the TMo Mode and $\varepsilon_{r2}'=8.28$.

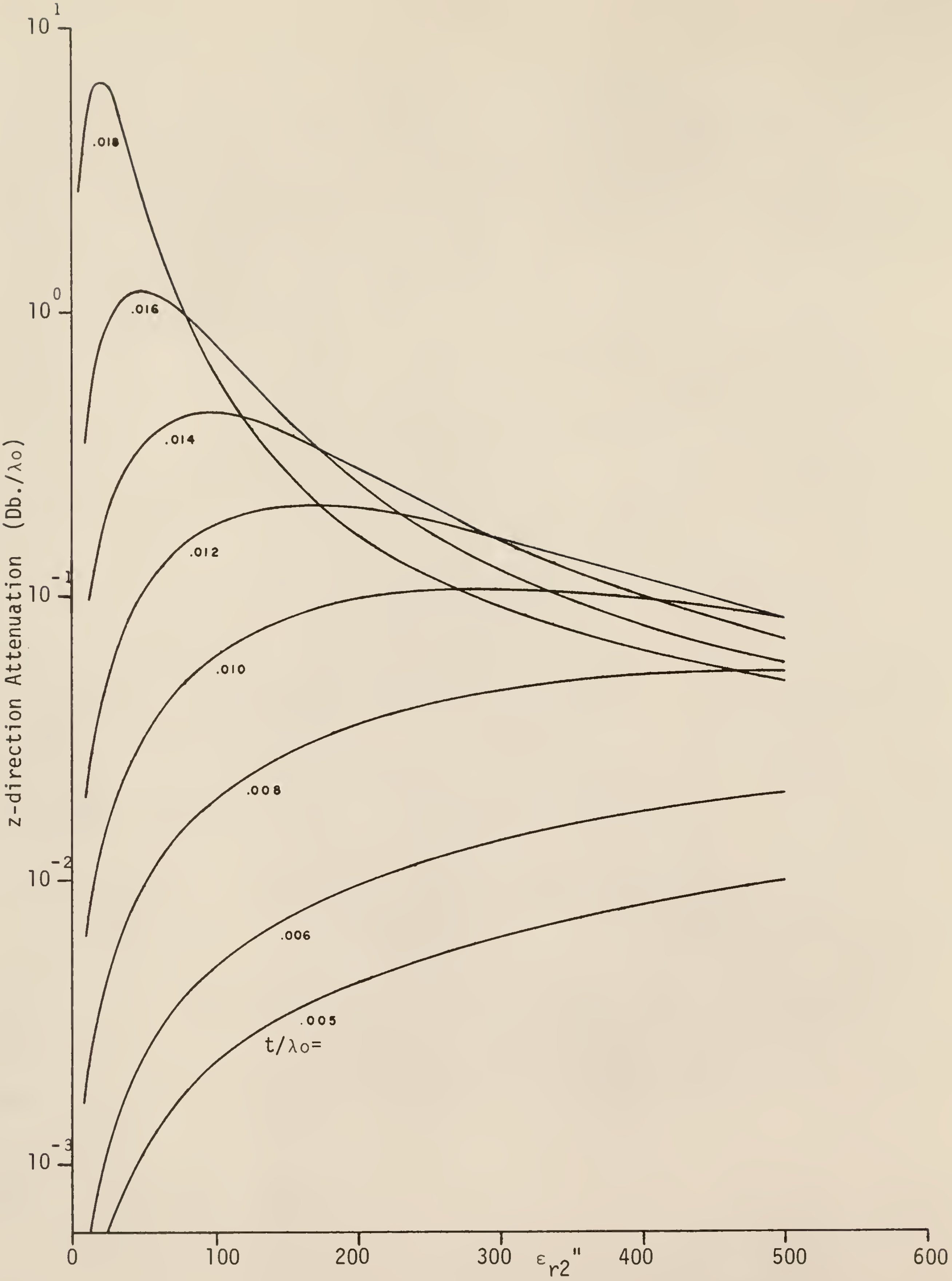

Figure 15. z-direction Attenuation for the TMo Mode and ε_{r2}'=165.

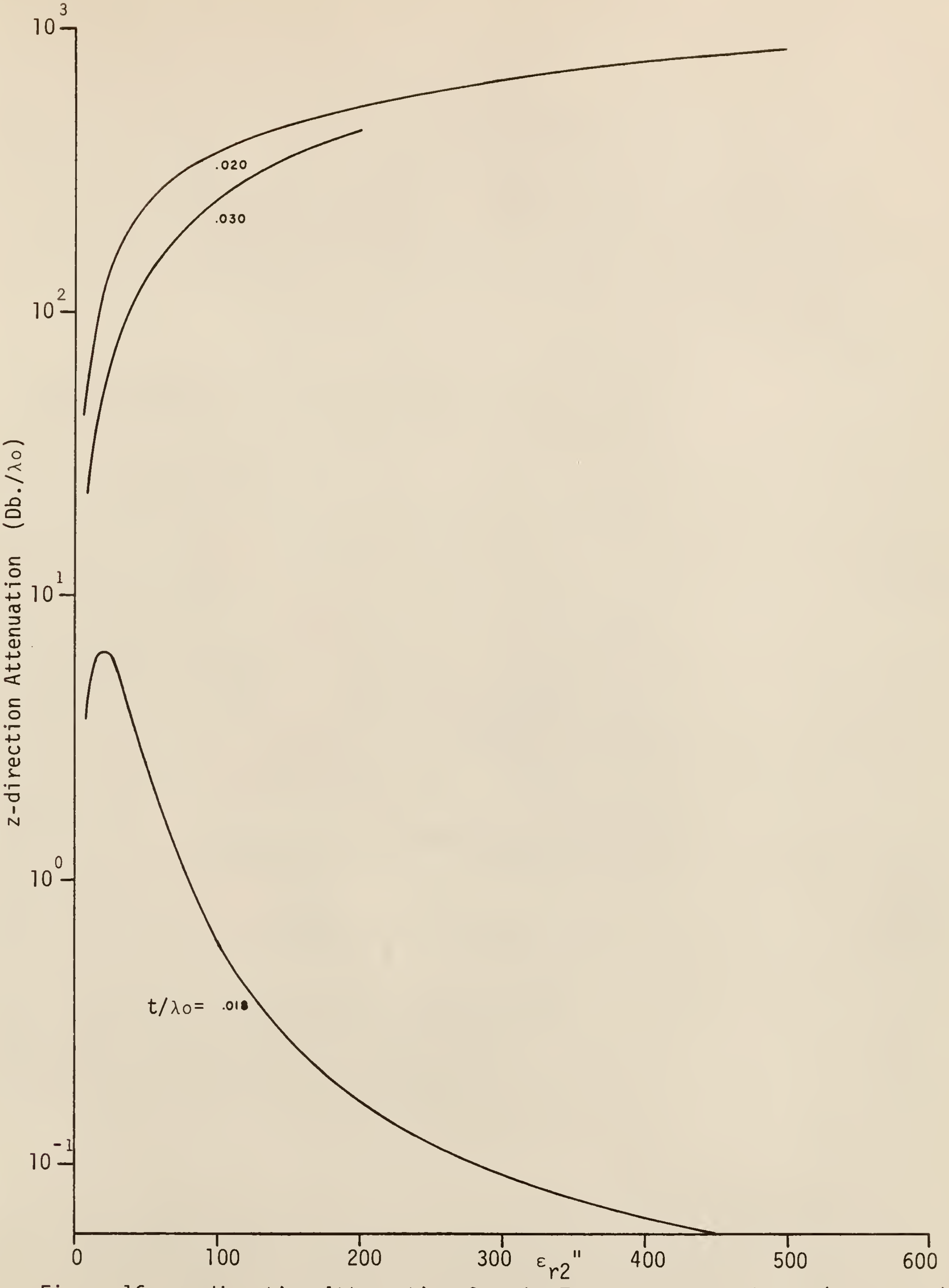

Figure 16. z-direction Attenuation for the TMo Mode and ε_{r2}'=165 (Continued).

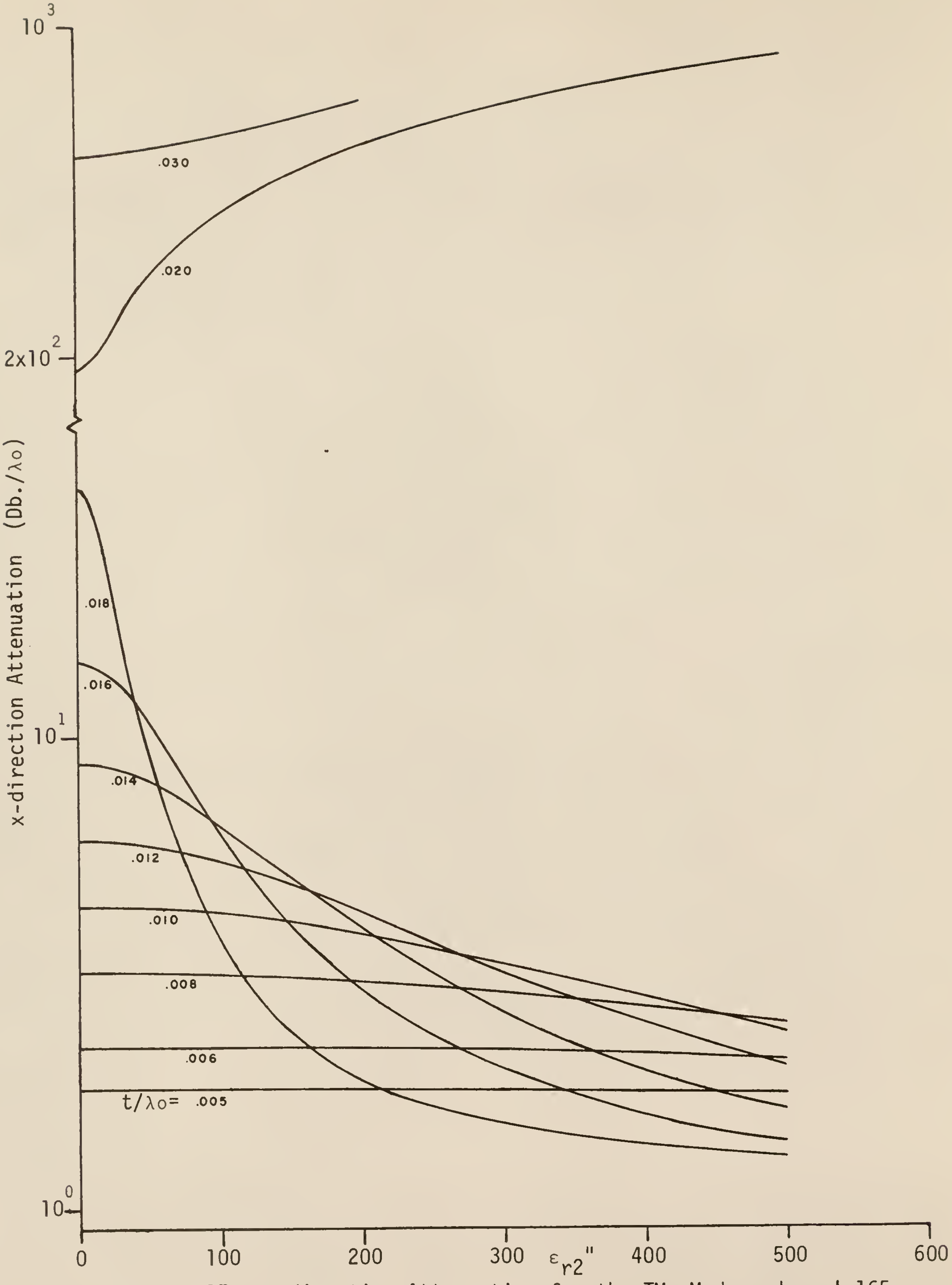

Figure 17. x-direction Attenuation for the TMo Mode and $\varepsilon_{r2}'=165$.

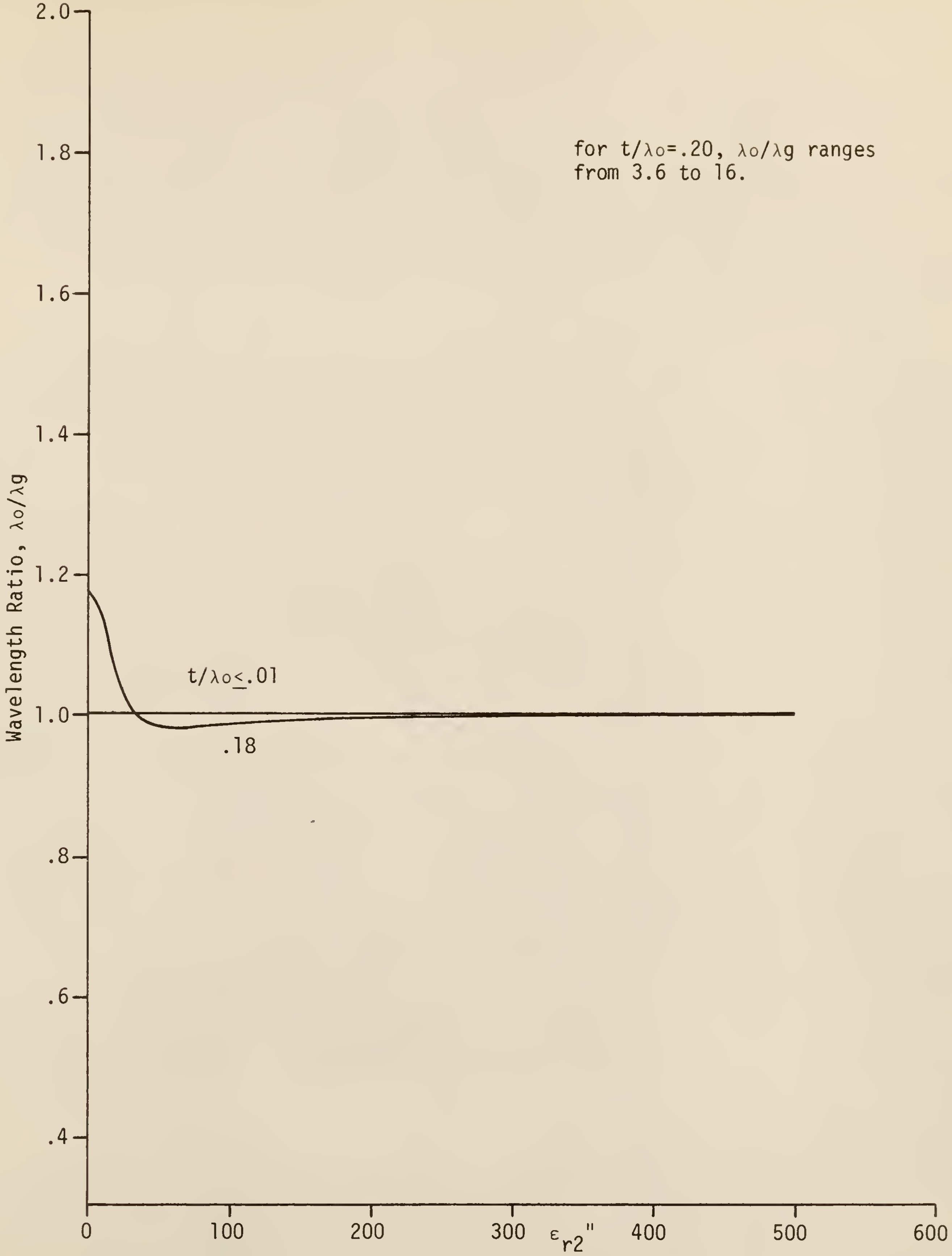

Figure 18. Wavelength Ratio for the TM_0 Mode and $\epsilon_{r2}'=165$.

Inspection of the computer output shows that, as losses are inserted, θ_β enters the fourth quadrant while θ_α enters the first quadrant. That is, the direction of propagation tilts so as to carry energy into the slab from without; one may hypothesize that this tilt occurs in order to overcome the losses of the dielectric. If region 1 is lossless, as is true in all cases considered in this research, the wave in region 1 is still an evanescent wave, that is $\vec{\alpha}\cdot\vec{\beta} = 0$ or $\theta_\alpha = \theta_\beta + \pi/2$; this is an immediate consequence of Equation 2.1.15. The angle of incidence is $\pi/2 + \theta_\beta = \theta_\alpha$. As might be expected from the data already presented, θ_β is zero in the lossless case, becoming more and more negative with the insertion of losses until the transition effect sets in (see Figure 21). For $t/\lambda o$ less than the transition value, θ_β reaches a maximum negative excursion for some value of ε_{r2}'' and then tends again to parallel incidence as losses are further increased. For $t/\lambda o$ greater than the transition value θ_β appears to tend toward a constant which tends to $-\pi/4$ as $t/\lambda o$ increases. This may be the best explanation of decreasing attenuation with increasing ε_{r2}''.

Though a small amount of research into the behavior of dielectrics having magnetic losses has been performed, sufficient data has not been collected to discuss the behavior of such cases. Their behavior can be expected to be slightly different since the ε_r term is not affected by magnetic losses.

4.2 The Behavior of the TM_1 Extraordinary Surface Wave Mode. When the transition effect was first encountered, it was suspected that there was some mathematical error in the program, such as an improper choice of sign preceding a square root. A hand check indicated, however, that the values obtained were indeed valid roots of Equation 2.1.18. The value of u (per free space wavelength) was plotted for the various values of t/λ_o; $\varepsilon_{r2}' = 2$ was being investigated at the time in question. This plot is included as Figure 19. The curves for the TM_o ordinary mode, i.e., those originating on the Real u axis, were the only ones plotted at this point in time. A run was made for $t/\lambda_o = .19$ and $.20$ for an initial ε_{r2}'' of 2.2 using a ZSTART near the U*RAT value previously produced by $t/\lambda_o = .18$ with the intention of verifying that the value of u would indeed meander away from this starting value to the values previously obtained for $t/\lambda_o = .19$ and $.20$. The DEBUG format option was specified to obtain visibility into the path of convergence and the error magnitude. The roots which were found, however, were not the same as before--they were quite near the u values for $t/\lambda_o = .18$. What a revolting development. The next logical step was to sweep ε_{r2}'' down to 0 and up to 6 and plot these results in order to obtain further insight. This was done for ratios of .19 and .20; also, for $t/\lambda_o = .18$ and the single point $\varepsilon_{r2}'' = 6$, $t/\lambda_o = .16$ solutions were anticipated corresponding to the ordinary mode behavior for $t/\lambda_o = .19$ and $.20$. All these values were indeed found; indicative curves of u values for this extraordinary mode are shown in Figure 19.

The curves extending below Re(u) = 8.75 are those of the ordinary mode while those not extending below Re(u) = 8.75 correspond to the extraordinary mode. The boundary separating the ordinary and extraordinary modes has been empirically determined. Those having decreasing Im(u) at high ε_{r2}'' produce decreasing z-direction attenuation at high ε_{r2}'' while those having increasing Im(u) at high ε_{r2}'' produce increasing z-direction attenuation at high ε_{r2}''.

Since the DEBUG format option was used during this investigation, the computer output is too bulky to include. However, tabular output for the

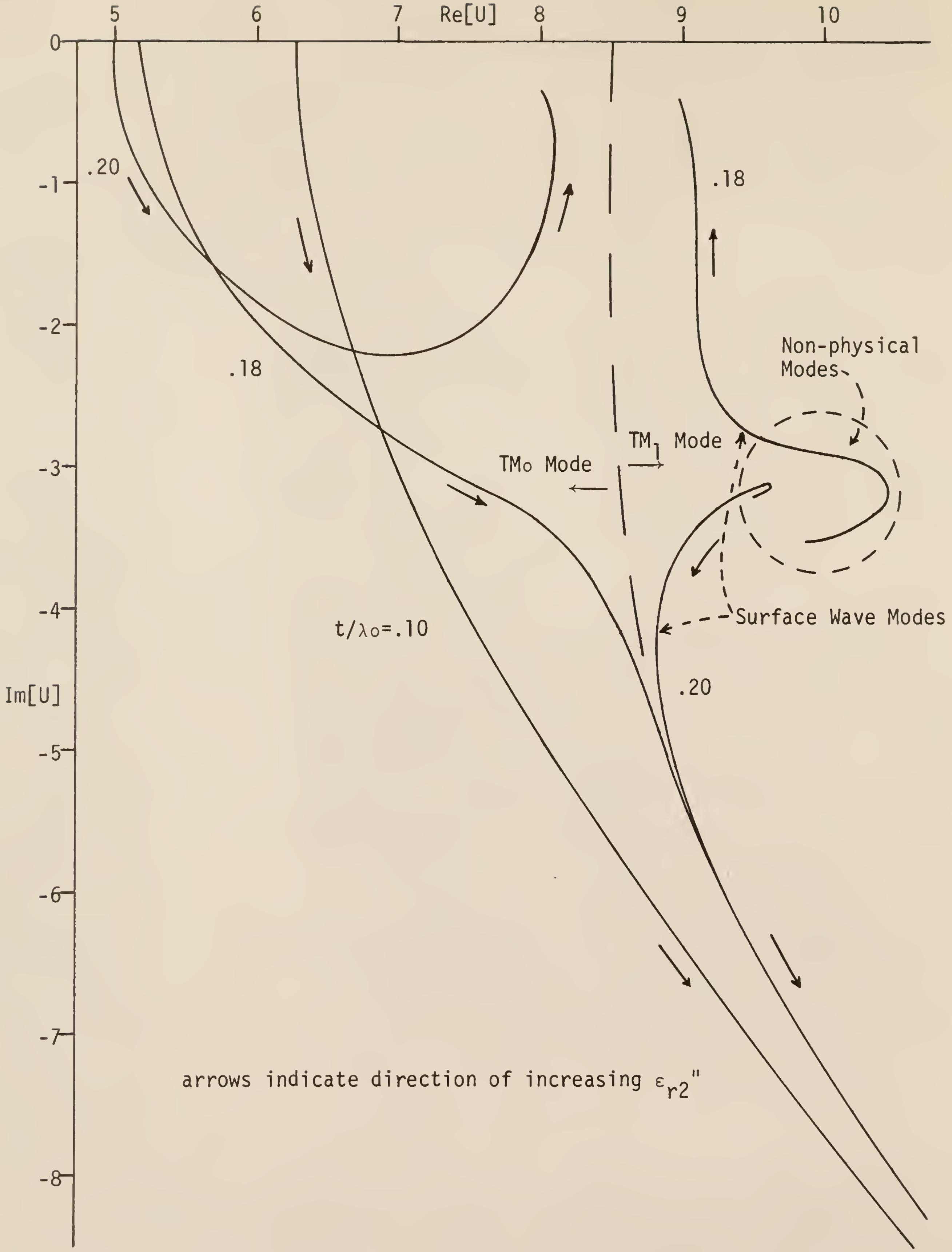

Figure 19. Root Paths in the Complex U Plane for the TMo and TM$_1$ Modes.

extraordinary mode with $\varepsilon_{r2}' = 165$, $t/\lambda o = .02$ is included in Appendix C (the mode subscript is incorrect, if indeed it is meaningful).

It is now apparent that this extraordinary mode corresponds to a mode numbered TM_1. Such modes are not physically real in the lossless case where there is a real intersection of the z·tan(z) curve with the circle of radius $2\pi[t/\lambda o]\sqrt{\mu_{r2}\varepsilon_{r2} - \mu_{r1}\varepsilon_{r1}}$; $\vec{\beta}$ lies in the $\vec{a}_z$ direction but $\vec{\alpha}$ lies in the $-\vec{a}_x$ direction. Examination of the computer results shows that this TM_1 mode has an $\vec{\alpha}$ lying in the third quadrant or on its boundary for low or zero losses, but as losses are increased $\vec{\alpha}$ passes through zero magnitude and enters the first quadrant; $\vec{\beta}$ remains in the fourth quadrant in both cases. The zero magnitude of $\vec{\alpha}$ is easy to believe for the case shown in Appendix C but may be an erroneous conclusion for the general case. That is, from the requirement $k_z'k_z'' = v'v''$, obtained from Equation 2.1.15 with k_1 real, and the smooth transition of v' through zero it is apparent that $k_z'k_z''$ passes through zero. k_z'' changes sign; k_z' does not change sign but may approach zero, possibly allowing k_z'' to be discontinuous. A closer investigation of the region $1.4 < \varepsilon_{r2}'' < 1.6$ should be made for $\varepsilon_{r2}' = 2$, $t/\lambda o = .18$ and $.19$.

The absolute value of the z-direction attenuation for the TM_1 extraordinary mode is shown in Figure 20. The dotted sections are actually negative, the change in direction of $\vec{\alpha}$ occurring between $\varepsilon_{r2}'' = 1.4$ and $\varepsilon_{r2}'' = 1.6$. The transition effect also appears in this mode. In fact, the extraordinary mode for $t/\lambda o \geq .19$ continues the trend of the TM_o surface wave mode for $t/\lambda o \leq .18$ and the extraordinary mode for $t/\lambda o \leq .18$ continues the trend of the TM_o wave mode for $t/\lambda o \geq .19$. Figure 21 shows this complementary relationship for the angle θ_β.

<u>4.3 Behavior of the TM_2 Leaky Wave Mode.</u> For a circle having a radius less than π, the TM_2 mode is a cutoff mode giving rise to a leaky wave. $\vec{\beta}$

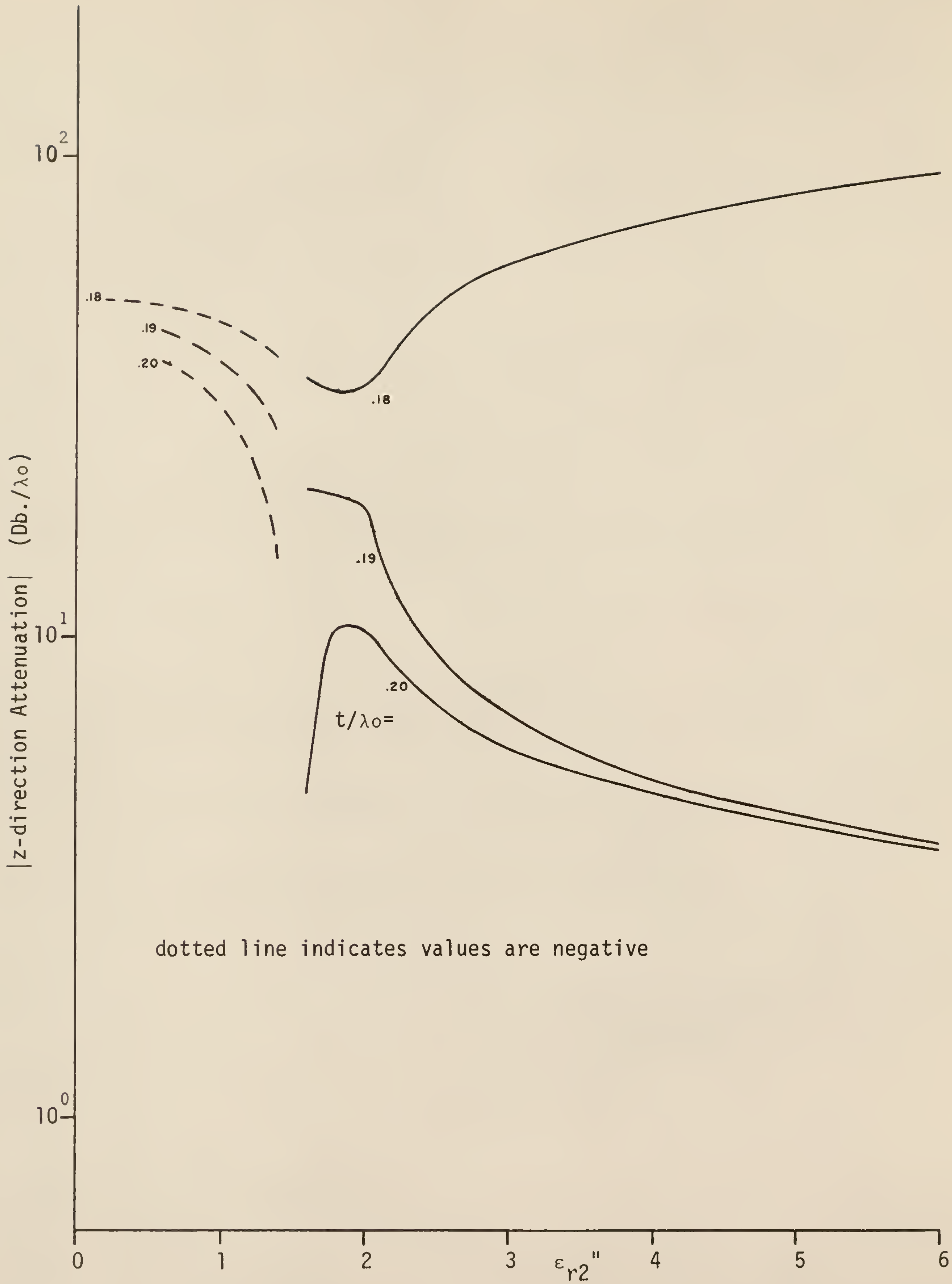

Figure 20. z-direction Attenuation for the TM_1 Mode and $\varepsilon_{r2}'=2$.

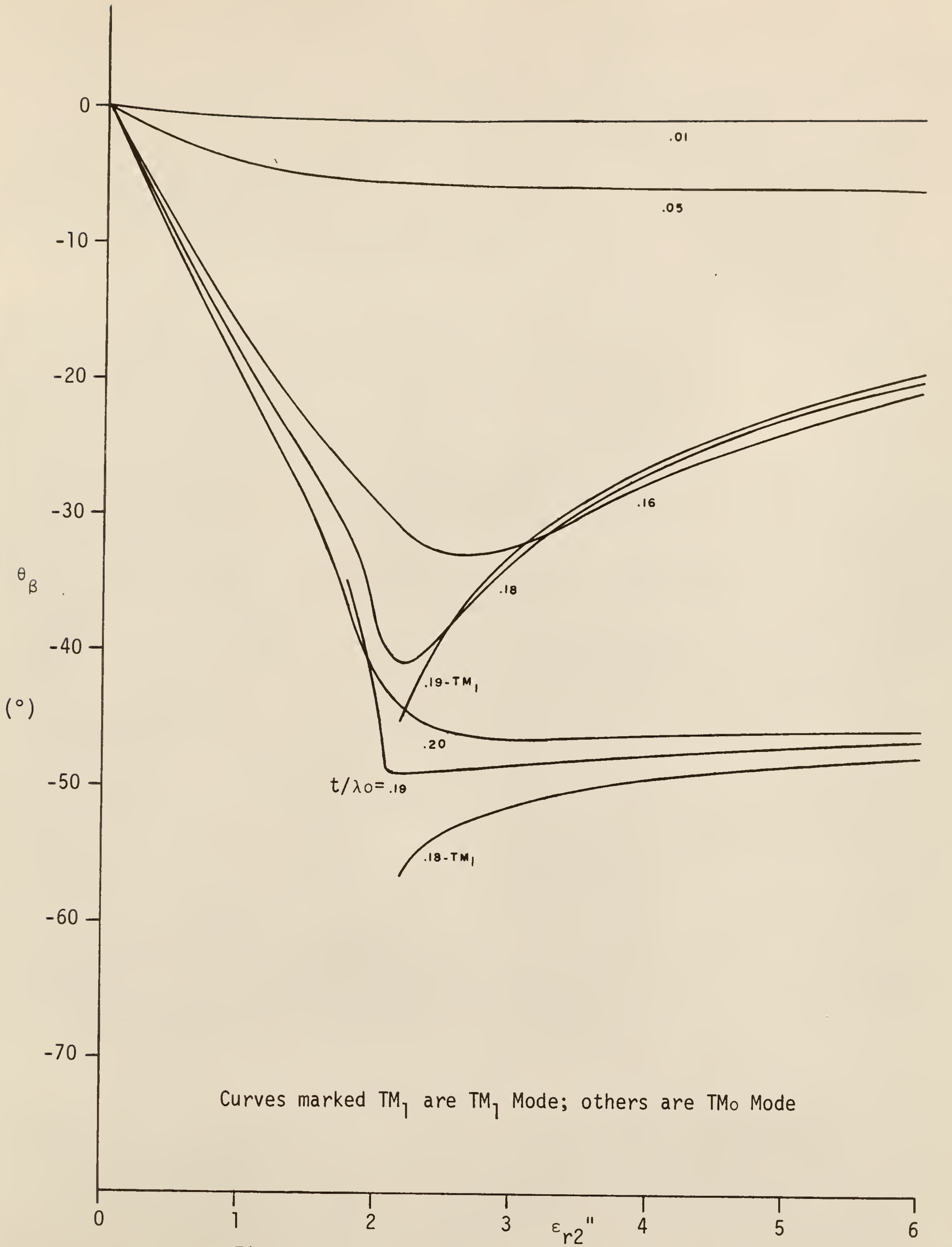

Figure 21. θ_β for the TMo, TM$_1$ Modes and $\varepsilon_{r2}'=2$.

lies in the first quadrant and $\vec{\alpha}$ in the fourth quadrant when region 1 is lossless.

Some representative computer output is included in Appendix C. Only cases in which region 2 is a dielectric having $\varepsilon_{r2}' = 2$ with the magnetic properties of free space and region 1 has the properties of free space were investigated. The z-direction attenuation is not of as much interest here as in the surface wave cases, so it is not plotted. In general, z-direction attenuation increases with decreasing $t/\lambda o$, i.e., a more severe degree of cutoff. θ_β is a much more interesting quantity. This angle, which might appropriately be termed the angle of departure or launch angle in the leaky wave cases, is plotted in Figure 22. θ_β increases as the degree of cutoff increases. For $t/\lambda o = .49$ the z-direction attenuation and launch angle are very nearly zero for $\varepsilon_{r2}'' = 0$ since the degree of cutoff is very mild. There may be effects of interest occurring in the range $.10 < t/\lambda o < .30$ which are not shown as evidenced by the dissimilarity of the $t/\lambda o = .20$ curve to the $t/\lambda o = .10$ and .30 curves. The wave seems to be affected very little by losses in severely cutoff cases.

A few notes are necessary concerning the cases $t/\lambda o = .49$ and $t/\lambda o = .01$. For $\varepsilon_{r2}'' = 0$ and $t/\lambda o = .49$ the computer oscillated between the proper solution and the conjugate solution, finally converging to the conjugate solution. This explains the sign discrepancy; format field width explains the 0.00000 value: the imaginary part of z is only 4.5E-10, thus the two solutions are extremely close together. It is simply fortuitous that the error surface is usually inclined such as to lead the iteration routine to the proper solution; no planning or constraints forced it. Only the first line of output is valid for $t/\lambda o = .01$; the degree of cutoff is extreme so that Re(z) is near $\pi/2$: 1.5710928 versus 1.5707963. This is an example of

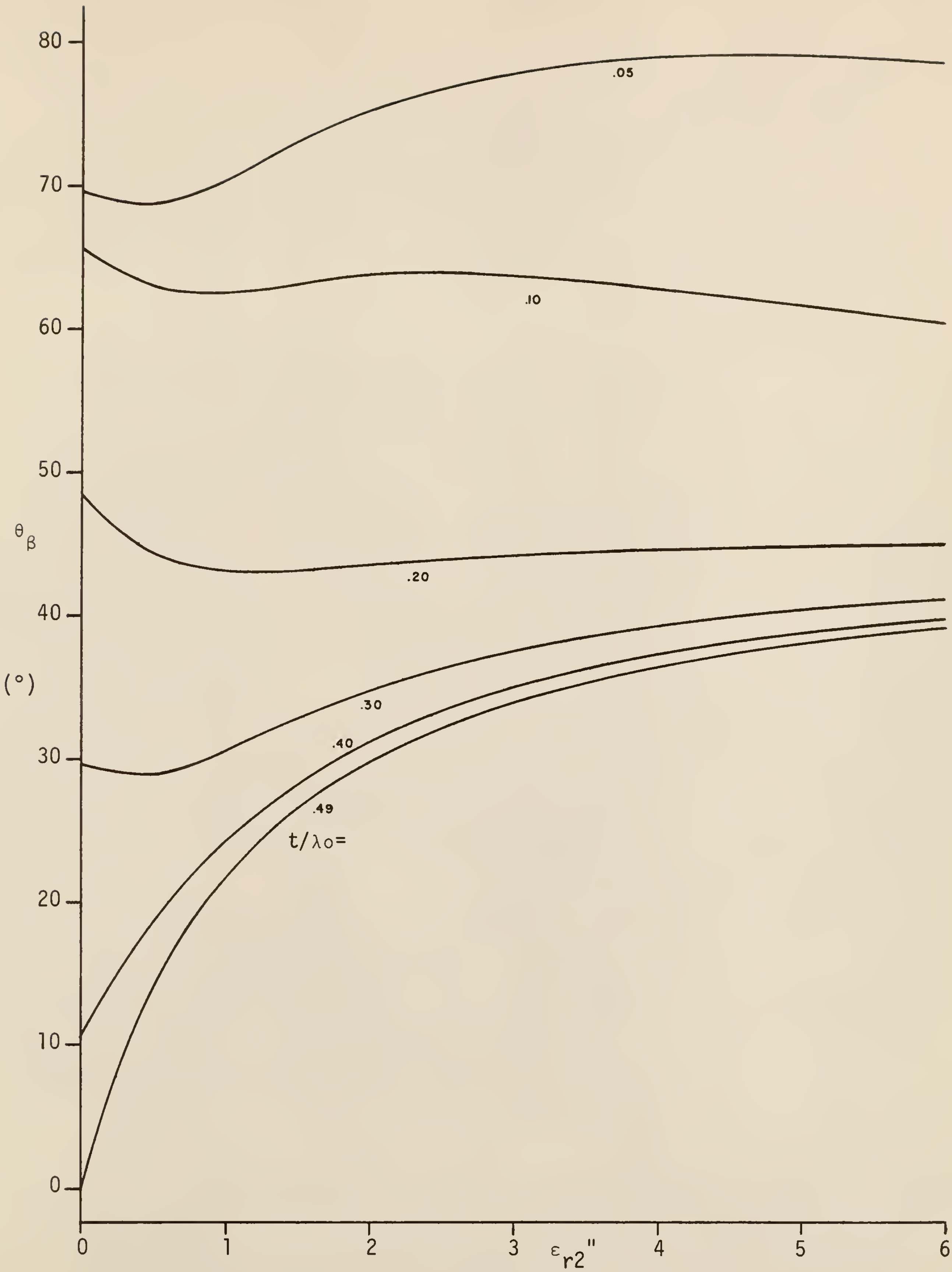

Figure 22. θ_β for the TM_2 Leaky Wave Mode and $\varepsilon_{r2}'=2$.

the increment magnitude problem mentioned in Section 3.4. At the time of this writing, attempts to obtain valid results for $t/\lambda o = .01$ have been unsuccessful.

Some conjecture about the possibility of an extraordinary cutoff mode seems appropriate. The conjugate solution to the TM_1 extraordinary mode could exhibit the characteristics of a leaky wave; referring to the TM_1 extraordinary mode $\varepsilon_{r2}' = 165$ computer output in Appendix C, a conjugate solution would, at low losses, give rise to a $\vec{\beta}$ in the first quadrant and an $\vec{\alpha}$ in the fourth quadrant.

4.4 Behavior of the TM_2 Surface Wave Mode. The case of $\varepsilon_{r2}' = 2$ was investigated for the TM_2 surface wave mode, the properties of region 1 and the magnetic properties of region 2 being those of free space. The z-direction attenuation, x-direction attenuation, and wavelength ratio are plotted in Figures 23, 24, and 25 respectively. The behavior of this mode is highly similar to that of the TMo mode. There are three notable differences: first, the value of $t/\lambda o$ at which the transition occurs is different; second, the value of ε_{r2}'' at which the transition occurs is different; third, for high losses and $t/\lambda o$ less than the transition value the curves for various $t/\lambda o$ values are so close together that it is impossible to distinguish one from another.

One might anticipate a difference in the TMo and TM_2 modes for circle radii near the cutoff value in each case since the $z \cdot \tan(z)$ curve has zero slope at $z = 0$ but non-zero slope at $z = \pi$. Such a difference is not apparent, however. On the other hand, compare the region $0 < \varepsilon_{r2}'' < 2$ for the TM_2 with the region $0 < \varepsilon_{r2}'' < 6$ for the TMo; the TMo might exhibit the same asymptotic behavior as the TM_2 if ε_{r2}'' were increased beyond 6. This might be the manifestation of the slope difference.

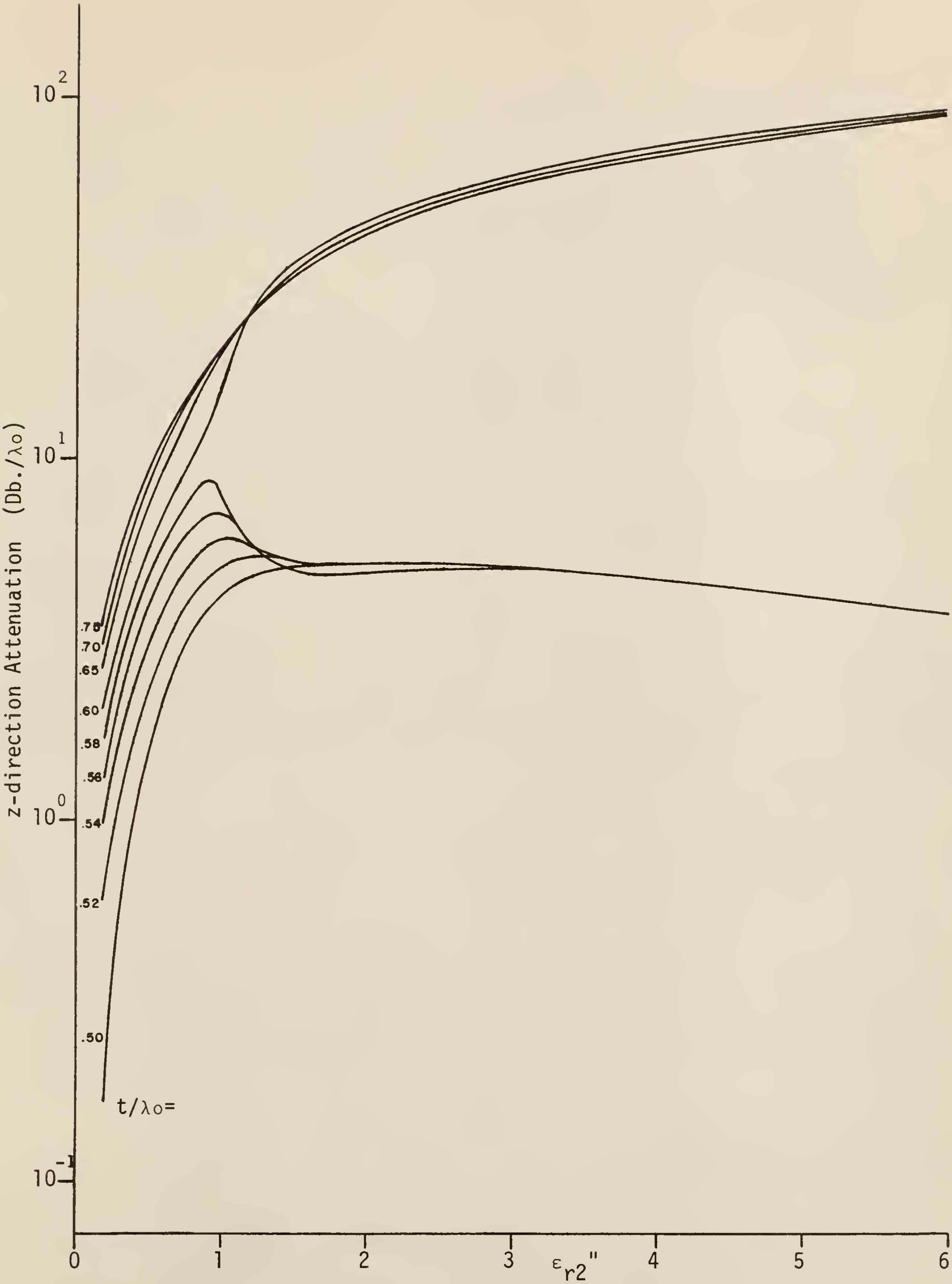

Figure 23. z-direction Attenuation for the TM_2 Surface Wave Mode and $\varepsilon_{r2}'=2$.

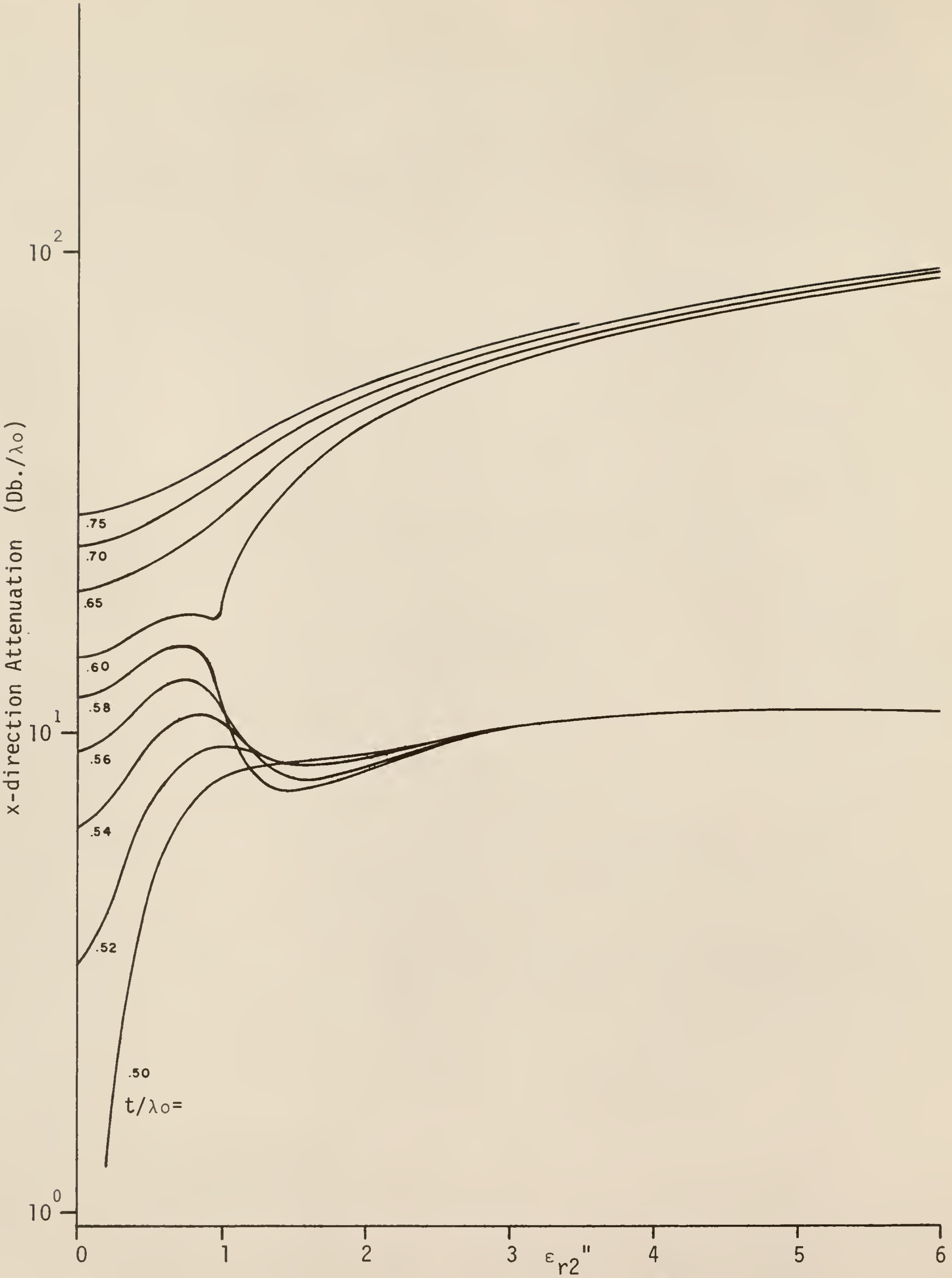

Figure 24. x-direction Attenuation for the TM_2 Surface Wave Mode and $\varepsilon_{r2}'=2$.

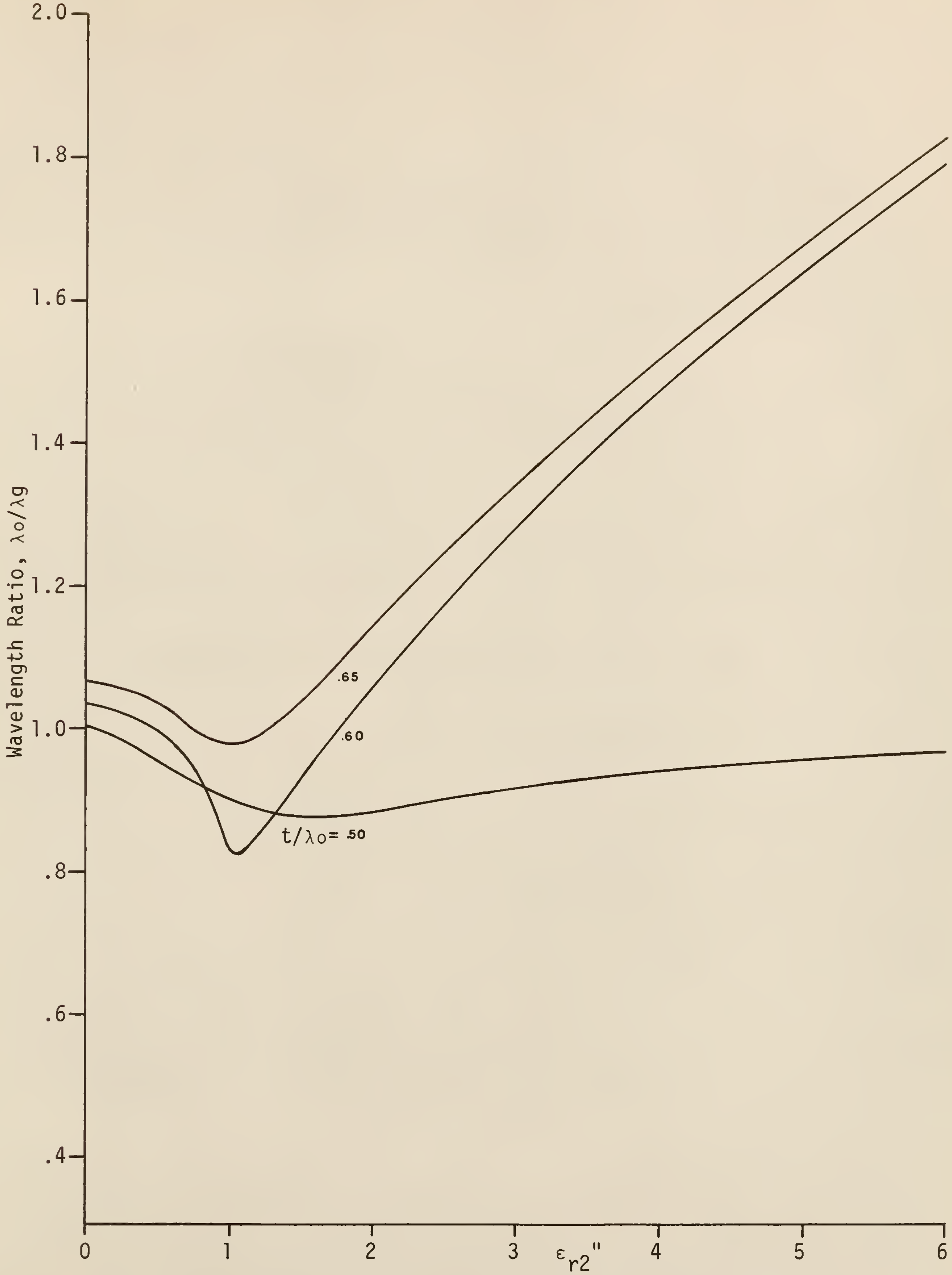

Figure 25. Wavelength Ratio for the TM_2 Surface Wave Mode and $\varepsilon_{r2}'=2$.

CHAPTER V

SUMMARY AND CONCLUSIONS

5.1 Summary. Chapter II begins with the derivation of the characteristic equation and the elimination of variables to obtain a single equation in one unknown. A graphical analysis of the real roots is presented; this graphical solution has been presented by several other authors [Collin, 1960; Harrington, 1961] and is not a significant contribution. Chapter II is concluded with a discussion of the location and nature of complex zeros of Equation 2.1.18.

Chapter III begins with a discussion of the numerical approaches with which early experiments were carried out. The final scheme of iteration, a combination of steepest descent and linear iteration, is described and the FORTRAN IV implementation explained. The remainder of the program is described in order that other researchers may understand the details of use of the program. The chapter is concluded with a discussion of problems and limitations within the program and recommendations for improving upon them.

Chapter IV presents the data compiled and its interpretation. The quantities of interest are the attenuation in directions parallel and normal to the slab (the z and x directions, respectively), the guide wavelength, and the tilt of the wave outside the slab. These quantities are functions of the properties of both regions and the thickness of the slab in relation to the free-space wavelength. Though the computer program was written to provide for more general properties, the electric and magnetic properties of the region above the slab and the magnetic properties of the slab were chosen to be the properties of free space in all cases presented in this research.

The TM_o mode, which is the dominant mode, shows the expected decrease in z-direction attenuation at high losses for small thicknesses. Another more interesting effect occurs as the thickness is increased; this is the sudden and drastic transition from decreasing to increasing attenuation at high losses. Comparison of families of curves for different ε_{r2}' values indicates that for small t/λ_o, the higher the ε_{r2}' the lower the attenuation while for large t/λ_o, the higher the ε_{r2}' the higher the attenuation. The case $\varepsilon_{r2}' = 165$ does not fit this pattern; the transition effects sets in at a much lower value of t/λ_o than in the other cases. Empirically, the relationship between the parameters at which transition occurs is given by the expressions

$$\varepsilon_{r2}'' \simeq \sqrt{2\varepsilon_{r2}'}$$

$$t/\lambda_o \simeq .24/\sqrt{\varepsilon_{r2}'} .$$

Except for t/λ_o values in the transition range, the attenuation in the x direction tends to increase slightly as losses are inserted and, as in the lossless case, tends to increase as t/λ_o increases. That is, as losses are added, $\vec{\alpha}$ increases in magnitude, since both components increase. $\vec{\beta}$ tends to tilt into the slab as losses are added, the degree of tilt increasing with increasing losses except near the transition t/λ_o values.

The behavior of the wave for t/λ_o in the transition range changes drastically. For t/λ_o slightly less than the transition value, the wave first tilts into the slab as losses are inserted, then tilts back toward parallel incidence at high losses. α increases at low losses but decreases at high losses also. The picture is that of a sufficiently high loss slab reflecting most of the wave so that it is less tightly bound and less energy is dissipated in the slab. For t/λ_0 greater than the transition value, the wave tilts into the slab, reaches some limiting angle, and continues to plow into the slab at a nearly constant angle as losses increase further; $\vec{\alpha}$ tends to increase in magnitude. Here the picture is that the thicker slab prevents the angle of incidence from returning toward zero so that a great deal of energy is concentrated in the slab and dissipated making the wave tightly bound.

It was discovered that, for sufficiently high losses, the TM_1-numbered solution has the proper attributes to be a surface wave. The behavior of this extraordinary mode is concisely but completely described by saying that it is complementary to the TM_0 mode.

Suppose that a source is designed to excite surface waves on some structure, and that the value of t/λ_0 is larger than the transition value but small enough that the TM_2 and higher modes are cut off. The load impedance which the source sees depends upon the $\vec{E}$ and $\vec{H}$ of each mode. The z directed wave impedance tends to be more and more reactive as ϵ, μ, ν, and k_z become more nearly pure imaginary. One would expect, then, that the TM_1 mode would carry most of the power in the structure, and that the TM_0 would be difficult to detect. As frequency is increased from a small t/λ_0 through transition, one might expect a reasonably smooth transition from the TM_0 mode to the TM_1 mode rather than an abrupt jump in attenuation.

The TM_2 leaky wave mode does not appear to exhibit any particularly noteworthy characteristics. It is expected that a solution complementary to the TM_2 leaky wave mode may arise from the extraordinary TM_1 mode.

The TM_2 surface wave mode exhibits properties very similar to those of the TMo mode. The merging of the curves at high losses might also occur for the TMo mode at higher losses.

5.2 Recommendations for Further Study. The geometry shown in Figure 1 will also support TE_n modes where n must be odd in the lossless case. The geometry having a mirror image half-slab and surrounding medium in place of the grounded conductor will support TE and TM modes having both even and odd subscripts. The separation equations are unchanged; the characteristic equations of the other three situations differ only by the appearance of μ_r in place of ε_r and/or the cotangent function in place of the tangent function [Harrington, 1961]. These geometries could be easily investigated with a minimum of simple changes in the program.

The cases involving losses both within and without the slab may be investigated with the present program. Such cases may well yield more possible zeros to be examined. $\vec{\alpha}$ and $\vec{\beta}$ are no longer orthogonal in this case; the angle between them can never exceed $\pi/2$, however.

Magnetic materials are extremely useful in the microwave region and are usually rather lossy. Thus, magnetic cases may well be of interest. Unfortunately, most such applications capitalize upon the anisotropy of such materials when subjected to a dc bias, so that the permeability is a tensor. A tensor permeability cannot be used with the present program.

Cylindrical geometries may also be of interest. It has been proposed that a lossy dielectric coating be used upon power lines to eliminate the propagation of RFI by surface waves. If the results of the present research are indicative, such a scheme is not practical.

To the best of the author's knowledge, there has been no experimental verification of either the transition phenomenon or of the existence of the

TM_1 extraordinary mode. The technology of constructing such lossy materials is available or soon will be; anechoic materials are commercially available, intended for uses such as the elimination of undesired reflections in microwave measurements. It should thus be practical to perform such experimental research.

REFERENCES

Barlow, H. M. and Cullen, A. L. (1953). "Surface Waves". Proceedings of the IEEE, Vol. 100, Part III, No. 68, November 1953, 329-347.

Collin, R. E. (1960). Field Theory of Guided Waves. New York: McGraw-Hill, 1960.

Goubau, Georg. (1950). "Surface Waves and Their Application to Transmission Lines". Journal of Applied Physics. Vol. 21, November, 1950, 1119-1128.

Harrington, R. F. (1961). Time-Harmonic Electromagnetic Fields. New York: McGraw-Hill, 1961.

Johnson, G. L. (1966). Unpublished Research.

Kunz, K. S. (1957). Numerical Analysis. New York: McGraw-Hill, 1957.

Romanovskiy, V. A. (1967). "Spectrum of 'Outflowing' and 'Inflowing' waves for a Dielectric Slab". Telecommunications and Radio Engineering (translation of RadioTekhnika), Vol. 22, June 1967, 139-140.

Zucker, F. J. (1961). "Surface and Leaky Wave Antennas." Antenna Engineering Handbook, Chapter 16, Ed. H. Jasik. New York: McGraw-Hill, 1961.

APPENDIX A

FLOWCHARTS

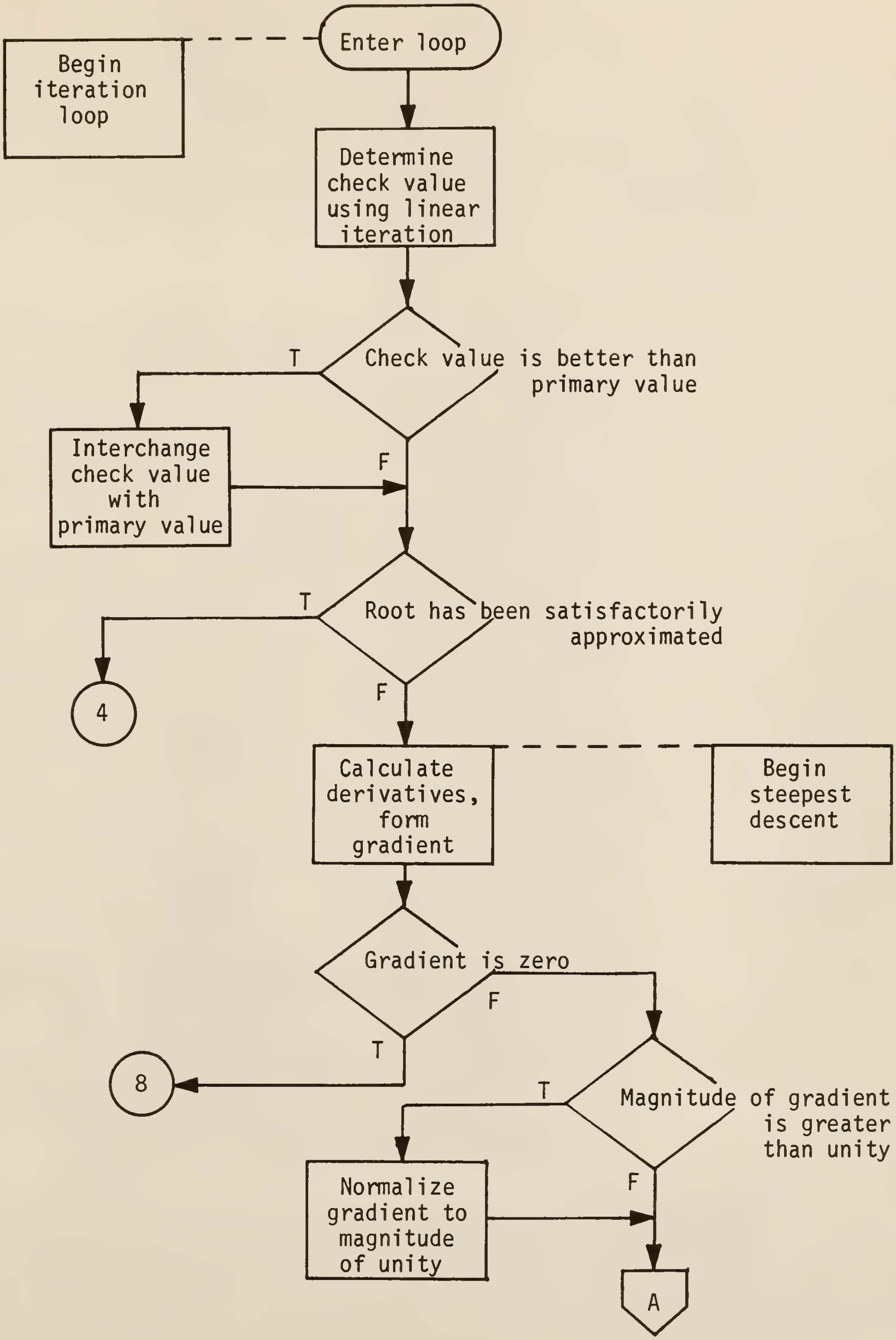

Enter loop
Begin iteration loop
Determine check value using linear iteration
Check value is better than primary value
T
F
Interchange check value with primary value
Root has been satisfactorily approximated
T
F
4
Calculate derivatives, form gradient
Begin steepest descent
Gradient is zero
F
T
8
Magnitude of gradient is greater than unity
T
F
Normalize gradient to magnitude of unity
A

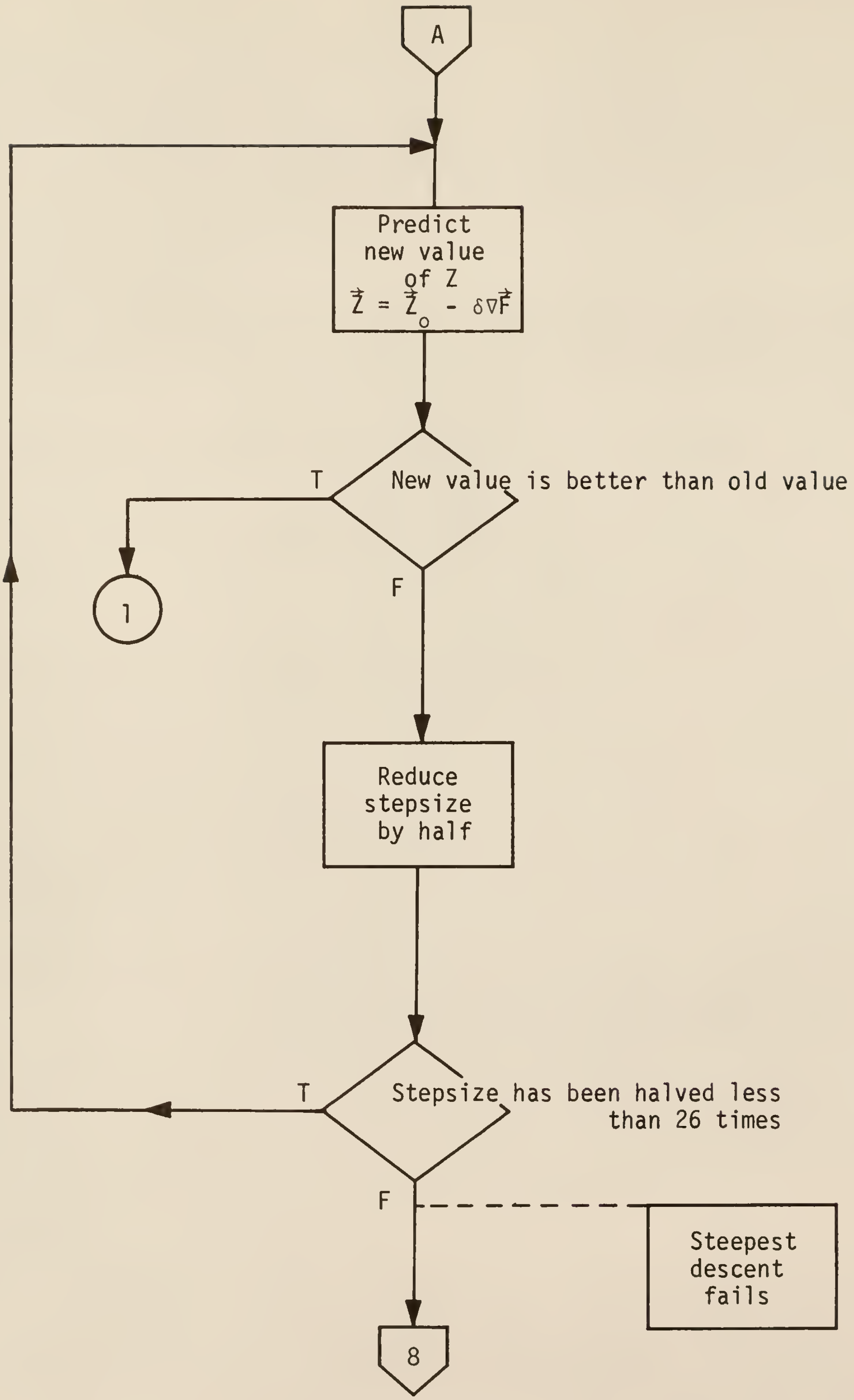
A
Predict
new value
of Z
$\vec{Z} = \vec{Z}_o - \delta\nabla\vec{F}$
T
New value is better than old value
1
F
Reduce
stepsize
by half
T
Stepsize has been halved less than 26 times
F
Steepest
descent
fails
8

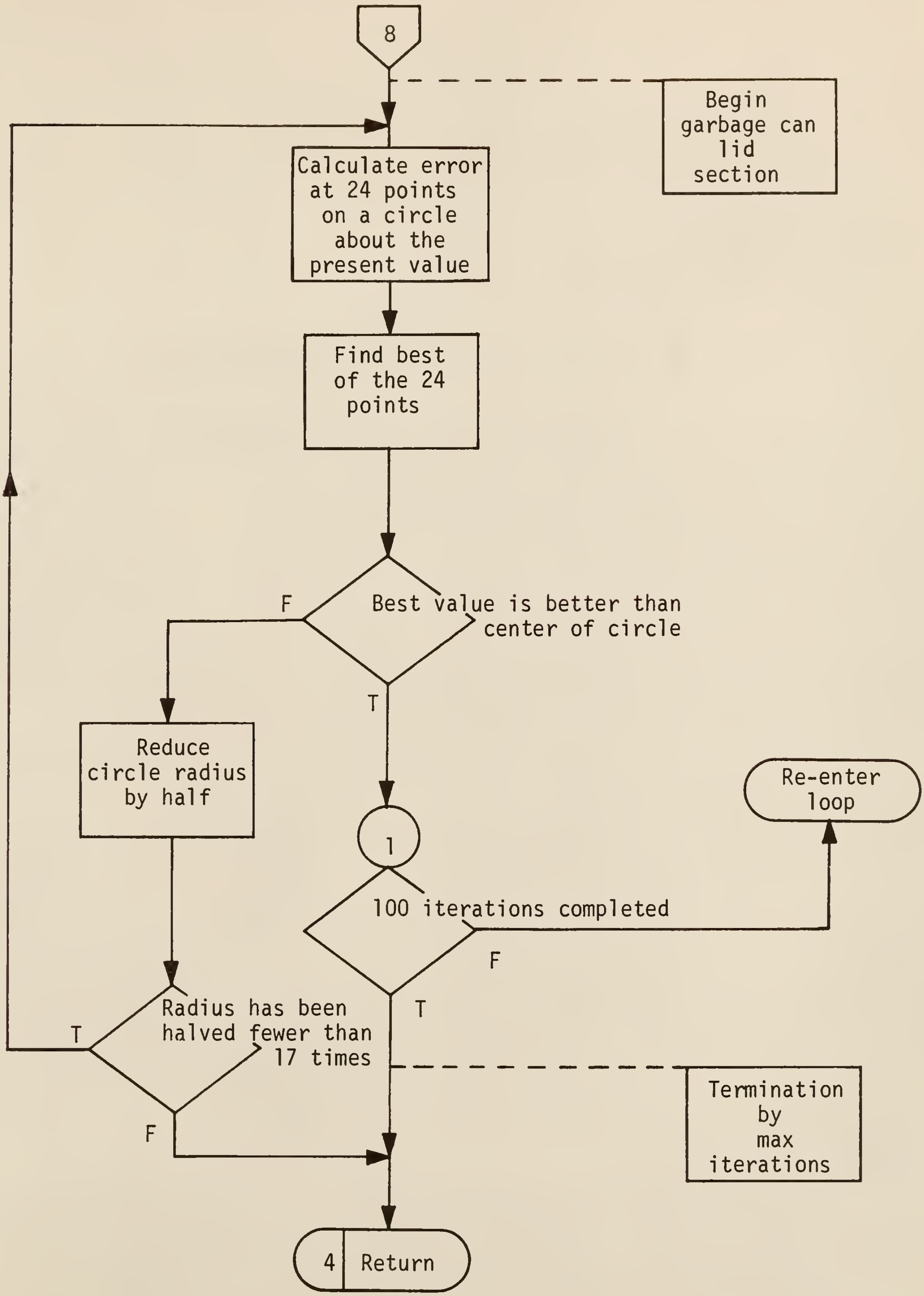
8
Begin garbage can lid section
Calculate error at 24 points on a circle about the present value
Find best of the 24 points
Best value is better than center of circle
F
T
Reduce circle radius by half
1
Re-enter loop
100 iterations completed
F
T
Radius has been halved fewer than 17 times
T
F
Termination by max iterations
4 Return

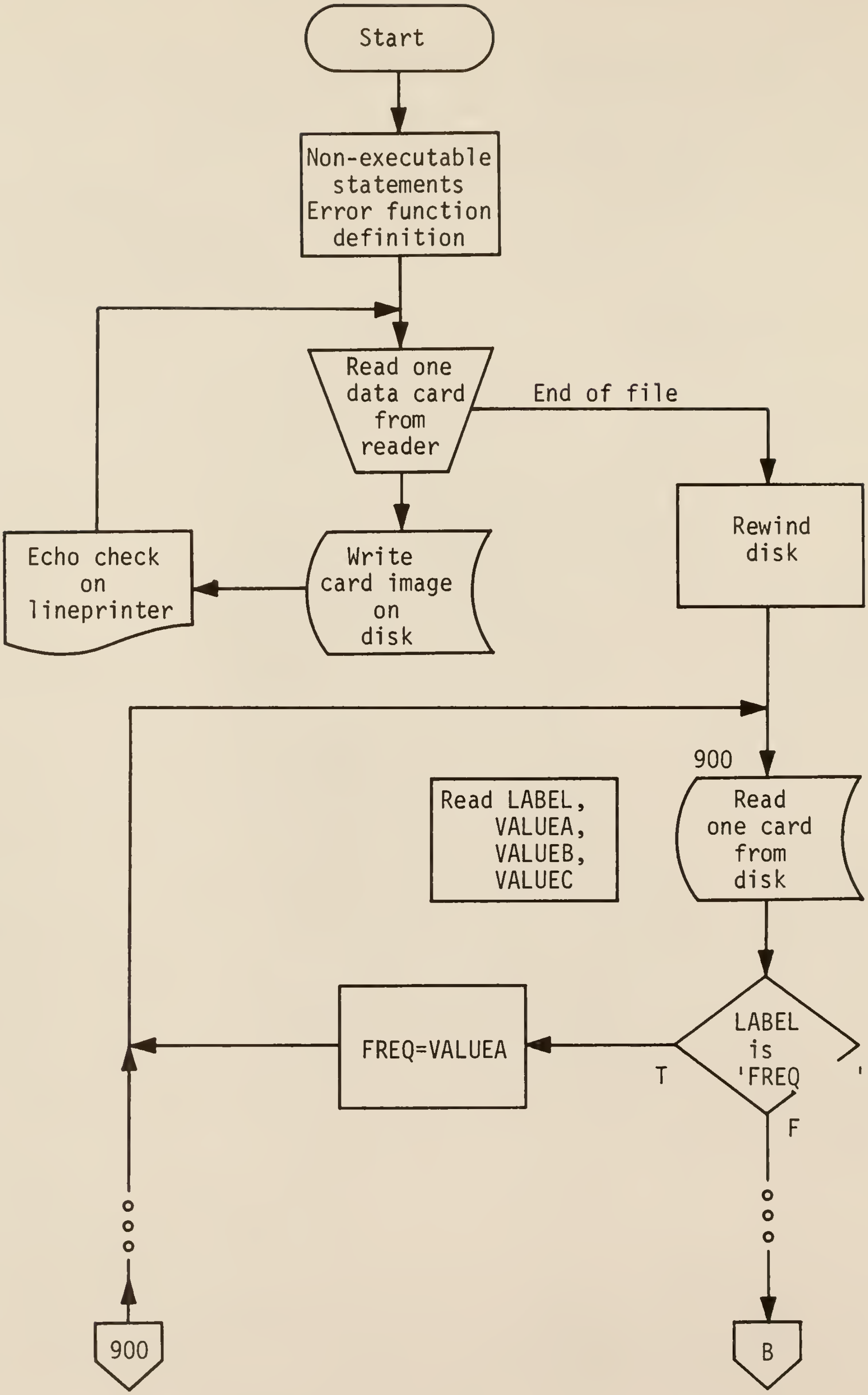

Start
Non-executable statements Error function definition
Read one data card from reader
End of file
Write card image on disk
Echo check on lineprinter
Rewind disk
900
Read one card from disk
Read LABEL, VALUEA, VALUEB, VALUEC
LABEL is 'FREQ'
T
F
FREQ=VALUEA
900
B

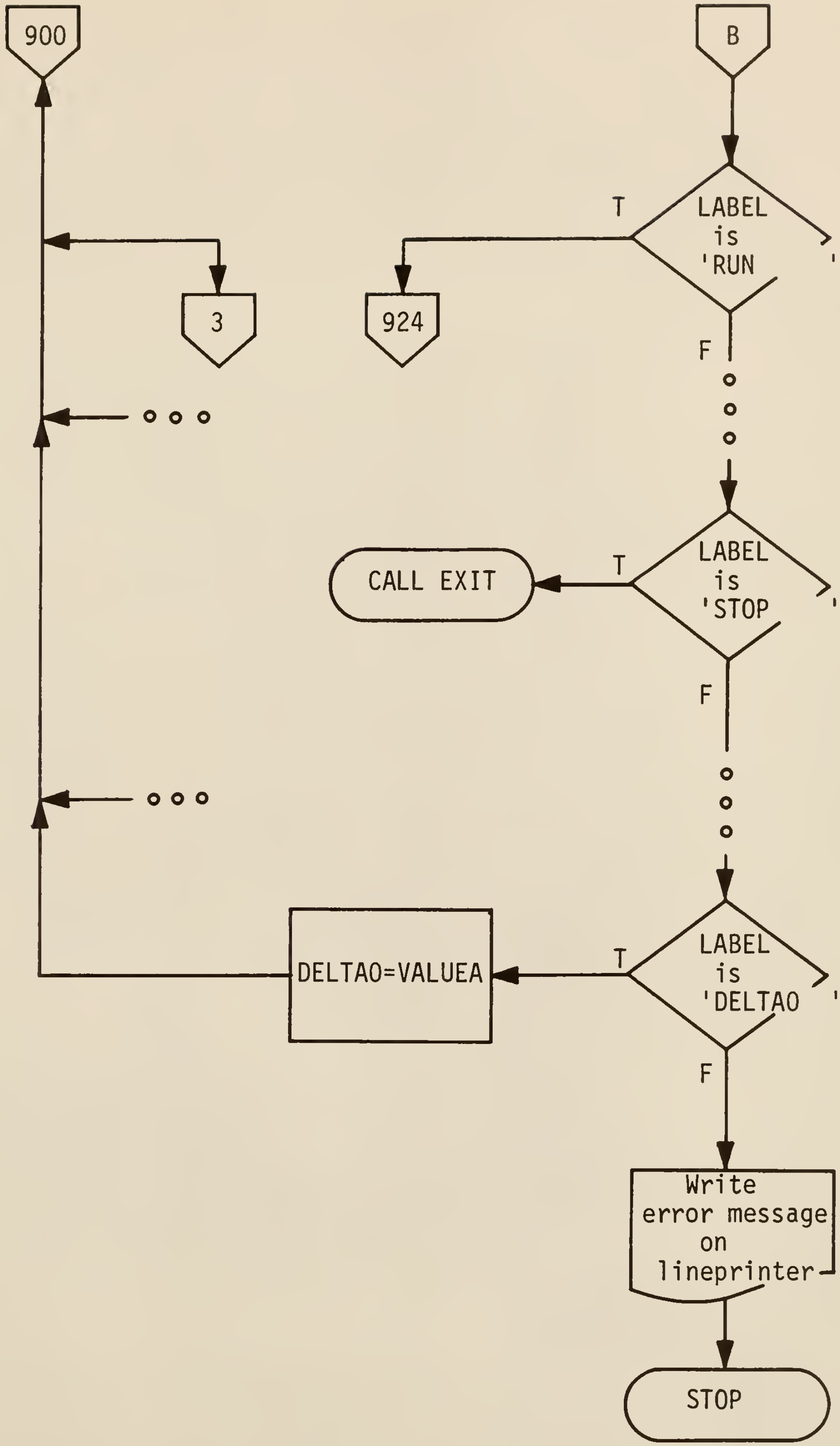
900
B
LABEL is 'RUN '
T
F
3
924
LABEL is 'STOP '
T
F
CALL EXIT
LABEL is 'DELTAO '
T
F
DELTAO=VALUEA
Write error message on lineprinter
STOP

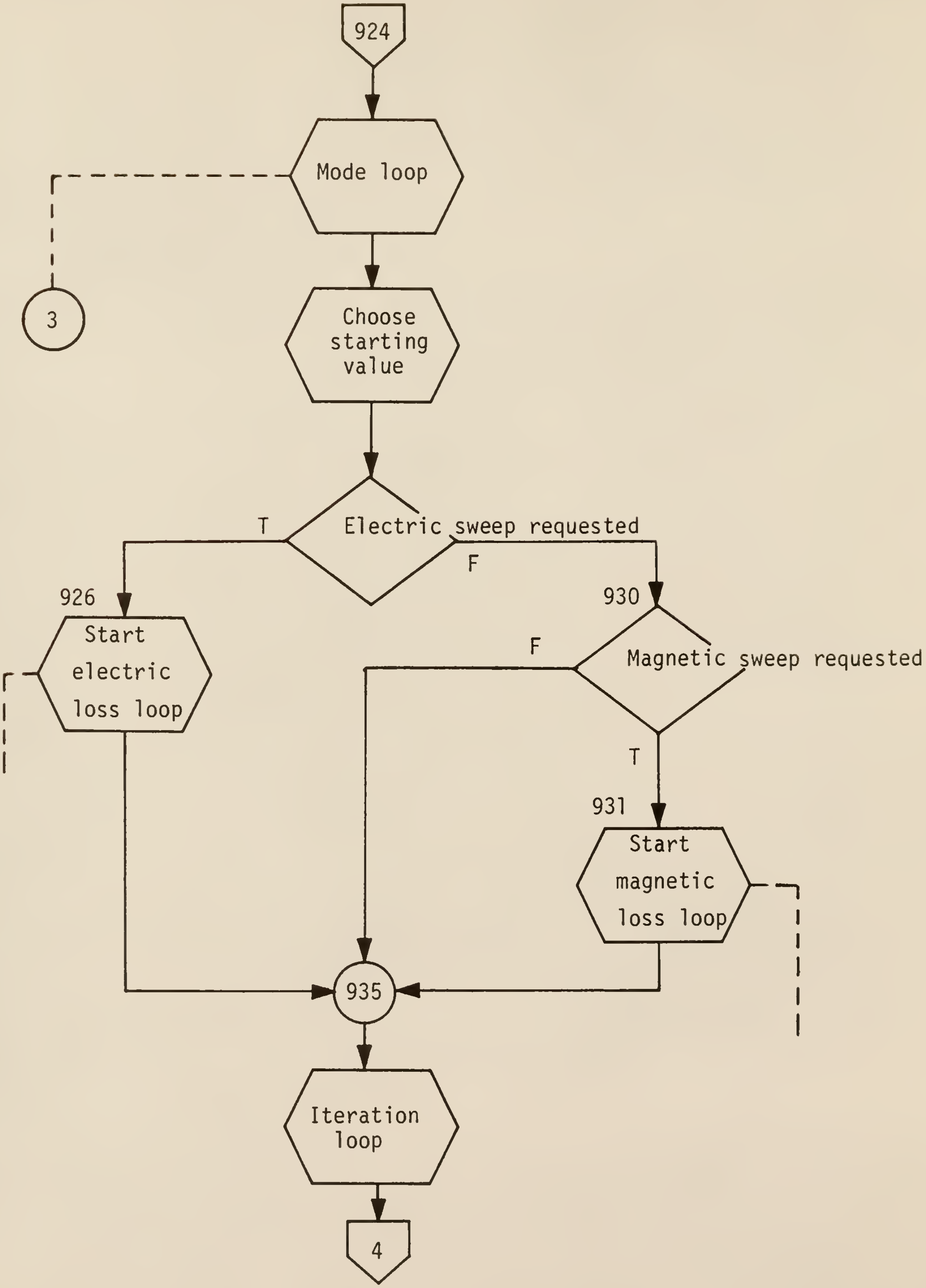
924
Mode loop
3
Choose starting value
Electric sweep requested
T
F
926
Start electric loss loop
930
Magnetic sweep requested
F
T
931
Start magnetic loss loop
935
Iteration loop
4

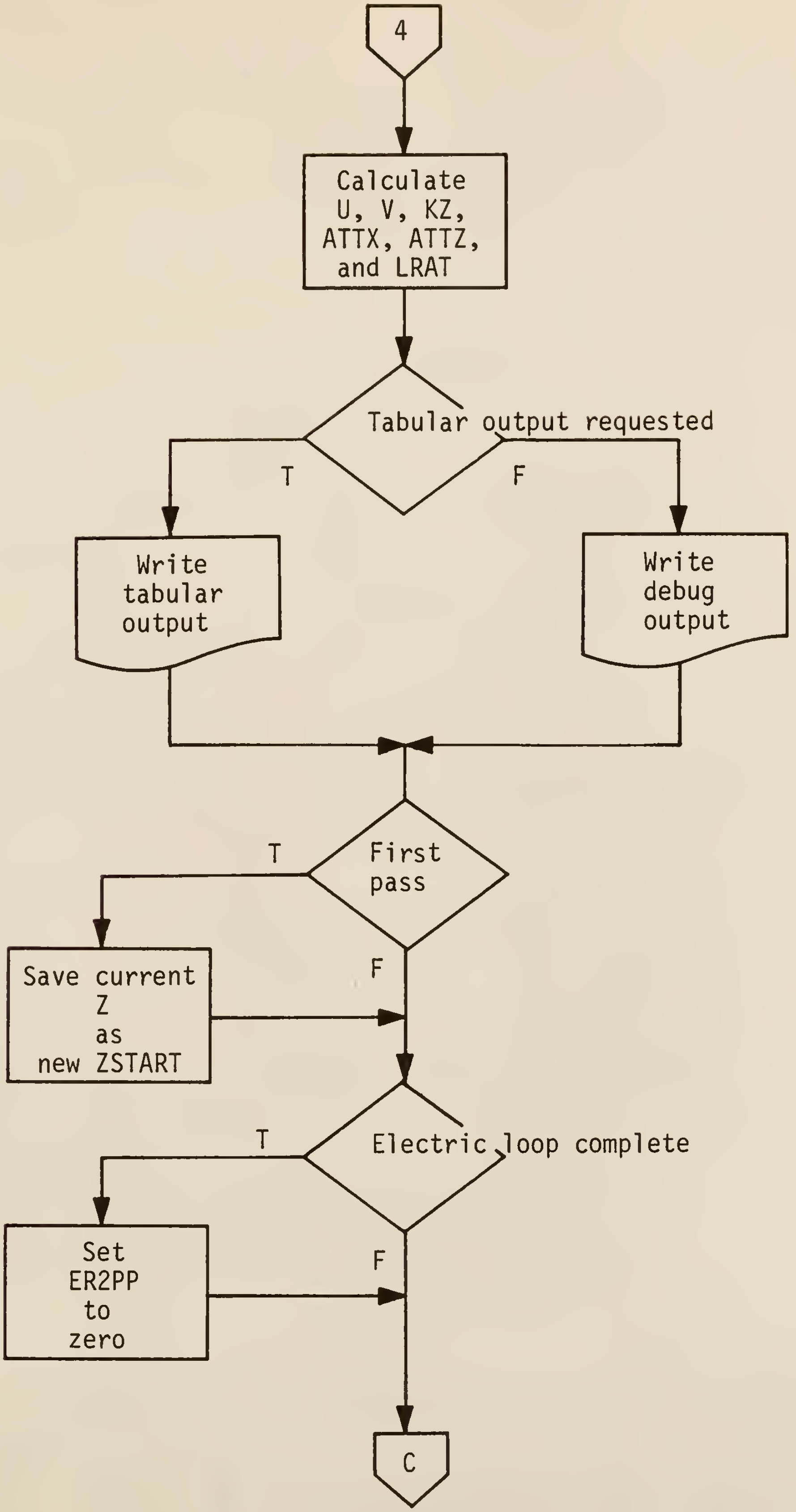
4
Calculate
U, V, KZ,
ATTX, ATTZ,
and LRAT
Tabular output requested
T
F
Write
tabular
output
Write
debug
output
First
pass
T
F
Save current
Z
as
new ZSTART
Electric loop complete
T
F
Set
ER2PP
to
zero
C

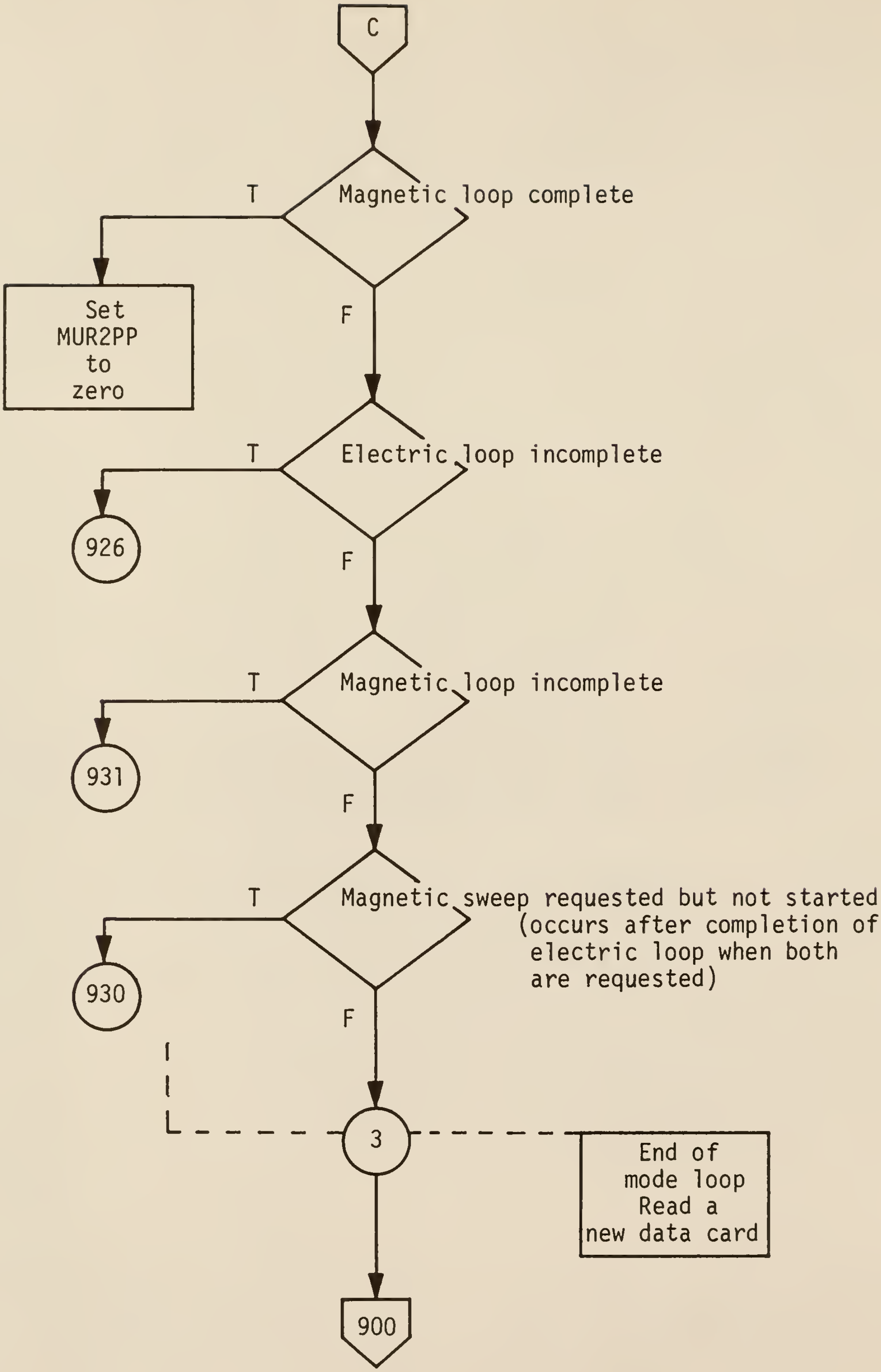
C
Magnetic loop complete
T
F
Set MUR2PP to zero
Electric loop incomplete
T
F
926
Magnetic loop incomplete
T
F
931
Magnetic sweep requested but not started (occurs after completion of electric loop when both are requested)
T
F
930
3
End of mode loop Read a new data card
900

APPENDIX B

PROGRAM LISTING

The "$JOB" card at the beginning of the listing and the statement numbers at the extreme left of some lines are included by the Waterloo FORTRAN (WATFOR) compiler and are not part of the FORTRAN card deck.

```
$JCF            JKS,RUN=CHECK,TIME=2,PAGES=50
C      PROGRAM PURPOSE: DETERMINATION OF THE PROPAGATION CONSTANTS OF
C                       SURFACE AND LEAKY WAVE TRANSVERSE MAGNETIC MODES
C                       OVER A GROUNDED DIELECTRIC SLAB INFINITELY LONG,
C                       INFINITELY WIDE, AND T CENTIMETERS THICK, WHERE
C                       BOTH THE DIELECTRIC SLAB AND SURROUNDING MEDIUM
C                       MAY HAVE EITHER ELECTRIC OR MAGNETIC LOSSES, OR
C                       BOTH.
C
C      ..................................................................
C
C                          REGION 1: SURROUNDING MEDIUM, HAVING RELATIVE
C                                    PERMITTIVITY ER1 AND RELATIVE PER-
C                                    MEABILITY MUR1.
C
C           X=T   -----------------------------------------------------
C
C                   REGION 2: DIELECTRIC SLAB HAVING RELATIVE PERMITTIV-
C                             ITY ER2 AND RELATIVE PERMEABILITY MUR2.
C           X=0   -----------------------------------------------------
C                 /////////////////////////////////////////////////////
C                             PERFECT CONDUCTOR
C
C
C          FIGURE INDICATING THE GEOMETRY OF THE SURFACE WAVEGUIDE.
C
C          THE CARTESIAN COORDINATE AXES ARE ORIENTED AS FOLLOWS: THE
C          Z-AXIS IS DIRECTED TO THE RIGHT; THE Y-AXIS IS DIRECTED OUT
C          OF THE PAGE; THE X-AXIS IS DIRECTED UPWARD, WITH X=0 AT THE
C          INTERFACE BETWEEN THE DIELECTRIC SLAB AND PERFECT CONDUCTOR.
C          THE STRUCTURE IS INFINITE IN EXTENT IN BOTH THE Y AND Z
C          DIRECTIONS; THE SLAB IS T CENTIMETERS THICK.
C
C      ..................................................................
C
C      BELOW THE SLAB-CONDUCTOR INTERFACE THE FIELDS ARE ZERO.
C
C      IN REGION 2 ( 0 <= X <= T ) THE FIELDS ARE
C
C              H(Y) =  -C2*U*COS(UX)*EXP(-J*KZ*Z)
C
C              E(X) =  -C2/(OMEGA*E2)*U*KZ*COS(UX)*EXP(-J*KZ*Z)
C
C              E(Z) =   C2/(J*OMEGA*E2)*U**2*SIN(UX)*EXP(-J*KZ*Z)
C
C      IN REGION 1 ( T <= X ) THE FIELDS ARE
C
C              H(Y) =   C1*V*EXP(-V*X)*EXP(-J*KZ*Z)
C
C              E(X) =   C1/(OMEGA*E1)*V*KZ*EXP(-V*X)*EXP(-J*KZ*Z)
C
C              E(Z) =  -C1/(J*OMEGA*E1)*V**2*EXP(-V*X)*EXP(-J*KZ*Z)
C
C
C      IN THE ABOVE EXPRESSIONS,
C
C      H(Y) IS THE Y-DIRECTED COMPONENT OF THE VECTOR H.
C
C      E(X) AND E(Z) ARE, RESPECTIVELY, THE X- AND Z-DIRECTED COMPONENTS
C          OF THE VECTOR E.
```

```
C
C     J IS THE IMAGINARY UNIT: J = CSQRT(-1.0).
C
C     OMEGA IS TWO TIMES PI TIMES FREQUENCY, THE "ANGULAR FREQUENCY".
C
C     E1 AND E2 ARE THE PERMITTIVITIES OF THE TWO REGIONS SPECIFIED.
C
C     C1 AND C2 ARE COMPLEX COEFFICIENTS WHICH DO NOT DEPEND ON X, Y,
C          OR Z, BUT DO DEPEND ON OMEGA, E1, E2, ETC.
C
C     U IS THE X-COMPONENT OF THE PROPAGATION CONSTANT IN REGION 2.
C
C     J*V IS THE X-COMPONENT OF THE PROPAGATION CONSTANT IN REGION 1.
C
C     KZ IS THE Z-COMPONENT OF THE PROPAGATION CONSTANT IN BOTH REGIONS.
C
C     ************************************************************************
C
C     THIS PROGRAM DETERMINES U, V, AND KZ FOR A GIVEN SET OF PARA-
C     METERS.  THE VALUES OF Z-DIRECTION ATTENUATION, X-DIRECTION
C     ATTENUATION (IN REGION 1), U, V, AND KZ, ALL EXPRESSED PER FREE
C     SPACE WAVELENGTH, PLUS THE RATIO OF GUIDE WAVELENGTH TO FREE SPACE
C     WAVELENGTH, ARE PRINTED OUT ALONG WITH THE PARAMETERS OF THE CASE.
C
C     ************************************************************************
C
C     DATA REQUIRED (NOTE THAT DEFAULT VALUES ARE PRESENT FOR ALL
C         PARAMETERS):
C
C     WITH THE EXCEPTION OF $DATA, ALL INPUT CARDS CONTAIN A CHARACTER
C         STRING TITLE IN COLUMNS 2 - 9, AND FLOATING POINT NUMBERS IN
C         COLUMNS 20-29, 40-49, AND 60-69; SOME OR ALL OF THE NUMBERS
C         MAY BE ZERO, AND TITLES MUST BE LEFT JUSTIFIED.
C
C     THE POSSIBLE INPUT CARDS ARE:
C
C     COLUMNS 2-9          20-29                  40-49                  60-69
C
C               FREQ       (FREQUENCY IN GHZ.)
C               SIZE       (THICKNESS IN CM.)
C               MODERNGE   (LOWER MODE NO.)     (UPPER MODE NO.) *SEE NOTE 1
C               ER1P       (REAL(ER1))
C               ER1PP      (-AIMAG(ER1))
C               ER2P       (REAL(ER2))
C               ER2PP      (-AIMAG(ER2))
C               MUR1P      (REAL(MUR1))
C               MUR1PP     (-AIMAG(MUR1))
C               MUR2P      (REAL(MUR1))
C               MUR2PP     (-AIMAG(MUR2))
C               RATIO      (T/LAMBDA_0)
C               ZSTART     (REAL(Z))            (AIMAG(Z)) *SEE NOTE 2
C               $DATA      (NO. OF VALUES) *SEE NOTE 3
C               DELTA      (DELTA)
C               DEBUG
C               TABLE
C               ELECTRIC
C               MAGNETIC
C               NOELECTR
C               NOMAGNET
C               RUN
```

```
C             STOP
C
C      NOTE 1: THESE VALUES ARE CONVERTED TO INTEGERS--A FLOATING POINT
C              NUMBER SLIGHTLY LARGER THAN THE INTEGER SHOULD BE USED TO
C              ENSURE THAT THE PROPER INTEGER WILL BE OBTAINED.  THE
C              INTEGERS MUST BE EVEN.
C
C      NOTE 2: Z HERE IS THE PROGRAM VARIABLE U*T, NOT THE COORDINATE
C              VALUE.  REAL(ZSTART) SHOULD BE >= 0 TO AVOID AN UNENDING
C              LOOP WITHIN ZTAN.
C
C      NOTE 3: THIS VALUE IS ALSO CONVERTED TO AN INTEGER, SO THE PRE-
C              CAUTION OF NOTE 1 APPLIES.  THE INTEGER MAY NOT BE LARGER
C              THAN 75 UNLESS $DATA IS DIMENSIONED ACCORDINGLY.  IMMEDIA-
C              TELY FOLLOWING THIS CARD MUST BE A CARD OR CARDS CONTAIN-
C              ING THE VALUES OF $DATA IN 10F8.0 FORMAT.
C
C      EITHER FREQ AND SIZE OR RATIO MAY BE USED.  IF FREQ AND SIZE ARE
C              PROVIDED, RAT IS CALCULATED FROM THEM.
C
C      ER1P THRU MUR2PP SET THE VALUE OF THAT PARAMETER.
C
C      DELTA SETS THE INITIAL INCREMENT VALUE FOR STEEPEST DESCENT.
C
C      $DATA DETERMINES THE VALUES OF ER2PP OR MUR2PP DURING PARAMETER
C              SWEEPS.
C
C      ZSTART PROVIDES A STARTING VALUE OF THE VARIABLE ITERATED UPON
C              FOR THE FIRST PASS WHICH MAY BE USED TO OVERRIDE THE VALUE
C              CALCULATED WITHIN THE PROGRAM IF NECESSARY.
C
C      ELECTRIC/NOELECTRIC CONTROLS WHETHER OR NOT ELECTRIC LOSSES ARE
C              SWEPT.
C
C      MAGNETIC/NOMAGNETIC CONTROLS WHETHER OR NOT MAGNETIC LOSSES ARE
C              SWEPT.  IF BOTH TYPES OF SWEEP ARE SPECIFIED THE ELECTRIC
C              SWEEP IS PERFORMED FIRST.
C
C      TABLE PRODUCES TABULAR OUTPUT; DEBUG PRODUCES AN OUTPUT WITH
C              THE DERIVATIVES, ERROR VALUES, AND Z VALUES TO ASSIST IN
C              DEBUGGING.
C
C      UPON ENCOUNTERING THE RUN CARD THE PROGRAM IS EXECUTED USING THE
C              PARAMETERS IN EFFECT AT THAT TIME.
C
C
C      UPON ENCOUNTERING THE STOP CARD SUBROUTINE EXIT IS EXECUTED.
C
C      UPON ENCOUNTERING ANY TITLE NOT LISTED IN THE ARRAY LABEL, THE
C              UNDECODEABLE TITLE IS PRINTED OUT AND EXECUTION IS
C              ABANDONED.
C
C      ********************************************************************
C
       COMPLEX Z, ER, K1SQ, K2SQ, J, U, V, CSQRT, KZ, ZTAN
       COMPLEX DELF, ZO
       COMPLEX ZCK, STORE
       COMPLEX ZSTART
       COMPLEX DZ(24)
       REAL MUR1P, MUR1PP, MUR2P, MUR2PP
```

```
      REAL LAMBDA, LRAT
      INTEGER FLAG
      DIMENSION ERR(24)
      DIMENSION CHAR(20)
      DIMENSION INVARI(2), LABEL(46), $DATA(75)
      COMMON IN, IERR
      DATA LABEL /'FREQ', '    ', 'SIZE', '    ', 'MODE', 'RNGE',
     &    'ELEC', 'TRIC', 'MAGN', 'ETIC', 'ER1P', '    ', 'ER1P', 'P   ',
     &,   'ER2P', '    ', 'ER2P', 'P   ', 'MUR1', 'P   ', 'MUR1', 'PP  ',
     &,   'MUR2', 'P   ', 'MUR2', 'PP  ', 'RUN ', '    ', 'RATI', 'O   ',
     &,   'ZSTA', 'RT  ', 'DEBU', 'G   ', 'TABL', 'E   ', 'NDEL', 'FCTR',
     &,   'NOMA', 'GNET', 'STOP', '    ', '$DAT', 'A   ', 'DELT', 'A   '
     &/
C
C     DEFAULT PARAMETERS
C
      DATA FGHZ/3.0/, T/1.0/, NL/1/, NF/1/, ER1P/1.0/, ER1PP/0.0/,
     &  ER2P/2.0/, ER2PP/0.0/, MUR1P/1.0/, MUR1PP/0.0/, MUR2P/1.0/,
     &  MUR2PP/0.0/
      DATA $DATA /0.0, 0.2, 0.3, 0.4, 0.5, 0.6, 0.7, 0.8, 0.9, 1.0, 1.2,
     & 1.4, 1.6, 1.8, 2.0, 2.5, 3.0, 3.5, 4.0, 4.5, 5.0, 5.5, 6.0,
     & 52*0.0                                                          /
C
C     DEFINE FUNCTION ITERATED UPON
C
      F(Z) = CABS(Z-ER*RAT*TWOPI*CSQRT((K2SQ-K1SQ)/(ER**2+ZTAN(Z)**2)))
C
C     INITIALIZE CONSTANTS AND SWITCHES
C
      IESW = 0
      IMSW = 0
      IZSW = 0
      NPASS = 0
      IFORM = 1
      NCT = 23
      J=(0., 1.)
      TWOPI=2.*3.1415927
      PI=3.1415927
      DELTAC = 0.05*PI
      RAT = FGHZ*T/29.9793
      WRITE (3, 9490)
      WRITE (3, 9491)
      WRITE (3, 9492)
      WRITE (3, 9493)
      WRITE (3, 8002)
C
C     IF THIS PROGRAM IS USED IN FORTRAN IV, A DD CARD MUST BE SUPPLIED
C    &      FOR UNIT 4
C
  800 READ (1, 8000, END=801) (CHAR(I), I = 1, 20)
      WRITE (4, 8000) (CHAR(I), I = 1, 20)
      WRITE (3, 8001) (CHAR(I), I = 1, 20)
      GO TO 800
  801 REWIND 4
  900 READ (4, 9099) INVARI(1), INVARI(2), VALUEA, VALUEB, VALUEC
C
C     MORE TESTS MAY BE ADDED IF THE DATA STATEMENT LIST IS ADDED TO
C    &      AND THE DIMENSION ARGUMENT OF LABEL IS INCREASED ACCORDINGLY
C
      IF ( INVARI(1) .EQ. LABEL(01) .AND. INVARI(2) .EQ. LABEL(02) )
```

```
     &                                                           GO TO 901
      IF ( INVARI(1) .EQ. LABEL(03) .AND. INVARI(2) .EQ. LABEL(04) )
     &                                                           GO TO 902
      IF ( INVARI(1) .EQ. LABEL(05) .AND. INVARI(2) .EQ. LABEL(06) )
     &                                                           GO TO 903
      IF ( INVARI(1) .EQ. LABEL(07) .AND. INVARI(2) .EQ. LABEL(08) )
     &                                                           GO TO 904
      IF ( INVARI(1) .EQ. LABEL(09) .AND. INVARI(2) .EQ. LABEL(10) )
     &                                                           GO TO 905
      IF ( INVARI(1) .EQ. LABEL(11) .AND. INVARI(2) .EQ. LABEL(12) )
     &                                                           GO TO 906
      IF ( INVARI(1) .EQ. LABEL(13) .AND. INVARI(2) .EQ. LABEL(14) )
     &                                                           GO TO 907
      IF ( INVARI(1) .EQ. LABEL(15) .AND. INVARI(2) .EQ. LABEL(16) )
     &                                                           GO TO 908
      IF ( INVARI(1) .EQ. LABEL(17) .AND. INVARI(2) .EQ. LABEL(18) )
     &                                                           GO TO 909
      IF ( INVARI(1) .EQ. LABEL(19) .AND. INVARI(2) .EQ. LABEL(20) )
     &                                                           GO TO 910
      IF ( INVARI(1) .EQ. LABEL(21) .AND. INVARI(2) .EQ. LABEL(22) )
     &                                                           GO TO 911
      IF ( INVARI(1) .EQ. LABEL(23) .AND. INVARI(2) .EQ. LABEL(24) )
     &                                                           GO TO 912
      IF ( INVARI(1) .EQ. LABEL(25) .AND. INVARI(2) .EQ. LABEL(26) )
     &                                                           GO TO 913
      IF ( INVARI(1) .EQ. LABEL(27) .AND. INVARI(2) .EQ. LABEL(28) )
     &                                                           GO TO 924
      IF ( INVARI(1) .EQ. LABEL(29) .AND. INVARI(2) .EQ. LABEL(30) )
     &                                                           GO TO 914
      IF ( INVARI(1) .EQ. LABEL(31) .AND. INVARI(2) .EQ. LABEL(32) )
     &                                                           GO TO 915
      IF ( INVARI(1) .EQ. LABEL(33) .AND. INVARI(2) .EQ. LABEL(34) )
     &                                                           GO TO 916
      IF ( INVARI(1) .EQ. LABEL(35) .AND. INVARI(2) .EQ. LABEL(36) )
     &                                                           GO TO 917
      IF ( INVARI(1) .EQ. LABEL(37) .AND. INVARI(2) .EQ. LABEL(38) )
     &                                                           GO TO 918
      IF ( INVARI(1) .EQ. LABEL(39) .AND. INVARI(2) .EQ. LABEL(40) )
     &                                                           GO TO 919
      IF ( INVARI(1) .EQ. LABEL(41) .AND. INVARI(2) .EQ. LABEL(42) )
     &                                                           GO TO 920
      IF ( INVARI(1) .EQ. LABEL(43) .AND. INVARI(2) .EQ. LABEL(44) )
     &                                                           GO TO 921
      IF ( INVARI(1) .EQ. LABEL(45) .AND. INVARI(2) .EQ. LABEL(46) )
     &                                                           GO TO 922
C
C     IF LABEL IS NOT IN LIBRARY, WRITE A MESSAGE AND STOP
C
      WRITE (3, 9098) INVARI(1), INVARI(2)
      WRITE (3, 9001)
      WRITE (3, 9002)
      WRITE (3, 9003)
      WRITE (3, 9004)
      STOP
  901 FGHZ = VALUEA
      RAT = FGHZ*T/29.9793
      GO TO 900
  902 T = VALUEA
      RAT = FGHZ*T/29.9793
      GO TO 900
```

```
  903 NL = VALUEA + 1.001
      NH = VALUEB + 1.001
      GO TO 900
  904 IESW = 1
      GO TO 900
  905 INSW = 1
      GO TO 900
  906 ER1P = VALUEA
      GO TO 900
  907 ER1PP = VALUEA
      GO TO 900
  908 ER2P = VALUEA
      GO TO 900
  909 ER2PP = VALUEA
      GO TO 900
  910 MUR1P = VALUEA
      GO TO 900
  911 MUR1PP = VALUEA
      GO TO 900
  912 MUR2P = VALUEA
      GO TO 900
  913 MUR2PP = VALUEA
      GO TO 900
  914 RAT = VALUEA
      GO TO 900
  915 ZSTART = VALUEA + J*VALUEB
      IZSW = 1
      GO TO 900
  916 IFORM = 0
      GO TO 900
  917 IFORM = 1
      GO TO 900
  918 IESW = 0
      GO TO 900
  919 INSW = 0
      GO TO 900
  920 CALL EXIT
  921 NCT = VALUEA
      READ (4, 9097) (IDATA(I), I = 1, NCT)
      GO TO 900
  922 DELTAO = VALUEA
      GO TO 900
  924 ER=(ER2P-J*ER2PP)/(ER1P-J*ER1PP)
      K1SQ = (MUR1P-J*MUR1PP)*(ER1P-J*ER1PP)
      K2SQ = (MUR2P-J*MUR2PP)*(ER2P-J*ER2PP)
      DO 3 I = NL, NH, 2
      IM = I - 1
C
C     CHOOSE STARTING VALUE FOR Z
C
      IF ( IZSW .EQ. 0 )  GO TO 950
      Z = ZSTART
      IZSW = 0
      GO TO 925
C
C     TEST FOR CUTOFF
C
  950 RADIUS = TWOPI*RAT*SQRT(MUR2P*ER2P-MUR1P*ER1P)
      IF ( RADIUS .GE. IM*PI/2. )  GO TO 955
      Z = (IM - 1 + 0.1)*PI/2. + J*0.5
```

```
          GO TO 925
      955 IF ( RADIUS  .GE. (IN+1)*PI/2. )  GO TO 960
          Z = 0.9*RADIUS + 0.1*IN*PI/2.
          GO TO 925
      960 Z = (IN+0.9)*PI/2.
      925 NPASS = 1
          IELEC = 0
          IMAG = 0
          IF ( ILSW .EQ. 0 )  GO TO 930
C
C         SWEEP ELECTRIC LOSSES
C
      926 IELEC = IELEC + 1
          ER2PP = $DATA(IELEC)
          K2SQ = (MUR2P-J*MUR2PP)*(ER2P-J*ER2PP)
          ER=(ER2P-J*ER2PP)/(ER1P-J*ER1PP)
          GO TO 935
      930 IF ( IMSW .EQ. 0 )  GO TO 935
          IF ( NPASS .GT. 1 )  Z = ZSTART
C
C         SWEEP MAGNETIC LOSSES
C
      931 IMAG = IMAG + 1
          MUR2PP = $DATA(IMAG)
          K2SQ = (MUR2P-J*MUR2PP)*(ER2P-J*ER2PP)
      935 CONTINUE
          IF ( IFORM .EQ. 0 )  WRITE (3, 9981)
C
C         ITERATION BEGINS HERE
C
          DO 1 K = 1, 100
          FLAG = 0
C
C         TRY LINEAR ITERATION AND CHECK WHETHER OR NOT IT IS USEFUL
C
          ZCK = ER*RAT*TWOPI*CSQRT((K2SQ-K1SQ)/(ER**2+ZTAN(Z)**2))
          IF ( IERR .EQ. 1 .AND. IFORM .EQ. 0 )  WRITE (3, 9401)
          FERR = F(Z)
          FCKERR = F(ZCK)
          IF ( FCKERR .GT. FERR  .OR.  CABS(Z-ZCK) .GT. 0.03*CABS(Z) )
         &                                                       GO TO 7
          STORE = ZCK
          ZCK = Z
          Z = STORE
          FERR = F(Z)
          FCKERR = F(ZCK)
          FLAG = 1
        7 IF ( FERR .LT. 1.E-07*RAT .AND. IFORM .EQ. 0 )  WRITE (3, 9940)
          IF ( FERR .LT. 1.E-07*RAT )  GO TO 4
C
C         GET DERIVATIVES FOR STEEPEST DESCENT
C
          FPX = (F(Z+0.0001)-F(Z-0.0001))/0.0002
          FPY = (F(Z+J*0.0001)-F(Z-J*0.0001))/0.0002
          DELF = FPX + J*FPY
          DELMAG = CABS(DELF)
C
C         IF DELMAG IS ZERO, RESORT TO THE GARBAGE CAN LID APPROACH
C
          IF ( DELMAG .EQ. 0. )  GO TO 8
```

```
      RZ = REAL(Z)
      AIZ = AIMAG(Z)
      IF ( IFORM .EQ. 0 )  WRITE (3, 9982) FERR, FLAG, FCKERR, RZ, AIZ,
     &                                    FFX, FFY
      IF ( DELMAG .GT. 1.0 )  DELF = DELF/DELMAG
      DELTA = DELTAO
      KC = 0
      ZO = Z
C
C     TRY STEEPEST DESCENT
C
    6 Z = ZO - DELTA*DELF
      IF ( F(Z) .LT. FERR )  GO TO 1
      DELTA = DELTA/2.
      KC = KC + 1
      IF ( KC .LE. 25 )  GO TO 6
      Z = ZO
      FLAG = FLAG + 2
C
C     BEGIN GARBAGE CAN LID ATTEMPT
C
    8 FLAG = FLAG + 2
      KC2 = 0
      DELZ = 0.0001
      IF (FERR .LT. DELZ )  DELZ = FERR
  310 DO 300 IDZ = 1, 24
      THETA = TWOPI*(IDZ-1)/24
      DZ(IDZ) = DELZ*(COS(THETA)+J*SIN(THETA))
      ERR(IDZ) = F(Z+DZ(IDZ))
  300 CONTINUE
      IDZ = 1
      IMIN = 1
      ERRMIN = ERR(1)
  301 IDZ = IDZ + 1
      IF ( ERR(IDZ) .LT. ERRMIN )  IMIN = IDZ
      IF ( ERR(IDZ) .LT. ERRMIN )  ERRMIN = ERR(IMIN)
      IF ( IDZ .LT. 24 )  GO TO 301
      FIMIN = IMIN
      IF ( ERRMIN .LT. FERR )  GO TO 302
      DELZ = DELZ/2
      KC2 = KC2 + 1
      FKC2 = KC2
      IF ( KC2 .LE. 17 )  GO TO 310
      RZ = REAL(Z)
      AIZ = AIMAG(Z)
      IF ( IFORM .EQ. 1 )  GO TO 4
      WRITE (3, 9982) FERR, FLAG, FCKERR, RZ, AIZ, FIMIN, FKC2
      WRITE (3, 9991)
      GO TO 4
  302 Z = Z + DZ(IMIN)
      IF ( IERR .EQ. 1 .AND. IFORM .EQ. 0 )  WRITE (3, 9401)
      RZ = REAL(Z)
      AIZ = AIMAG(Z)
      IF ( IFORM .EQ. 1 )  GO TO 1
      WRITE (3, 9982) FERR, FLAG, FCKERR, RZ, AIZ, FIMIN, FKC2
    1 CONTINUE
C
C     END OF ITERATION LOOP
C
      WRITE (3, 9980)
```

```
    4 CONTINUE
      U = Z/RAT
      V = Z*ZTAN(Z)/(ER*RAT)
      KZ = CSQRT(4.0*PI*PI*(MURIF-J*MURIFF)*(ERIF-J*ERIFP) + V**2)
      URAT = REAL(KZ)/TWOPI
      ATTX=8.685889638*REAL(V)
      ATTZ=-8.685889638*AIMAG(KZ)
      C5=REAL(U)
      C6=AIMAG(U)
      C7=REAL(V)
      C8=AIMAG(V)
      C9=REAL(KZ)
      C10=AIMAG(KZ)
C
C     CHOOSE OUTPUT FORMAT HERE
C
      IF ( IFORM .EQ. 1 )  GO TO 400
      X=REAL(Z)
      Y=AIMAG(Z)
      WRITE (3, 9989)
      WRITE (3, 9988) K, KC, DELTA, X, Y, ERRZ, DELMAG
      XCK = REAL(ZCK)
      YCK = AIMAG(ZCK)
      WRITE (3, 9985)
      WRITE (3, 9984) XCK, YCK
      IF ( IERR .EQ. 1 .AND. IFORM .EQ. 0 )  WRITE (3, 9401)
      FA=REAL(Z*ZTAN(Z) )
      FB=AIMAG(Z*ZTAN(Z))
      FC = REAL(ER*CSQRT((TWOPI*RAT)**2*(K2SQ-K1SQ)-Z**2))
      FD = AIMAG(ER*CSQRT((TWOPI*RAT)**2*(K2SQ-K1SQ)-Z**2))
      WRITE (3, 9987) FA, FB, FC, FD
      WRITE (3, 9992) FERR, FCKERR
      WRITE (3, 9996) IN
      WRITE (3, 9995) ERIF, ERIFP, MURIF, MURIFP, ER2P, ER2FP, MUR2P,
     &MUR2FP, RAT, URAT
      WRITE (3, 9994) C5, C6, C7, C8, C9, C10, ATTX, ATTZ
      GO TO 450
  400 IF ( NPASS .GT. 1 )  GO TO 402
      WRITE (3, 9499) IN, RAT
      WRITE (3, 9498) ERIF, ERIFF, MURIF, MURIFP, ER2P, ER2FP, MUR2P,
     &                MUR2FP
      IF ( IELEC .GT. 0 .OR. IMAG .GT. 0 )  GO TO 402
      WRITE (3, 9497) URAT, ATTZ, ATTX, C5, C6, C7, C8, C9, C10
      GO TO 450
  402 IF ( IELEC .EQ. 0 .OR. NPASS .GT. NCT )  GO TO 404
      IF ( IELEC .GT. 1 )  GO TO 403
      WRITE (3, 9496)
  403 WRITE (3, 9495) ER2FP, URAT, ATTZ, ATTX, C5, C6, C7, C8, C9, C10
      GO TO 450
  404 IF ( IMAG .EQ. 1 )  WRITE (3, 9494)
      WRITE (3, 9495) MUR2FP, URAT, ATTZ, ATTX, C5, C6, C7, C8, C9, C10
  450 IF ( NPASS .EQ. 1 )  ZSTART = Z
      NPASS = NPASS + 1
      IF ( IELEC .EQ. NCT )  ER2FP = 0.0
      IF ( IMAG .EQ. NCT )  MUR2FP = 0.0
      IF ( IELEC .GT. 0 .AND. IELEC .LT. NCT )  GO TO 926
      IF ( IMAG .GT. 0 .AND. IMAG .LT. NCT )  GO TO 931
      IF ( INSW .EQ. 1 .AND. IMAG .EQ. 0 )  GO TO 930
    3 CONTINUE
      GO TO 900
```

```
      C
      C      END OF MODE LOOP --- READ A NEW DATA CARD
      C
274    8000 FORMAT ( 20A4 )
275    8001 FORMAT (5X, 20A4)
276    8002 FORMAT ('1', 5X, 'ECHO CHECK:', /// )
277    9001 FORMAT ('1DESCRIPTION OF DATA INPUT CARDS:', ///, ' DEFAULT VALUES
          & STORED IN PROGRAM ARE:',T51, 'FREQUENCY = 3.0 GHZ.', T81, 'THICKN
          &ESS = 1 CM.', /, T51, 'TM(0) MODE ONLY', T81, 'ER1P = 1.0', /,
          &T51, 'ER1PP = 0.0', T81, 'ER2P = 2.0', /, T51, 'ER2PP = 0.0', T81,
          &'MUR1P = 1.0', /, T51, 'MUR1PP = 0.0', T81, 'MUR2P = 1.0', /,
          &T51, 'MUR2PP = 0.0', T81, 'DELTA = 0.05*PI', //,T21, '#DATA = 0.0,
          & 0.2, 0.3, 0.4, 0.5, 0.6, 0.7, 0.8, 0.9, 1.0, 1.2, 1.4,', /, T29,
          &'1.6, 1.8, 2.0, 2.5, 3.0, 3.5, 4.0, 4.5, 5.0, 5.5, 6.0', ///,
          &' WITH THE EXCEPTION OF #DATA, ALL INPUT CARDS CONTAIN A CHARACTER
          & STRING TITLE IN COLUMNS 2-9, AND FLOATING POINT NUMBERS IN', /,
          &' COLUMNS 20-29, 40-49, AND 60-69; SOME OR ALL OF THE NUMBERS MAY
          &BE ZERO; TITLES MUST BE LEFT JUSTIFIED.', //,
          &' THE POSSIBLE INPUT CARDS ARE:', //,
          &' COLUMNS  2-9', T26, '20-29', T56, '40-49', T86, '60-69', //,
          &T11, 'FREQ', T26, '(FREQUENCY IN GHZ.)', /, T11, 'SIZE', T26,
          &'(THICKNESS IN CM.)', /, T11, 'MODERNGE', T26, '(LOWER MODE NO.)',
          &T56, '(UPPER MODE NO.)  * SEE NOTE 1', /, T11, 'ER1P', T26, '(REAL
          &(ER1))', /, T11, 'ER1PP', T26, '(-AIMAG(ER1))'  )
278    9002 FORMAT (T11, 'ER2P', T26, '(REAL(ER2))',/, T11, 'ER2PP', T26, '(-A
          &IMAG(ER2))', /, T11, 'MUR1P', T26, '(REAL(MUR2))', /, T11, 'MUR2PP
          &', T26, '(-AIMAG(MUR2))', /, T11, 'MUR2P', T26, '(REAL(MUR2))', /,
          &T11, 'MUR2PP', T26, '(-AIMAG(MUR2))', /, T11, 'RATIO', T26, '(T/LA
          &MBDA_0)', /, T11, 'ZSTART', T26, '(REAL(ZSTART))', T56, '(AIMAG(ZS
          &TART))  * SEE NOTE 2', /, T11, '#DATA', T26, '(NO. OF VALUES)  * S
          &EE NOTE 3', /, T11, 'DELTA', T26, '(DELTA)', /, T11, 'DEBUG', /,
          &T11, 'TABLE', /, T11, 'ELECTRIC', /, T11, 'MAGNETIC', /, T11,
          &'NOELECTR', /, T11, 'NOMAGNET', /, T11, 'RUN', /, T11, 'STOP', /,
          &'1NOTE 1: THESE VALUES ARE CONVERTED TO INTEGERS--A FLOATING POINT
          & NUMBER SLIGHTLY LARGER THAN THE PROPER INTEGER SHOULD BE', /,
          &' USED TO ENSURE THAT THE PROPER INTEGER WILL BE OBTAINED.  THE IN
          &TEGERS MUST BE EVEN.', //,
          &' NOTE 2: Z HERE IS THE PROGRAM VARIABLE, NOT THE COORDINATE VALUE
          &.  REAL(ZSTART) SHOULD BE >= 0 TO AVOID AN UNENDING LOOP', /,
          &' WITHIN THE FUNCTION ZTAN.', //,
          &' NOTE 3: THIS VALUE IS ALSO CONVERTED TO AN INTEGER, SO THE PRECA
          &UTION OF NOTE 1 APPLIES.  THE INTEGER MAY NOT BE LARGER'       )
279    9003 FORMAT (' THAN 75 UNLESS #DATA IS DIMENSIONED ACCORDINGLY.  IMMEDI
          &ATELY FOLLOWING THIS CARD MUST BE A CARD OR CARDS CONTAINING THE',
          &/, ' VALUES OF #DATA IN 10F8.0 FORMAT.', //,
          &' EITHER FREQ AND SIZE OR RATIO MAY BE USED.  IF FREQ AND SIZE ARE
          & SPECIFIED, RAT IS CALCULATED FROM THEM.', //,
          &' ER1P THRU MUR2PP SETS THAT VALUE OF THAT PARAMETER.', //,
          &' DELTA SETS THE INITIAL INCREMENT VALUE FOR STEEPEST DESCENT.',
          &//, ' #DATA DETERMINES THE VALUES OF ER2PP OR MUR2PP DURING PARAME
          &TER SWEEPS.', //,
          &' ZSTART PROVIDES A STARTING VALUE OF THE VARIABLE ITERATED UPON F
          &OR THE FIRST PASS WHICH MAY BE USED TO OVERRIDE THE VALUE', /,
          &' CALCULATED WITHIN THE PROGRAM IF NECESSARY.', //,
          &' ELECTRIC/NOELECTRIC CONTROLS WHETHER OR NOT ELECTRIC LOSSES ARE
          &SWEPT.  NOELECTRIC IS DEFAULT.', //,
          &' MAGNETIC/NOMAGNETIC CONTROLS WHETHER OR NOT MAGNETIC LOSSES ARE
          &SWEPT.  IF BOTH TYPES OF SWEEP ARE SPECIFIED THE ELECTRIC', /,
          &' SWEEP IS PERFORMED FIRST.  NOMAGNETIC IS DEFAULT.', //    )
280    9004 FORMAT (' TABLE PRODUCES A TABULAR OUTPUT; DEBUG PRODUCES AN OUTPU
```

```
     &T WITH THE DERIVATIVES, ERROR VALUES, AND Z VALUES TO ASSIST', /,
     &' IN DEBUGGING.  TABLE IS DEFAULT.', //,
     &' UPON ENCOUNTERING THE RUN CARD THE PROGRAM IS EXECUTED USING THE
     & PARAMETERS IN EFFECT AT THAT TIME.', //,
     &' UPON ENCOUNTERING THE STOP CARD SUBROUTINE EXIT IS EXECUTED.',
     &//, ' UPON ENCOUNTERING ANY TITLE NOT LISTED IN THE ARRAY LABEL, T
     &HE UNRECOGNIZABLE TITLE IS PRINTED OUT, FOLLOWED BY THIS', /,
     &' TABLE, AND EXECUTION IS ABANDONED.'  )
281   9097 FORMAT ( 10F8.4 )
282   9098 FORMAT (1H1, 'MESSAGE "', A4, A4, '" NOT IN LIBRARY', //
     &                  ' EXECUTION INHIBITED'  )
283   9099 FORMAT (1X, A4, A4, 10X, F10.5, 10X, F10.5, 10X, F10.5 )
284   9401 FORMAT (60X, 'TANGENT' )
285   9490 FORMAT ('1DEBUG OUTPUT:',//, ' THE FIRST INFORMATION PRINTED IS IN
     &TENDED TO SHOW THE PATH OF CONVERGENCE AND TO GIVE OTHER INFORMATI
     &ON', /, '       ABOUT THE VALIDITY OF THE SOLUTION.', //,
     &' FERR IS THE VALUE OF THE FUNCTION FOR Z -- ITS ZEROS ARE SOLUTIO
     &NS.', /,
     &' FCKERR IS THE VALUE OF THE FUNCTION FOR ZCK.', /,
     &' Z = U*T IS THE VARIABLE ITERATED UPON.', /,
     &' FPX IS (APPROXIMATELY) THE PARTIAL DERIVATIVE OF F WITH RESPECT
     &TO THE REAL PART OF Z.', /,
     &' FPY IS (APPROXIMATELY) THE PARTIAL DERIVATIVE OF F WITH RESPECT
     &TO THE IMAGINARY PART OF Z.', /,
     &' FLAG IS PRINTED BETWEEN FERR AND FCKERR.  IF IT IS EVEN, Z AND Z
     &CK WERE NOT INTERCHANGED, EITHER BECAUSE', /,
     &'       FERR WAS LESS THAN FCKERR OR ZCK WAS NOT SUFFICIENTLY CLOSE
     &TO Z TO BE CERTAIN THAT THEY WERE APPROACHING', /,
     &'       THE SAME ROOT; IF ODD, Z AND ZCK WERE INTERCHANGED.  IF FLAG
     & IS ZERO OR ONE, ONLY STEEPEST DESCENT WAS', /,
     &'       USED; IF TWO OR THREE, ONLY THE GARBAGE CAN LID APPROACH WAS
     & USED (THIS HAPPENS WHEN THE GRADIENT IS ZERO);' )
286   9491 FORMAT (
     &'       IF FOUR OR FIVE BOTH STEEPEST DESCENT AND THE GARBAGE CAN AP
     &PROACH WERE USED.  IF FLAG IS TWO OR FOUR,', /,
     &'       IMIN AND KC2 WILL BE PRINTED IN PLACE OF FPX AND FPY.  IF FL
     &AG IS FOUR OR FIVE, TWO LINES HAVE BEEN', /,
     &'       PRINTED DURING ONE PASS THROUGH THE ITERATION LOOP, I.E., TH
     &E LINE IN WHICH THE 4 OR 5 APPEARS AND', /,
     &'       THE LINE IMMEDIATELY PRECEEDING IT.', /,
     &' FOLLOWING THIS, A MESSAGE INDICATING HOW THE ITERATION WAS TERMI
     &NATED APPEARS.', /,
     &' K IS THE ITERATION LOOP INDEX.', /,
     &' KC INDICATES HOW MANY TIMES THE INCREMENT WAS HALVED DURING THE
     &LAST STEEPEST DESCENT ATTEMPT.', /,
     &' DELTA IS THE INCREMENT USED IN THE LAST STEEPEST DESCENT ATTEMPT
     &.', /,
     &' DELMAG IS THE MAGNITUDE OF THE GRADIENT DURING THE LAST STEEPEST
     & DESCENT ATTEMPT.', /,
     &' F1 - F2 SHOULD BE ZERO; F1-F2 IS ANOTHER EXPRESSION FOR F(Z).' )
287   9492 FORMAT (
     &' ER2 IS THE COMPLEX PERMITTIVITY OF THE SLAB MATERIAL RELATIVE TO
     & FREE SPACE.', /,
     &' MUR2 IS THE COMPLEX PERMEABILITY OF THE SLAB MATERIAL RELATIVE T
     &O FREE SPACE.', /,
     &' ER1 AND MUR1 ARE SIMILARLY DEFINED FOR THE SURROUNDING MEDIUM.',
     & /,
     &' T IS THE SLAB THICKNESS.', /,
     &' LAMBDA_0 IS THE FREE SPACE WAVELENGTH.', /,
     &' LAMBDA_G IS THE GUIDE WAVELENGTH.', /,
```

```
          &' U, V, AND KZ ARE AS DEFINED ON PAGE 164 OF ''TIME-HARMONIC ELECT
          &ROMAGNETIC FIELDS'', R.F. HARRINGTON.', /,
          &'      MCGRAW-HILL (1961).')
288     9493 FORMAT (
          &' WHERE THE WORD ''WAVELENGTH'' APPEARS IT REFERS TO THE FREE SPAC
          &E WAVELENGTH.', ///,
          &' TABULATED OUTPUT:', //,
          &' T, LAMBDA_C, ER1, MUR1, ER2, AND MUR2 ARE AS PREVIOUSLY DEFINED.
          &', /,
          &' ER2PP IS THE NEGATIVE OF THE IMAGINARY COMPONENT OF ER2.', /,
          &' MUR2PP IS THE NEGATIVE OF THE IMAGINARY COMPONENT OF MUR2.', /,
          &' L_RATIO IS THE RATIO OF FREE SPACE WAVELENGTH TO GUIDE WAVELENGT
          &H.', /,
          &' ATTEN.-X AND ATTEN.-Z ARE THE X- AND Z-DIRECTION ATTENUATION (DE
          &CIBELS) PER FREE SPACE WAVELENGTH.', /,
          &' U, V, AND KZ ARE (NEPERS) PER FREE SPACE WAVELENGTH.' )
289     9494 FORMAT (//, '  MUR2PP       L_RATIO      ATTEN.-Z      ATTEN.-X
          &REAL(U)      AIMAG(U)       REAL(V)      AIMAG(V)      REAL(KZ)     AIM
          &AG(KZ)' )
290     9495 FORMAT (1X, F7.3, 9(2X, F11.5) )
291     9496 FORMAT (//, '   ER2PP       L_RATIO      ATTEN.-Z      ATTEN.-X
          &REAL(U)      AIMAG(U)       REAL(V)      AIMAG(V)      REAL(KZ)     AIM
          &AG(KZ)' )
292     9497 FORMAT (//, '               L_RATIO      ATTEN.-Z      ATTEN.-X
          &REAL(U)      AIMAG(U)       REAL(V)      AIMAG(V)      REAL(KZ)     AIM
          &AG(KZ)', //, 8X, 9(2X, F11.5)  )
293     9498 FORMAT (//, 34X, 'ER1 = ', F8.3, ' -J* ', F8.3,
          &              10X, 'MUR1 = ', F8.3, ' -J* ', F8.3,
          &          //, 34X, 'ER2 = ', F8.3, ' -J* ', F8.3,
          &              10X, 'MUR2 = ', F8.3, ' -J* ', F8.3  )
294     9499 FORMAT (1H1, 45X, 'TM(', I1, ') MODE', 10X, 'T/LAMBDA_C = ', F8.4)
295     9980 FORMAT (55X, '***   WARNING   ***',
          &/, 51X, 'D I D   N O T   C O N V E R G E')
296     9981 FORMAT (1H1, 9X, 'FERR', 18X, 'FCKERR', 16X, 'REAL(Z)', 15X,
          &               'AIMAG(Z)', 14X, 'FPX', 19X, 'FPY'  )
297     9982 FORMAT (7X, E15.7, 3X, I1, 3X, E15.7, 4(7X, E15.7) )
298     9984 FORMAT (40X, E15.7, 7X, E15.7 )
299     9985 FORMAT (/, 42X, 'REAL(ZCK)', 13X, 'AIMAG(ZCK)' )
300     9986 FORMAT ( 1H1 )
301     9987 FORMAT (/, 21X, 'F1 = ', E15.7, ' +J* ', E15.7,
          &             10X, 'F2 = ', E15.7, ' +J* ', E15.7 )
302     9988 FORMAT (6X, I2, 2X, I2, 6X, 5(E15.7, 7X) )
303     9989 FORMAT (/, 6X, 'K    KC          DELTA                      REAL(Z)
          &          AIMAG(Z)             FERR                       DELMAG  ' )
304     9990 FORMAT (/, 54X, 'TERMINATED BY SMALL FERR')
305     9991 FORMAT (/, 52X, 'TERMINATED BY SMALL CABS(DZ)')
306     9992 FORMAT (/, 38X, 'FERR = ', E15.7, '           FCKERR = ', E15.7 )
307     9994 FORMAT (//, 42X, 'U = ', F12.5, ' +J* ', F12.5, ' PER WAVELENGTH',
          &          //, 42X, 'V = ', F12.5, ' +J* ', F12.5, ' PER WAVELENGTH',
          &         //, 41X, 'KZ = ', F12.5, ' +J* ', F12.5, ' PER WAVELENGTH',
          &//, 29X, 'X-DIRECTION ATTENUATION = ', F12.5, ' DB./WAVELENGTH',
          &//, 29X, 'Z-DIRECTION ATTENUATION = ', F12.5, ' DB./WAVELENGTH' )
308     9995 FORMAT (//, 34X, 'ER1 = ', F8.3, ' -J* ', F8.3,
          &              10X, 'MUR1 = ', F8.3, ' -J* ', F8.3,
          &          //, 34X, 'ER2 = ', F8.3, ' -J* ', F8.3,
          &              10X, 'MUR2 = ', F8.3, ' -J* ', F8.3,
          &//, 35X, 'T/LAMBDA_C = ', F10.5, 10X, 'LAMBDA_0/LAMBDA_G = ',
          &                            F10.5  )
309     9996 FORMAT ( ///, 61X, 'TM(', I1, ') MODE' )
      C      PUNCHED DECK
```

```
310         END
```

```
      COMPLEX FUNCTION ZTAN(Z)
      COMPLEX J, Z
C     ZTAN RETURNS THE TANGENT OF A COMPLEX NUMBER UNLESS THE REAL PART
C     OF THE ARGUMENT IS SUFFICIENTLY CLOSE TO PI/2 TO GENERATE AN
C     ERROR, IN WHICH CASE A BOUNDED APPROXIMATION IS RETURNED.
      COMMON IN, IERR
      J = (0., 1.)
      PI = 3.1415927
      X = REAL(Z)
      Y = AIMAG(Z)
    2 IF ( ABS(X) .LE. PI/2 )  GO TO 3
      X = X - 3.141592653589793
      GO TO 2
    3 DELTA = PI/2 - ABS(X)
      IF ( DELTA .LT. 5.E-06*PI )  GO TO 1
      X = REAL(Z)
      ZTAN = (TAN(X) + J*TANH(Y))/(1. - J*TAN(X)*TANH(Y))
      IERR = 0
      RETURN
    1 TANX = 1.E+36*(1.0-DELTA/(5.E-06*PI)) + 60342.94
      IF ( X .LT. 0. )  TANX = -TANX
      ZTAN = (TANX + J*TANH(Y))/(1. - J*TANX*TANH(Y))
      IERR = 1
      RETURN
      END
```

APPENDIX C

SELECTED COMPUTER OUTPUT

TM(0) MODE T/LAMBDA_0 = 0.0100

ER1 = 1.000 -J* 0.0 MUR1 = 1.000 -J* 0.0

ER2 = 2.000 -J* 0.0 MUR2 = 1.000 -J* 0.0

ER2FP	L_RATIO	ATTEN.-Z	ATTEN.-X	REAL(U)	AIMAG(U)	REAL(V)	AIMAG(V)	REAL(KZ)	AIMAG(KZ)
0.0	1.00049	-0.0	1.71508	6.28008	0.0	0.19746	0.0	6.28629	0.0
0.200	1.00050	0.00541	1.73200	6.31105	-0.62492	0.19940	-0.01960	6.28633	-0.00062
0.300	1.00051	0.00811	1.75268	6.34875	-0.93182	0.20178	-0.02905	6.28637	-0.00093
0.400	1.00051	0.01079	1.78081	6.39976	-1.23253	0.20502	-0.03808	6.28642	-0.00124
0.500	1.00053	0.01348	1.81559	6.46255	-1.52569	0.20903	-0.04660	6.28650	-0.00155
0.600	1.00054	0.01612	1.85617	6.53553	-1.81039	0.21370	-0.05452	6.28659	-0.00186
0.700	1.00056	0.01872	1.90156	6.61710	-2.08609	0.21893	-0.06178	6.28670	-0.00216
0.800	1.00058	0.02124	1.95077	6.70576	-2.35260	0.22459	-0.06834	6.28683	-0.00245
0.900	1.00060	0.02365	2.00284	6.80019	-2.60995	0.23059	-0.07419	6.28698	-0.00272
1.000	1.00063	0.02599	2.05684	6.89919	-2.85837	0.23680	-0.07932	6.28715	-0.00299
1.200	1.00069	0.03023	2.16743	7.10712	-3.32978	0.24953	-0.08755	6.28753	-0.00348
1.400	1.00076	0.03388	2.27710	7.32341	-3.77015	0.26216	-0.09332	6.28796	-0.00390
1.600	1.00083	0.03680	2.38209	7.54387	-4.18301	0.27425	-0.09699	6.28842	-0.00424
1.800	1.00091	0.03909	2.48007	7.76573	-4.57166	0.28553	-0.09898	6.28890	-0.00450
2.000	1.00098	0.04080	2.56991	7.98716	-4.93903	0.29587	-0.09965	6.28937	-0.00470
2.500	1.00115	0.04288	2.75793	8.53213	-5.78015	0.31752	-0.09756	6.29045	-0.00494
3.000	1.00130	0.04283	2.89950	9.05886	-6.53356	0.33382	-0.09268	6.29137	-0.00493
3.500	1.00142	0.04173	3.00513	9.56506	-7.21971	0.34598	-0.08690	6.29210	-0.00480
4.000	1.00151	0.03989	3.08442	10.05106	-7.85269	0.35511	-0.08111	6.29267	-0.00459
4.500	1.00159	0.03793	3.14467	10.51805	-8.44253	0.36204	-0.07569	6.29315	-0.00437
5.000	1.00164	0.03614	3.19111	10.96752	-8.99655	0.36739	-0.07076	6.29350	-0.00416
5.500	1.00169	0.03426	3.22747	11.40095	-9.52033	0.37158	-0.06636	6.29380	-0.00394
6.000	1.00173	0.03253	3.25633	11.81970	-10.01815	0.37490	-0.06244	6.29403	-0.00375

TM(0) MODE   T/LAMBDA_0 = 0.0200

ER1 = 1.000 -J* 0.0   MUR1 = 1.000 -J* 0.0

ER2 = 2.000 -J* 0.0   MUR2 = 1.000 -J* 0.0

ER2FP	L_RATIO	ATTEN.-Z	ATTEN.-X	REAL(U)	AIMAG(U)	REAL(V)	AIMAG(V)	REAL(KZ)	AIMAG(KZ)
0.0	1.00198	-0.00000	3.43349	6.27073	-0.00000	0.39530	-0.00000	6.29561	0.00000
0.200	1.00200	0.02179	3.46700	6.30158	-0.62398	0.39915	-0.03956	6.29573	-0.00251
0.300	1.00202	0.03267	3.50794	6.33911	-0.93043	0.40387	-0.05863	6.29588	-0.00376
0.400	1.00206	0.04354	3.56360	6.38988	-1.23071	0.41028	-0.07689	6.29610	-0.00501
0.500	1.00210	0.05432	3.63248	6.45239	-1.52350	0.41820	-0.09413	6.29639	-0.00625
0.600	1.00216	0.06498	3.71279	6.52504	-1.80787	0.42745	-0.11019	6.29675	-0.00748
0.700	1.00223	0.07547	3.80262	6.60624	-2.08329	0.43779	-0.12493	6.29719	-0.00869
0.800	1.00231	0.08566	3.90003	6.69450	-2.34958	0.44901	-0.13830	6.29770	-0.00986
0.900	1.00240	0.09556	4.00308	6.78850	-2.60676	0.46087	-0.15026	6.29828	-0.01100
1.000	1.00251	0.10499	4.10999	6.88707	-2.85507	0.47318	-0.16082	6.29893	-0.01209
1.200	1.00274	0.12230	4.32900	7.09414	-3.32645	0.49839	-0.17789	6.30043	-0.01408
1.400	1.00301	0.13721	4.54635	7.30963	-3.76699	0.52342	-0.19009	6.30210	-0.01580
1.600	1.00330	0.14957	4.75457	7.52940	-4.18017	0.54739	-0.19816	6.30390	-0.01722
1.800	1.00359	0.15934	4.94912	7.75068	-4.56926	0.56979	-0.20288	6.30573	-0.01834
2.000	1.00388	0.16671	5.12772	7.97166	-4.93716	0.59035	-0.20499	6.30756	-0.01919
2.500	1.00456	0.17674	5.50222	8.51602	-5.77965	0.63347	-0.20272	6.31181	-0.02035
3.000	1.00513	0.17849	5.78493	9.04269	-6.53432	0.66601	-0.19480	6.31541	-0.02055
3.500	1.00559	0.17574	5.99623	9.54915	-7.22152	0.69034	-0.18501	6.31832	-0.02023
4.000	1.00596	0.17073	6.15493	10.03558	-7.85531	0.70861	-0.17513	6.32061	-0.01966
4.500	1.00625	0.16485	6.27545	10.50308	-8.44575	0.72249	-0.16593	6.32243	-0.01898
5.000	1.00647	0.15903	6.36821	10.95308	-9.00023	0.73317	-0.15769	6.32386	-0.01831
5.500	1.00665	0.15355	6.44057	11.38702	-9.52433	0.74150	-0.15047	6.32500	-0.01768
6.000	1.00680	0.14844	6.49775	11.80627	-10.02239	0.74808	-0.14421	6.32593	-0.01709

TM(0) MODE T/LAMBDA_0 = 0.0300

ER1 = 1.000 -J* 0.0 MUR1 = 1.000 -J* 0.0

ER2 = 2.000 -J* 0.0 MUR2 = 1.000 -J* 0.0

ER2PP	L_RATIO	ATTEN.-Z	ATTEN.-X	REAL(U)	AIMAG(U)	REAL(V)	AIMAG(V)	REAL(KZ)	AIMAG(KZ)
0.0	1.00446	-0.0	5.15831	6.25505	0.0	0.59387	0.0	6.31119	0.0
0.200	1.00450	0.04968	5.20770	6.28569	-0.62233	0.59956	-0.06021	6.31144	-0.00572
0.300	1.00455	0.07451	5.26805	6.32295	-0.92799	0.60651	-0.08927	6.31176	-0.00858
0.400	1.00462	0.09927	5.35008	6.37335	-1.22754	0.61595	-0.11714	6.31223	-0.01143
0.500	1.00472	0.12394	5.45155	6.43540	-1.51964	0.62763	-0.14350	6.31284	-0.01427
0.600	1.00484	0.14832	5.56987	6.50751	-1.80341	0.64125	-0.16811	6.31361	-0.01708
0.700	1.00499	0.17231	5.70218	6.58811	-2.07832	0.65649	-0.19080	6.31454	-0.01984
0.800	1.00516	0.19575	5.84565	6.67572	-2.34417	0.67300	-0.21146	6.31563	-0.02254
0.900	1.00536	0.21846	5.99743	6.76904	-2.60102	0.69048	-0.23004	6.31687	-0.02515
1.000	1.00558	0.24025	6.15490	6.86690	-2.84909	0.70861	-0.24657	6.31827	-0.02766
1.200	1.00609	0.28051	6.47758	7.07258	-3.32027	0.74576	-0.27369	6.32145	-0.03229
1.400	1.00666	0.31564	6.79804	7.28675	-3.76094	0.78265	-0.29364	6.32503	-0.03634
1.600	1.00727	0.34526	7.10537	7.50535	-4.17451	0.81804	-0.30749	6.32887	-0.03975
1.800	1.00790	0.36939	7.39285	7.72566	-4.56417	0.85113	-0.31640	6.33281	-0.04253
2.000	1.00852	0.38844	7.65707	7.94586	-4.93276	0.88155	-0.32143	6.33673	-0.04472
2.500	1.00998	0.41773	8.21218	8.48907	-5.77717	0.94546	-0.32272	6.34590	-0.04809
3.000	1.01122	0.42857	8.63191	9.01548	-6.53366	0.99379	-0.31543	6.35365	-0.04934
3.500	1.01221	0.42933	8.94537	9.52224	-7.22234	1.02987	-0.30514	6.35990	-0.04943
4.000	1.01299	0.42498	9.17985	10.00924	-7.85728	1.05687	-0.29455	6.36482	-0.04893
4.500	1.01360	0.41863	9.35655	10.47747	-8.44855	1.07721	-0.28486	6.36866	-0.04820
5.000	1.01408	0.41194	9.49083	10.92824	-9.00363	1.09267	-0.27652	6.37166	-0.04743
5.500	1.01445	0.40595	9.59365	11.36295	-9.52813	1.10451	-0.26961	6.37399	-0.04674
6.000	1.01474	0.40082	9.67285	11.78294	-10.02644	1.11363	-0.26409	6.37579	-0.04615

TM(0) MODE T/LAMBDA_0 = 0.0400

ER1 = 1.000 -J* 0.0 MUR1 = 1.000 -J* 0.0

ER2 = 2.000 -J* 0.0 MUR2 = 1.000 -J* 0.0

ER2FP	L_RATIO	ATTEN.-Z	ATTEN.-X	REAL(U)	AIMAG(U)	REAL(V)	AIMAG(V)	REAL(KZ)	AIMAG(KZ)
0.0	1.00794	-0.0	6.89212	6.23288	0.0	0.79348	0.0	6.33309	0.0
0.200	1.00801	0.08994	6.95630	6.26322	-0.61985	0.80087	-0.08188	6.33350	-0.01035
0.300	1.00809	0.13490	7.03472	6.30012	-0.92433	0.80990	-0.12146	6.33402	-0.01553
0.400	1.00821	0.17979	7.14127	6.35004	-1.22276	0.82217	-0.15948	6.33478	-0.02070
0.500	1.00837	0.22449	7.27304	6.41148	-1.51382	0.83734	-0.19554	6.33577	-0.02585
0.600	1.00857	0.26877	7.42662	6.48289	-1.79664	0.85502	-0.22932	6.33702	-0.03094
0.700	1.00881	0.31242	7.59832	6.56269	-2.07071	0.87479	-0.26060	6.33854	-0.03597
0.800	1.00905	0.35514	7.78440	6.64944	-2.33585	0.89621	-0.28925	6.34032	-0.04089
0.900	1.00942	0.39669	7.98124	6.74184	-2.59211	0.91887	-0.31520	6.34236	-0.04567
1.000	1.00978	0.43674	8.18543	6.83877	-2.83972	0.94238	-0.33848	6.34464	-0.05028
1.200	1.01061	0.51135	8.60382	7.04257	-3.31033	0.99055	-0.37734	6.34986	-0.05887
1.400	1.01155	0.57745	9.01937	7.25497	-3.75085	1.03839	-0.40689	6.35575	-0.06648
1.600	1.01255	0.63443	9.41802	7.47198	-4.16463	1.08429	-0.42852	6.36206	-0.07304
1.800	1.01359	0.68219	9.79112	7.69093	-4.55476	1.12724	-0.44369	6.36854	-0.07854
2.000	1.01461	0.72143	10.13416	7.91004	-4.92399	1.16674	-0.45377	6.37500	-0.08306
2.500	1.01701	0.78822	10.85465	8.45154	-5.77032	1.24969	-0.46399	6.39006	-0.09075
3.000	1.01903	0.82352	11.39756	8.97741	-6.52867	1.31219	-0.46259	6.40275	-0.09481
3.500	1.02063	0.84064	11.79940	9.48439	-7.21887	1.35846	-0.45686	6.41283	-0.09678
4.000	1.02187	0.84855	12.09498	9.97205	-7.85491	1.39249	-0.45040	6.42059	-0.09769
4.500	1.02280	0.85239	12.31166	10.44116	-8.44693	1.41743	-0.44485	6.42645	-0.09814
5.000	1.02349	0.85491	12.46960	10.89293	-9.00245	1.43562	-0.44083	6.43075	-0.09843
5.500	1.02398	0.85775	12.58325	11.32868	-9.52717	1.44870	-0.43850	6.43386	-0.09875
6.000	1.02432	0.86178	12.66296	11.74970	-10.02550	1.45788	-0.43781	6.43597	-0.09922

TM(0) MODE T/LAMBDA_0 = 0.0500

ER1 = 1.000 -J* 0.0 MUR1 = 1.000 -J* 0.0

ER2 = 2.000 -J* 0.0 MUR2 = 1.000 -J* 0.0

ER2FP	L_RATIO	ATTEN.-Z	ATTEN.-X	REAL(U)	AIMAG(U)	REAL(V)	AIMAG(V)	REAL(KZ)	AIMAG(KZ)
0.0	1.01244	-0.0	8.63674	6.20400	0.0	0.99434	0.0	6.36138	0.0
0.200	1.01253	0.14365	8.71420	6.23400	-0.61640	1.00326	-0.10487	6.36194	-0.01654
0.300	1.01265	0.21549	8.80885	6.27049	-0.91921	1.01416	-0.15564	6.36265	-0.02481
0.400	1.01281	0.28724	8.93738	6.31983	-1.21605	1.02895	-0.20451	6.36368	-0.03307
0.500	1.01303	0.35873	9.09622	6.38056	-1.50562	1.04724	-0.25100	6.36505	-0.04130
0.600	1.01330	0.42966	9.28122	6.45113	-1.78706	1.06854	-0.29473	6.36677	-0.04947
0.700	1.01364	0.49970	9.48790	6.52999	-2.05989	1.09233	-0.33541	6.36886	-0.05753
0.800	1.01403	0.56842	9.71174	6.61573	-2.32392	1.11811	-0.37291	6.37133	-0.06544
0.900	1.01448	0.63549	9.94837	6.70706	-2.57921	1.14535	-0.40714	6.37415	-0.07316
1.000	1.01498	0.70037	10.19363	6.80289	-2.82600	1.17358	-0.43814	6.37732	-0.08063
1.200	1.01614	0.82230	10.69571	7.00447	-3.29541	1.23139	-0.49083	6.38457	-0.09467
1.400	1.01744	0.93205	11.19383	7.21476	-3.73524	1.28874	-0.53224	6.39277	-0.10731
1.600	1.01884	1.02842	11.67117	7.42988	-4.14875	1.34369	-0.56405	6.40154	-0.11840
1.800	1.02027	1.11145	12.11725	7.64721	-4.53894	1.39505	-0.58798	6.41056	-0.12796
2.000	1.02170	1.18195	12.52660	7.86499	-4.90844	1.44218	-0.60568	6.41950	-0.13608
2.500	1.02499	1.31188	13.38186	8.40441	-5.75594	1.54064	-0.63130	6.44020	-0.15104
3.000	1.02771	1.39386	14.01725	8.92964	-6.51554	1.61380	-0.64208	6.45726	-0.16047
3.500	1.02978	1.44723	14.47534	9.43694	-7.20669	1.66654	-0.64684	6.47033	-0.16662
4.000	1.03129	1.48450	14.79766	9.92554	-7.84333	1.70364	-0.65002	6.47977	-0.17091
4.500	1.03231	1.51335	15.01727	10.39596	-8.43561	1.72893	-0.65365	6.48619	-0.17423
5.000	1.03294	1.53837	15.15888	10.84924	-8.99109	1.74523	-0.65854	6.49013	-0.17711
5.500	1.03325	1.56091	15.24061	11.28663	-9.51558	1.75464	-0.66490	6.49209	-0.17971
6.000	1.03330	1.58298	15.27553	11.70936	-10.01353	1.75866	-0.67267	6.49244	-0.18225

TM(0) MODE T/LAMBDA_0 = 0.0600

ER1 = 1.000 -J* 0.0 MUR1 = 1.000 -J* 0.0

ER2 = 2.000 -J* 0.0 MUR2 = 1.000 -J* 0.0

ER2PP	L_RATIO	ATTEN.-Z	ATTEN.-X	REAL(U)	AIMAG(U)	REAL(V)	AIMAG(V)	REAL(KZ)	AIMAG(KZ)
0.0	1.01797	-0.0	10.39295	6.16820	0.0	1.19653	0.0	6.39610	0.0
0.200	1.01808	0.21205	10.48183	6.19783	-0.61177	1.20677	-0.12941	6.39676	-0.02441
0.300	1.01821	0.31812	10.59028	6.23386	-0.91235	1.21925	-0.19217	6.39761	-0.03662
0.400	1.01841	0.42407	10.73751	6.28259	-1.20703	1.23620	-0.25272	6.39884	-0.04882
0.500	1.01867	0.52972	10.91922	6.34256	-1.49455	1.25712	-0.31049	6.40048	-0.06099
0.600	1.01900	0.63463	11.13065	6.41224	-1.77406	1.28146	-0.36504	6.40255	-0.07306
0.700	1.01940	0.73839	11.36657	6.49010	-2.04511	1.30862	-0.41607	6.40508	-0.08501
0.800	1.01987	0.84041	11.62171	6.57476	-2.30751	1.33800	-0.46339	6.40806	-0.09676
0.900	1.02042	0.94021	11.89104	6.66496	-2.56135	1.36901	-0.50693	6.41150	-0.10825
1.000	1.02104	1.03713	12.16981	6.75963	-2.80684	1.40110	-0.54672	6.41536	-0.11940
1.200	1.02244	1.22064	12.73915	6.95888	-3.27412	1.46665	-0.61552	6.42420	-0.14053
1.400	1.02403	1.38783	13.30216	7.16698	-3.71242	1.53147	-0.67127	6.43419	-0.15978
1.600	1.02573	1.53721	13.83957	7.38015	-4.12487	1.59334	-0.71584	6.44485	-0.17698
1.800	1.02746	1.66862	14.33948	7.59583	-4.51436	1.65089	-0.75121	6.45573	-0.19211
2.000	1.02917	1.78296	14.79561	7.81230	-4.88345	1.70341	-0.77923	6.46645	-0.20527
2.500	1.03303	2.00485	15.73518	8.34987	-5.73061	1.81158	-0.82697	6.49074	-0.23082
3.000	1.03605	2.15839	16.41019	8.87493	-6.49018	1.88929	-0.85618	6.50973	-0.24849
3.500	1.03816	2.26800	16.86865	9.38330	-7.18126	1.94208	-0.87699	6.52297	-0.26111
4.000	1.03944	2.35028	17.15848	9.87378	-7.81763	1.97544	-0.89451	6.53098	-0.27059
4.500	1.04002	2.41473	17.31871	10.34661	-8.40949	1.99389	-0.91113	6.53462	-0.27801
5.000	1.04002	2.46756	17.37907	10.80264	-8.96444	2.00084	-0.92778	6.53465	-0.28409
5.500	1.03957	2.51123	17.36192	11.24296	-9.48835	1.99887	-0.94471	6.53184	-0.28912
6.000	1.03877	2.54727	17.28395	11.66873	-9.98575	1.98989	-0.96184	6.52677	-0.29327

TM(0) MODE   T/LAMBDA_0 =   0.0800

ER1 = 1.000 -J* 0.0   MUR1 = 1.000 -J* 0.0

ER2 = 2.000 -J* 0.0   MUR2 = 1.000 -J* 0.0

ER2FP	L_RATIO	ATTEN.-Z	ATTEN.-X	REAL(U)	AIMAG(U)	REAL(V)	AIMAG(V)	REAL(KZ)	AIMAG(KZ)
0.0	1.03209	-0.0	13.93660	6.07486	0.0	1.60451	0.0	6.48482	0.0
0.200	1.03218	0.39777	14.04094	6.10383	-0.59812	1.61652	-0.18373	6.48536	-0.04580
0.300	1.03229	0.59665	14.16801	6.13906	-0.89203	1.63115	-0.27314	6.48608	-0.06869
0.400	1.03246	0.79526	14.33999	6.18669	-1.18023	1.65095	-0.35976	6.48714	-0.09156
0.500	1.03269	0.99323	14.55157	6.24531	-1.46152	1.67531	-0.44288	6.48861	-0.11435
0.600	1.03300	1.19995	14.79669	6.31342	-1.73509	1.70353	-0.52196	6.49051	-0.13700
0.700	1.03338	1.38469	15.06884	6.38957	-2.00050	1.73486	-0.59663	6.49289	-0.15942
0.800	1.03383	1.57658	15.36161	6.47239	-2.25764	1.76857	-0.66666	6.49575	-0.18151
0.900	1.03436	1.76477	15.66873	6.56071	-2.50656	1.80393	-0.73198	6.49908	-0.20318
1.000	1.03496	1.94636	15.98453	6.65348	-2.74751	1.84029	-0.79262	6.50286	-0.22431
1.200	1.03634	2.29869	16.62230	6.84912	-3.20680	1.91371	-0.90046	6.51152	-0.26465
1.400	1.03788	2.62264	17.24207	7.05408	-3.63844	1.98507	-0.99191	6.52121	-0.30194
1.600	1.03949	2.91747	17.82127	7.26479	-4.04540	2.05175	-1.06920	6.53129	-0.33589
1.800	1.04105	3.18238	18.34604	7.47882	-4.43038	2.11217	-1.13463	6.54114	-0.36638
2.000	1.04250	3.41803	18.80920	7.69448	-4.79575	2.16549	-1.19031	6.55025	-0.39352
2.500	1.04524	3.89215	19.68840	8.23356	-5.63609	2.26671	-1.29827	6.56747	-0.44810
3.000	1.04641	4.23032	20.19952	8.76438	-6.39127	2.32556	-1.37689	6.57480	-0.48703
3.500	1.04601	4.46449	20.40662	9.28151	-7.07957	2.34940	-1.43784	6.57228	-0.51399
4.000	1.04479	4.61802	20.37589	9.78265	-7.71450	2.34586	-1.48706	6.56146	-0.53167
4.500	1.04156	4.70634	20.16461	10.26714	-8.30616	2.32154	-1.52740	6.54435	-0.54184
5.000	1.03816	4.74054	19.81963	10.73513	-8.86211	2.28182	-1.56018	6.52294	-0.54578
5.500	1.03434	4.72944	19.37852	11.18720	-9.38813	2.23104	-1.58605	6.49898	-0.54450
6.000	1.03036	4.67985	18.87123	11.62415	-9.88865	2.17263	-1.60542	6.47392	-0.53879

TM(0) MODE T/LAMBDA_0 = 0.1000

ER1 = 1.000 -J* 0.0 MUR1 = 1.000 -J* 0.0

ER2 = 2.000 -J* 0.0 MUR2 = 1.000 -J* 0.0

ER2FP	L_RATIO	ATTEN.-Z	ATTEN.-X	REAL(U)	AIMAG(U)	REAL(V)	AIMAG(V)	REAL(KZ)	AIMAG(KZ)
0.0	1.05015	-0.0	17.49901	5.95143	0.0	2.01465	0.0	6.59828	0.0
0.200	1.05010	0.65354	17.60783	5.98013	-0.57714	2.02718	-0.24489	6.59800	-0.07524
0.300	1.05006	0.97984	17.73988	6.01504	-0.86076	2.04238	-0.36441	6.59770	-0.11281
0.400	1.05000	1.30525	17.91771	6.06226	-1.13889	2.06285	-0.48059	6.59738	-0.15027
0.500	1.04996	1.62908	18.13503	6.12042	-1.41041	2.08787	-0.59261	6.59710	-0.18756
0.600	1.04993	1.95035	18.38475	6.18806	-1.67455	2.11662	-0.69983	6.59691	-0.22454
0.700	1.04992	2.26793	18.65933	6.26377	-1.93094	2.14824	-0.80180	6.59687	-0.26110
0.800	1.04994	2.58050	18.95137	6.34624	-2.17947	2.18186	-0.89827	6.59699	-0.29709
0.900	1.04999	2.88675	19.25374	6.43433	-2.42025	2.21667	-0.98913	6.59728	-0.33235
1.000	1.05006	3.18537	19.56007	6.52707	-2.65351	2.25194	-1.07443	6.59771	-0.36673
1.200	1.05022	3.75504	20.16248	6.72331	-3.09882	2.32129	-1.22893	6.59875	-0.43231
1.400	1.05035	4.28171	20.72240	6.92996	-3.51830	2.38576	-1.36360	6.59954	-0.49295
1.600	1.05033	4.76040	21.21570	7.14358	-3.91482	2.44255	-1.48076	6.59941	-0.54806
1.800	1.05007	5.18860	21.62817	7.36178	-4.29099	2.49004	-1.58278	6.59776	-0.59736
2.000	1.04948	5.56598	21.95317	7.58281	-4.64905	2.52745	-1.67183	6.59409	-0.64081
2.500	1.04638	6.29500	22.38240	8.13981	-5.47717	2.57687	-1.84905	6.57457	-0.72474
3.000	1.04097	6.74505	22.32114	8.69293	-6.22788	2.56982	-1.97643	6.54058	-0.77655
3.500	1.03386	6.95584	21.87643	9.23397	-6.91848	2.51862	-2.06542	6.49594	-0.80082
4.000	1.02594	6.96887	21.16304	9.75816	-7.56135	2.43649	-2.12265	6.44615	-0.80232
4.500	1.01803	6.82740	20.28441	10.26298	-8.16513	2.33533	-2.15289	6.39650	-0.78603
5.000	1.01077	6.57430	19.32518	10.74759	-8.73582	2.22489	-2.16049	6.35087	-0.75689
5.500	1.00453	6.24993	18.34818	11.21223	-9.27773	2.11241	-2.14980	6.31163	-0.71955
6.000	0.99943	5.88718	17.39607	11.65793	-9.79410	2.00280	-2.12499	6.27960	-0.67779

TM(0) MODE   T/LAMBDA_0 =   0.1200

ER1 =   1.000 -J*   0.0   MUR1 =   1.000 -J*   0.0

ER2 =   2.000 -J*   0.0   MUR2 =   1.000 -J*   0.0

ER2FP	L_RATIO	ATTEN.-Z	ATTEN.-X	REAL(U)	AIMAG(U)	REAL(V)	AIMAG(V)	REAL(KZ)	AIMAG(KZ)
0.0	1.07166	-0.0	21.02782	5.79806	0.0	2.42092	0.0	6.73344	0.0
0.200	1.07136	0.97577	21.13205	5.82717	-0.54771	2.43292	-0.31083	6.73153	-0.11234
0.300	1.07099	1.46227	21.25774	5.86261	-0.81685	2.44739	-0.46289	6.72920	-0.16835
0.400	1.07048	1.94676	21.42552	5.91061	-1.08080	2.46671	-0.61114	6.72606	-0.22413
0.500	1.06987	2.42804	21.62833	5.96984	-1.33848	2.49005	-0.75464	6.72216	-0.27954
0.600	1.06914	2.90458	21.85794	6.03888	-1.58922	2.51649	-0.89266	6.71760	-0.33440
0.700	1.06831	3.37465	22.10590	6.11637	-1.83271	2.54504	-1.02470	6.71242	-0.38852
0.800	1.06740	3.83631	22.36386	6.20104	-2.06888	2.57474	-1.15046	6.70665	-0.44167
0.900	1.06639	4.28759	22.62387	6.29180	-2.29788	2.60467	-1.26981	6.70030	-0.49363
1.000	1.06528	4.72652	22.87885	6.38770	-2.51999	2.63403	-1.38276	6.69332	-0.54416
1.200	1.06273	5.56003	23.34938	6.59188	-2.94495	2.68820	-1.59002	6.67731	-0.64012
1.400	1.05966	6.32383	23.73601	6.80870	-3.34681	2.73271	-1.77385	6.65805	-0.72806
1.600	1.05599	7.00781	24.01292	7.03471	-3.72859	2.76459	-1.93631	6.63498	-0.80680
1.800	1.05165	7.60461	24.16570	7.26735	-4.09302	2.78218	-2.07934	6.60771	-0.87551
2.000	1.04662	8.10930	24.18900	7.50458	-4.44247	2.78486	-2.20460	6.57611	-0.93362
2.500	1.03143	8.95241	23.70541	8.10688	-5.26324	2.72919	-2.44742	6.48069	-1.03068
3.000	1.01432	9.21138	22.59285	8.70513	-6.02620	2.60110	-2.59838	6.37317	-1.06050
3.500	0.99827	8.97792	21.11319	9.28265	-6.74420	2.43075	-2.66711	6.27230	-1.03362
4.000	0.98562	8.41566	19.52948	9.82997	-7.42186	2.24842	-2.66858	6.19283	-0.96889
4.500	0.97713	7.69900	18.07451	10.34499	-8.06038	2.07515	-2.62238	6.13949	-0.88638
5.000	0.97230	6.95694	16.68500	10.83021	-8.66123	1.92093	-2.54713	6.10915	-0.80095
5.500	0.97017	6.26017	15.53107	11.28974	-9.22715	1.78808	-2.45694	6.09576	-0.72073
6.000	0.96982	5.63819	14.55048	11.72756	-9.76160	1.67519	-2.36104	6.09354	-0.64912

TM(0) MODE T/LAMBDA_0 = 0.1400

ER1 = 1.000 -J* 0.0 MUR1 = 1.000 -J* 0.0

ER2 = 2.000 -J* 0.0 MUR2 = 1.000 -J* 0.0

ER2FP	L_RATIO	ATTEN.-Z	ATTEN.-X	REAL(U)	AIMAG(U)	REAL(V)	AIMAG(V)	REAL(KZ)	AIMAG(KZ)
0.0	1.09575	-0.0	24.44768	5.61749	0.0	2.81464	0.0	6.88481	0.0
0.200	1.09511	1.34642	24.54436	5.64766	-0.51016	2.82577	-0.37745	6.88077	-0.15501
0.300	1.09431	2.01766	24.65988	5.68447	-0.76077	2.83908	-0.56257	6.87577	-0.23229
0.400	1.09321	2.68611	24.81227	5.73446	-1.00646	2.85662	-0.74360	6.86887	-0.30925
0.500	1.09182	3.35015	24.99321	5.79632	-1.24625	2.87745	-0.91954	6.86013	-0.38570
0.600	1.09015	4.00780	25.19342	5.86871	-1.47954	2.90050	-1.08963	6.84959	-0.46142
0.700	1.08819	4.65673	25.40298	5.95034	-1.70609	2.92463	-1.25336	6.83728	-0.53613
0.800	1.08594	5.29433	25.61237	6.04001	-1.92589	2.94873	-1.41041	6.82317	-0.60953
0.900	1.08340	5.91787	25.81221	6.13668	-2.13917	2.97174	-1.56066	6.80722	-0.68132
1.000	1.08055	6.52448	25.99414	6.23947	-2.34625	2.99269	-1.70410	6.78932	-0.75116
1.200	1.07386	7.67538	26.27477	6.46060	-2.74352	3.02500	-1.97098	6.74723	-0.88366
1.400	1.06568	8.72381	26.40451	6.69883	-3.12141	3.03993	-2.21224	6.69585	-1.00437
1.600	1.05588	9.64636	26.34761	6.95077	-3.48376	3.03338	-2.42892	6.63428	-1.11058
1.800	1.04440	10.41845	26.08136	7.21357	-3.83436	3.00273	-2.62132	6.56218	-1.19947
2.000	1.03137	11.01489	25.59644	7.48438	-4.17676	2.94690	-2.78864	6.48030	-1.26814
2.500	0.99500	11.59705	23.51483	8.17406	-5.01598	2.70725	-3.08319	6.25174	-1.33516
3.000	0.96342	10.91039	20.75687	8.83354	-5.84295	2.38972	-3.18178	6.05337	-1.25611
3.500	0.94603	9.55730	18.19707	9.42658	-6.63515	2.09502	-3.12185	5.94409	-1.10032
4.000	0.94094	8.17919	16.21246	9.95943	-7.36885	1.86653	-2.98258	5.91212	-0.94166
4.500	0.94250	7.02140	14.74956	10.45040	-8.04173	1.69811	-2.81900	5.92188	-0.80837
5.000	0.94682	6.10139	13.66482	10.91237	-8.66146	1.57322	-2.65622	5.94905	-0.70245
5.500	0.95198	5.37568	12.84208	11.35265	-9.23692	1.47850	-2.50384	5.98146	-0.61892
6.000	0.95711	4.79843	12.20183	11.77545	-9.77567	1.40479	-2.36477	6.01369	-0.55244

TM(0) MODE T/LAMBDA_0 = 0.1600

ER1 = 1.000 -J* 0.0 MUR1 = 1.000 -J* 0.0

ER2 = 2.000 -J* 0.0 MUR2 = 1.000 -J* 0.0

ER2PP	L_RATIO	ATTEN.-Z	ATTEN.-X	REAL(U)	AIMAG(U)	REAL(V)	AIMAG(V)	REAL(KZ)	AIMAG(KZ)
0.0	1.12124	-0.0	27.67657	5.41529	0.0	3.18638	0.0	7.04496	0.0
0.200	1.12028	1.73557	27.77037	5.44680	-0.46658	3.19718	-0.43991	7.03895	-0.19982
0.300	1.11909	2.60229	27.88153	5.48533	-0.69552	3.20998	-0.65627	7.03146	-0.29960
0.400	1.11743	3.46723	28.02644	5.53780	-0.91968	3.22666	-0.86859	7.02102	-0.39918
0.500	1.11530	4.32900	28.19550	5.60303	-1.13814	3.24613	-1.07591	7.00761	-0.49839
0.600	1.11268	5.18580	28.37801	5.67976	-1.35032	3.26714	-1.27757	6.99120	-0.59704
0.700	1.10958	6.03541	28.56238	5.76683	-1.55599	3.28837	-1.47315	6.97169	-0.69485
0.800	1.10595	6.87513	28.73712	5.86318	-1.75521	3.30848	-1.66247	6.94890	-0.79153
0.900	1.10176	7.70210	28.89084	5.96794	-1.94820	3.32618	-1.84551	6.92259	-0.88674
1.000	1.09697	8.51308	29.01271	6.08040	-2.13536	3.34021	-2.02241	6.89245	-0.98010
1.200	1.08528	10.07247	29.11935	6.32643	-2.49421	3.35249	-2.35870	6.81901	-1.15964
1.400	1.07027	11.51865	28.97731	6.59848	-2.83657	3.33614	-2.67309	6.72470	-1.32613
1.600	1.05120	12.80209	28.50734	6.89523	-3.16854	3.28203	-2.96612	6.60489	-1.47390
1.800	1.02739	13.84323	27.62555	7.21557	-3.49832	3.18051	-3.23474	6.45528	-1.59376
2.000	0.99867	14.51218	26.25269	7.55633	-3.83712	3.02245	-3.46864	6.27485	-1.67078
2.500	0.92412	13.56469	21.00970	8.40520	-4.79229	2.41883	-3.74882	5.80641	-1.56169
3.000	0.89828	10.51340	16.61861	9.05669	-5.78423	1.91329	-3.57053	5.64406	-1.21040
3.500	0.90423	8.24432	14.25628	9.58027	-6.64852	1.64131	-3.28546	5.68145	-0.94916
4.000	0.91684	6.78247	12.93669	10.05868	-7.40242	1.48939	-3.02012	5.76066	-0.78086
4.500	0.92923	5.79515	12.12676	10.51465	-8.07740	1.39614	-2.79002	5.83853	-0.66719
5.000	0.93995	5.08735	11.58804	10.95457	-8.69380	1.33412	-2.59267	5.90588	-0.58570
5.500	0.94889	4.55410	11.20456	11.38075	-9.26474	1.28997	-2.42313	5.96202	-0.52431
6.000	0.95626	4.13623	10.91507	11.79432	-9.79912	1.25664	-2.27677	6.00836	-0.47620

TM(0) MODE T/LAMBDA_C = 0.1800

ER1 = 1.000 -J* 0.0 MUR1 = 1.000 -J* 0.0

ER2 = 2.000 -J* 0.0 MUR2 = 1.000 -J* 0.0

ER2PP	L_RATIO	ATTEN.-Z	ATTEN.-X	REAL(U)	AIMAG(U)	REAL(V)	AIMAG(V)	REAL(KZ)	AIMAG(KZ)
0.0	1.14688	-0.0	30.64619	5.19901	0.0	3.52827	0.0	7.20605	0.0
0.200	1.14573	2.11093	30.74640	5.23154	-0.42020	3.53981	-0.49425	7.19885	-0.24303
0.300	1.14430	3.16814	30.86499	5.27140	-0.62589	3.55346	-0.73800	7.18985	-0.36475
0.400	1.14229	4.22699	31.01927	5.32585	-0.82670	3.57123	-0.97803	7.17721	-0.48665
0.500	1.13969	5.28733	31.19888	5.39380	-1.02165	3.59191	-1.21356	7.16086	-0.60873
0.600	1.13647	6.34872	31.39189	5.47415	-1.21009	3.61413	-1.44413	7.14066	-0.73092
0.700	1.13260	7.41038	31.58559	5.56589	-1.39171	3.63643	-1.66958	7.11635	-0.85315
0.800	1.12802	8.47145	31.76717	5.66818	-1.56643	3.65733	-1.89005	7.08755	-0.97531
0.900	1.12264	9.53096	31.92363	5.78041	-1.73435	3.67534	-2.10593	7.05377	-1.09729
1.000	1.11636	10.58806	32.04207	5.90218	-1.89570	3.68898	-2.31782	7.01432	-1.21900
1.200	1.10050	12.69201	32.11198	6.17410	-2.20002	3.69703	-2.73296	6.91466	-1.46122
1.400	1.07878	14.77742	31.86003	6.48624	-2.48265	3.66802	-3.14386	6.77816	-1.70131
1.600	1.04829	16.83080	31.12187	6.84711	-2.74857	3.58304	-3.56203	6.58660	-1.93772
1.800	1.00313	18.78825	29.57886	7.27755	-3.00884	3.40539	-4.00351	6.30285	-2.16308
2.000	0.92780	20.19162	26.28392	7.83173	-3.31047	3.02605	-4.47833	5.82957	-2.32465
2.500	0.82701	11.62767	14.61117	8.77875	-4.82892	1.68217	-4.13514	5.19623	-1.33869
3.000	0.86356	8.02327	12.14590	9.21712	-5.88097	1.39835	-3.58417	5.42592	-0.92371
3.500	0.89263	6.42380	11.25413	9.65735	-6.72434	1.29568	-3.20126	5.60857	-0.73957
4.000	0.91408	5.50062	10.86295	10.09918	-7.45799	1.25064	-2.90816	5.74335	-0.63328
4.500	0.93015	4.88155	10.67090	10.53682	-8.11837	1.22853	-2.67349	5.84431	-0.56201
5.000	0.94242	4.42527	10.56296	10.96675	-8.72447	1.21611	-2.48066	5.92141	-0.50948
5.500	0.95196	4.06763	10.48935	11.38716	-9.28805	1.20763	-2.31938	5.98135	-0.46830
6.000	0.95949	3.77577	10.42735	11.79728	-9.81705	1.20049	-2.18267	6.02863	-0.43470

TM(0) MODE T/LAMBDA_0 = 0.2000

ER1 = 1.000 -J* 0.0 MUR1 = 1.000 -J* 0.0

ER2 = 2.000 -J* 0.0 MUR2 = 1.000 -J* 0.0

ER2FP	L_RATIO	ATTEN.-Z	ATTEN.-X	REAL(U)	AIMAG(U)	REAL(V)	AIMAG(V)	REAL(KZ)	AIMAG(KZ)
0.0	1.17161	-0.0	33.31587	4.97657	0.0	3.83563	0.0	7.36142	0.0
0.200	1.17044	2.44799	33.43155	5.00939	-0.37434	3.84895	-0.53849	7.35407	-0.28184
0.300	1.16897	3.67763	33.56937	5.04966	-0.55685	3.86482	-0.80465	7.34487	-0.42340
0.400	1.16691	4.91375	33.75035	5.10475	-0.73419	3.88565	-1.06746	7.33194	-0.56572
0.500	1.16425	6.15816	33.96405	5.17365	-0.90521	3.91026	-1.32634	7.31520	-0.70898
0.600	1.16095	7.41261	34.19879	5.25536	-1.06907	3.93728	-1.58108	7.29446	-0.85341
0.700	1.15697	8.67910	34.44217	5.34896	-1.22522	3.96530	-1.83183	7.26946	-0.99922
0.800	1.15225	9.96012	34.68230	5.45374	-1.37327	3.99295	-2.07912	7.23977	-1.14670
0.900	1.14669	11.25911	34.90758	5.56921	-1.51295	4.01888	-2.32385	7.20485	-1.29625
1.000	1.14018	12.58093	35.10736	5.69516	-1.64397	4.04189	-2.56724	7.16398	-1.44843
1.200	1.12370	15.32458	35.39313	5.97894	-1.87830	4.07479	-3.05702	7.06044	-1.76431
1.400	1.10119	18.29770	35.48160	6.30926	-2.06987	4.08497	-3.56807	6.91897	-2.10660
1.600	1.07049	21.75122	35.37938	6.69572	-2.20128	4.07320	-4.13519	6.72612	-2.50420
1.800	1.03213	26.33374	35.42155	7.14334	-2.22153	4.07806	-4.82125	6.48509	-3.03178
2.000	1.01005	32.85294	37.03668	7.56143	-2.04650	4.26401	-5.62942	6.34632	-3.78234
2.500	1.09779	47.46875	46.24916	7.96167	-1.46353	5.32463	-7.07951	6.89762	-5.46504
3.000	1.21685	57.13080	54.65329	8.06162	-1.10756	6.29219	-7.99227	7.64567	-6.57743
3.500	1.32734	64.58676	61.83167	8.09062	-0.87421	7.11864	-8.71152	8.33993	-7.43583
4.000	1.42814	70.86336	68.14508	8.09330	-0.71030	7.84549	-9.33121	8.97329	-8.15845
4.500	1.52084	76.40424	73.82982	8.08510	-0.59005	8.49997	-9.88896	9.55573	-8.79636
5.000	1.60697	81.43816	79.03629	8.07255	-0.49901	9.09939	-10.40374	10.09690	-9.37592
5.500	1.68774	86.09720	83.86713	8.05862	-0.42834	9.65556	-10.88628	10.60437	-9.91231
6.000	1.76405	90.46446	88.39615	8.04472	-0.37234	10.17698	-11.34327	11.08388	-10.41511

TM(0) MODE T/LAMBDA_0 = 0.3000

ER1 = 1.000 -J* 0.0 MUR1 = 1.000 -J* 0.0

ER2 = 2.000 -J* 0.0 MUR2 = 1.000 -J* 0.0

ER2FP	L_RATIO	ATTEN.-Z	ATTEN.-X	REAL(U)	AIMAG(U)	REAL(V)	AIMAG(V)	REAL(KZ)	AIMAG(KZ)
0.0	1.26650	-0.0	42.41528	3.95377	0.0	4.88324	0.0	7.95767	0.0
0.200	1.26644	3.42143	42.63385	3.97938	-0.20441	4.90840	-0.63858	7.95728	-0.39391
0.300	1.26640	5.14465	42.90091	4.01053	-0.30141	4.93915	-0.95419	7.95701	-0.59230
0.400	1.26640	6.88235	43.26453	4.05265	-0.39254	4.98101	-1.26576	7.95705	-0.79236
0.500	1.26652	8.63859	43.71628	4.10445	-0.47635	5.03302	-1.57249	7.95778	-0.99455
0.600	1.26682	10.41688	44.24783	4.16449	-0.55170	5.09422	-1.87387	7.95968	-1.19929
0.700	1.26740	12.22012	44.85149	4.23124	-0.61776	5.16372	-2.16966	7.96332	-1.40689
0.800	1.26836	14.05039	45.52107	4.30313	-0.67393	5.24081	-2.45978	7.96936	-1.61761
0.900	1.26983	15.90871	46.25247	4.37856	-0.71988	5.32501	-2.74426	7.97858	-1.83156
1.000	1.27194	17.79465	47.04240	4.45593	-0.75550	5.41596	-3.02305	7.99183	-2.04869
1.200	1.27864	21.63828	48.79114	4.61016	-0.79670	5.61729	-3.56294	8.03393	-2.49120
1.400	1.28947	25.53789	50.75108	4.75426	-0.80219	5.84293	-4.07689	8.10196	-2.94016
1.600	1.30494	29.42334	52.89027	4.87995	-0.78034	6.08922	-4.56128	8.19920	-3.38749
1.800	1.32488	33.22032	55.15834	4.98364	-0.74092	6.35034	-5.01359	8.32447	-3.82463
2.000	1.34855	36.87318	57.49821	5.06588	-0.69251	6.61973	-5.43378	8.47318	-4.24518
2.500	1.41806	45.23682	63.37344	5.19761	-0.56649	7.29614	-6.36000	8.90991	-5.20808
3.000	1.49380	52.56558	69.00388	5.26289	-0.45905	7.94437	-7.14993	9.38585	-6.05164
3.500	1.57016	59.07697	74.28688	5.29412	-0.37522	8.55259	-7.84567	9.86560	-6.80149
4.000	1.64495	64.96754	79.23506	5.30806	-0.31093	9.12227	-8.47446	10.33554	-7.47967
4.500	1.71747	70.37907	83.88927	5.31311	-0.26138	9.65811	-9.05326	10.79118	-8.10269
5.000	1.78757	75.41061	88.28944	5.31355	-0.22272	10.16470	-9.59319	11.23161	-8.68197
5.500	1.85531	80.13242	92.47197	5.31163	-0.19211	10.64623	-10.10166	11.65726	-9.22559
6.000	1.92084	84.59590	96.46539	5.30856	-0.16754	11.10599	-10.58397	12.06902	-9.73946

TM(0) MODE T/LAMBDA_0 = 0.0200

ER1 = 1.000 -J* 0.0 MUR1 = 1.000 -J* 0.0

ER2 = 165.000 -J* 0.0 MUR2 = 1.000 -J* 0.0

ER2PP	L RATIO	ATTEN.-Z	ATTEN.-X	REAL(U)	AIMAG(U)	REAL(V)	AIMAG(V)	REAL(KZ)	AIMAG(KZ)
0.0	1.01158	-0.0	-110.33115	80.45830	0.0	-12.70234	0.0	6.35576	0.0
10.000	0.98068	-33.55554	-35.76834	80.61279	-2.74394	-4.11798	-5.78073	6.16177	3.66323
20.000	0.80706	-11.14886	-13.39255	80.71303	-4.97185	-1.54187	-4.22260	5.07059	1.28556
30.000	0.87931	-3.22277	-5.76521	80.85518	-7.34926	-0.66374	-3.09136	5.52439	0.37104
40.000	0.92644	-1.12277	-2.73839	81.08678	-9.74660	-0.31527	-2.39507	5.62099	0.12426
50.000	0.95153	-0.41481	-1.28580	81.39600	-12.12892	-0.14803	-1.94515	5.97867	0.04776
60.000	0.96585	-0.12929	-0.48517	81.77351	-14.48442	-0.05566	-1.63493	6.06853	0.01489
70.000	0.97493	0.01056	0.00128	82.21245	-16.80690	0.00015	-1.40939	6.12554	-0.00122
80.000	0.98080	0.07536	0.31844	82.70721	-19.09244	0.03666	-1.23850	6.16252	-0.00865
90.000	0.98477	0.10539	0.53661	83.25243	-21.33815	0.06178	-1.10476	6.18751	-0.01213
100.000	0.98763	0.12302	0.69306	83.84303	-23.54199	0.07979	-0.99737	6.20548	-0.01415
125.000	0.99213	0.13335	0.93378	85.48726	-28.86165	0.10751	-0.80350	6.23375	-0.01535
150.000	0.99452	0.12760	1.06446	87.31908	-33.90770	0.12255	-0.67416	6.24676	-0.01459
175.000	0.99601	0.12199	1.14252	89.28375	-38.68871	0.13154	-0.58197	6.25813	-0.01404
200.000	0.99705	0.10832	1.19204	91.33868	-43.22112	0.13724	-0.51308	6.26468	-0.01247
225.000	0.99775	0.10013	1.22459	93.45169	-47.52454	0.14099	-0.45977	6.26904	-0.01153
250.000	0.99815	0.10550	1.24633	95.59883	-51.61909	0.14349	-0.41737	6.27153	-0.01215
300.000	0.99859	0.08652	1.27008	99.93047	-59.25816	0.14622	-0.35442	6.27433	-0.00996
350.000	0.99923	0.07566	1.27836	104.24380	-66.27411	0.14718	-0.31015	6.27838	-0.00871
400.000	0.99943	0.07834	1.27768	108.49309	-72.77536	0.14710	-0.27752	6.27952	-0.00902
450.000	0.99948	0.07024	1.27135	112.65591	-78.84706	0.14637	-0.25260	6.27993	-0.00809
500.000	0.99948	0.07564	1.26121	116.72253	-84.55562	0.14520	-0.23301	6.27993	-0.00371

Mode Number is Incorrect (See Section 4.2)

TM(2) MODE   T/LAMBDA_0 =   0.0100

ER1 =   1.000 -J*   0.0   MUR1 =   1.000 -J*   0.0

ER2 =   2.000 -J*   0.0   MUR2 =   1.000 -J*   0.0

ER2PP	L_RATIC	ATTEN.-Z	ATTEN.-X	REAL(U)	AIMAG(U)	REAL(V)	AIMAG(V)	REAL(KZ)	AIMAG(KZ)
0.C	8.76089	1362.68799	-477.78320	157.10928	54.96779	-55.00684	156.99728	55.04626	-156.88527
0.2C0	1.0005C	0.00541	1.73200	6.31105	-0.62492	0.19940	-0.01960	6.28633	-0.00062
0.3C0	1.00051	0.00811	1.75268	6.34875	-0.93182	0.20178	-0.02905	6.28637	-0.00093
0.4C0	1.00051	0.01079	1.78081	6.39976	-1.23253	0.20502	-0.03808	6.28642	-0.00124
0.5C0	1.00053	0.01348	1.81559	6.46255	-1.52569	0.20903	-0.04660	6.28650	-0.00155
0.6C0	1.00054	0.01612	1.85617	6.53553	-1.81039	0.21370	-0.05452	6.28659	-0.00186
0.7C0	1.00056	0.01872	1.90156	6.61710	-2.08609	0.21893	-0.06178	6.28670	-0.00216
0.8C0	1.00058	0.02124	1.95077	6.70576	-2.35260	0.22459	-0.06834	6.28683	-0.00245
0.9C0	1.0006C	0.02365	2.00284	6.80019	-2.60995	0.23059	-0.07419	6.28698	-0.00272
1.CC0	1.00063	0.02599	2.05684	6.89919	-2.85837	0.23680	-0.07932	6.28715	-0.00299
1.2C0	1.00069	0.03023	2.16743	7.10712	-3.32978	0.24953	-0.08755	6.28753	-0.00348
1.4C0	1.00076	0.03388	2.27710	7.32341	-3.77015	0.26216	-0.09332	6.28796	-0.00390
1.6C0	1.00083	0.03680	2.38209	7.54387	-4.18301	0.27425	-0.09699	6.28842	-0.00424
1.8C0	1.00091	0.03909	2.48007	7.76573	-4.57166	0.28553	-0.09898	6.28890	-0.00450
2.CC0	1.00098	0.04080	2.56991	7.98716	-4.93903	0.29587	-0.09965	6.28937	-0.00470
2.5C0	1.00115	0.04288	2.75793	8.53213	-5.78015	0.31752	-0.09756	6.29045	-0.00494
3.CC0	1.00130	0.04283	2.89950	9.05886	-6.53356	0.33382	-0.09268	6.29137	-0.00493
3.5C0	1.00142	0.04173	3.00513	9.56506	-7.21971	0.34598	-0.08690	6.29210	-0.00480
4.CC0	1.00151	0.03989	3.08442	10.05106	-7.85269	0.35511	-0.08111	6.29267	-0.00459
4.5C0	1.00159	0.03793	3.14467	10.51805	-8.44253	0.36204	-0.07569	6.29315	-0.00437
5.CC0	1.00164	0.03614	3.19111	10.96752	-8.99655	0.36739	-0.07076	6.29350	-0.00416
5.5C0	1.00169	0.03426	3.22747	11.40095	-9.52033	0.37158	-0.06636	6.29380	-0.00394
6.CC0	1.00173	0.03253	3.25633	11.81970	-10.01815	0.37490	-0.06244	6.29403	-0.00375

Only the line of values for ER2PP=0 is valid (See Sections 3.4 and 4.3)

TM(2) MODE   T/LAMBDA_O =   0.0500

ER1 =   1.000 -J*   0.0   MUR1 =   1.000 -J*   0.0

ER2 =   2.000 -J*   0.0   MUR2 =   1.000 -J*   0.0

ER2PP	L_RATIO	ATTEN.-Z	ATTEN.-X	REAL(U)	AIMAG(U)	REAL(V)	AIMAG(V)	REAL(KZ)	AIMAG(KZ)
0.0	1.84328	264.47705	-98.76837	31.57115	11.17003	-11.37113	31.01277	11.58166	-30.44905
0.2C0	1.83948	253.36287	-98.42555	30.28633	11.00127	-11.33166	29.75166	11.55782	-29.16948
0.3C0	1.81868	248.18137	-97.23753	29.68831	10.79836	-11.19489	29.16574	11.42713	-28.57294
0.4C0	1.78756	243.40742	-95.49776	29.13789	10.53095	-10.99459	28.62724	11.23154	-28.02332
0.5C0	1.74826	239.11206	-93.32518	28.64314	10.21273	-10.74446	28.14418	10.98463	-27.52879
0.6C0	1.70299	235.32961	-90.83940	28.20786	9.85760	-10.45827	27.72018	10.70023	-27.09332
0.7C0	1.6538C	232.06299	-88.15105	27.83223	9.47839	-10.14877	27.35530	10.39112	-26.71724
0.8C0	1.60242	229.29271	-85.35440	27.51390	9.08613	-9.82679	27.04707	10.06830	-26.39830
0.9C0	1.55029	226.98419	-82.52675	27.24878	8.68979	-9.50124	26.79138	9.74078	-26.13252
1.CC0	1.49853	225.09529	-79.72658	27.03191	8.29631	-9.17886	26.58322	9.41553	-25.91505
1.2C0	1.39915	222.39594	-74.37144	26.72189	7.53704	-8.56233	26.28854	8.79115	-25.60428
1.4C0	1.30834	220.84764	-69.49791	26.54350	6.83335	-8.00124	26.12288	8.22054	-25.42603
1.6C0	1.22770	220.15448	-65.18567	26.46248	6.19502	-7.50478	26.05243	7.71389	-25.34622
1.8C0	1.15748	220.08264	-61.44124	26.45181	5.62319	-7.07368	26.05063	7.27265	-25.33795
2.CC0	1.09718	220.45427	-58.23360	26.49103	5.11459	-6.70439	26.09761	6.89377	-25.38074
2.5C0	0.98425	222.53708	-52.24713	26.71701	4.08339	-6.01517	26.34061	6.18425	-25.62053
3.CC0	0.91406	225.37468	-48.54320	27.02359	3.32313	-5.58874	26.66434	5.74321	-25.94722
3.5C0	0.87458	228.38603	-46.47311	27.34474	2.75745	-5.35042	27.00516	5.49514	-26.29391
4.CC0	0.85696	231.32039	-45.56387	27.65224	2.33038	-5.24574	27.33597	5.38443	-26.63174
4.5C0	0.85497	234.08058	-45.48444	27.93541	2.00265	-5.23659	27.64639	5.37194	-26.94952
5.CC0	0.86428	236.63907	-46.00385	28.19150	1.74701	-5.29639	27.93352	5.43041	-27.24408
5.5C0	0.88184	239.00085	-46.96167	28.42134	1.54441	-5.40666	28.19820	5.54077	-27.51599
6.CC0	0.90552	241.18266	-48.24544	28.62712	1.38145	-5.55446	28.44257	5.68952	-27.76718

TM(2) MODE T/LAMBDA_O = 0.1000

ER1 = 1.000 -J* 0.0 MUR1 = 1.000 -J* 0.0

ER2 = 2.000 -J* 0.0 MUR2 = 1.000 -J* 0.0

ER2PP	L_RATIO	ATTEN.-Z	ATTEN.-X	REAL(U)	AIMAG(U)	REAL(V)	AIMAG(V)	REAL(KZ)	AIMAG(KZ)
0.C	1.08081	120.01863	-54.49863	16.05951	5.84293	-6.27439	14.95518	6.79092	-13.81766
0.2C0	1.11418	115.16638	-55.93671	15.45389	5.75087	-6.43995	14.41336	7.00060	-13.25902
0.3C0	1.12147	112.92308	-56.17070	15.17292	5.64734	-6.46689	14.16573	7.04638	-13.00075
0.4C0	1.12358	110.87865	-56.14470	14.91520	5.51272	-6.46390	13.94191	7.05965	-12.76538
0.5C0	1.12156	109.06781	-55.91624	14.68456	5.35380	-6.43760	13.74545	7.04695	-12.55690
0.6C0	1.11647	107.50742	-55.54372	14.48270	5.17740	-6.39471	13.57783	7.01499	-12.37725
0.7C0	1.10930	106.19916	-55.07961	14.30961	4.98977	-6.34127	13.43878	6.96995	-12.22663
0.8C0	1.10091	105.13353	-54.56859	14.16399	4.79625	-6.28244	13.32687	6.91720	-12.10395
0.900	1.09198	104.29396	-54.04622	14.04379	4.60116	-6.22230	13.23995	6.86108	-12.00729
1.CC0	1.08305	103.65987	-53.53932	13.94650	4.40781	-6.16394	13.17543	6.80499	-11.93428
1.2C0	1.06669	102.92053	-52.64326	13.81027	4.03532	-6.06078	13.10323	6.70223	-11.84916
1.4C0	1.0538C	102.74747	-51.96902	13.73558	3.69035	-5.98316	13.09073	6.62122	-11.82924
1.6C0	1.04515	102.99738	-51.54526	13.70587	3.37721	-5.93437	13.12188	6.56689	-11.85801
1.8C0	1.04087	103.55721	-51.36864	13.70826	3.09611	-5.91403	13.18437	6.53999	-11.92246
2.CC0	1.04074	104.34088	-51.42015	13.73306	2.84527	-5.91996	13.26909	6.53914	-12.01269
2.5C0	1.05593	106.89984	-52.38458	13.85095	2.33240	-6.03100	13.53896	6.63459	-12.30730
3.CC0	1.0881C	109.88226	-54.24655	14.00176	1.94771	-6.24537	13.84853	6.83671	-12.65066
3.500	1.13177	113.00217	-56.70891	14.15571	1.65500	-6.52886	14.17014	7.11113	-13.00986
4.CC0	1.18300	116.13092	-59.56403	14.30055	1.42812	-6.85756	14.49187	7.43299	-13.37007
4.5C0	1.23904	119.21306	-62.67085	14.43197	1.24887	-7.21525	14.80890	7.78512	-13.72491
5.CC0	1.29804	122.22684	-65.93230	14.54916	1.10465	-7.59074	15.11948	8.15582	-14.07189
5.5C0	1.35873	125.16656	-69.28258	14.65284	0.98667	-7.97645	15.42328	8.53714	-14.41033
6.CC0	1.42024	128.03352	-72.67664	14.74432	0.88868	-8.36721	15.72059	8.92365	-14.74041

TM(2) MODE T/LAMBDA_O = 0.2000

ER1 = 1.000 -J* 0.0 MUR1 = 1.000 -J* 0.0

ER2 = 2.000 -J* 0.0 MUR2 = 1.000 -J* 0.0

ER2PP	L_RATIC	ATTEN.-Z	ATTEN.-X	REAL(U)	AIMAG(U)	REAL(V)	AIMAG(V)	REAL(KZ)	AIMAG(KZ)
0.0	0.94104	41.20868	-36.46402	8.76110	3.20188	-4.19808	6.68209	5.91274	-4.74432
0.2C0	0.99897	41.47372	-39.46040	8.47297	3.07123	-4.54305	6.59695	6.27671	-4.77484
0.3C0	1.02283	41.61693	-40.72931	8.33728	2.98303	-4.68914	6.56670	6.42664	-4.79133
0.4C0	1.04379	41.81087	-41.87485	8.21146	2.88303	-4.82102	6.54830	6.55833	-4.81365
0.5C0	1.06233	42.07706	-42.92339	8.09741	2.77437	-4.94174	6.54320	6.67481	-4.84430
0.6C0	1.07894	42.42790	-43.90051	7.99599	2.66019	-5.05423	6.55181	6.77921	-4.88469
0.7C0	1.09411	42.86809	-44.82880	7.90725	2.54332	-5.16111	6.57380	6.87448	-4.93537
0.8C0	1.10822	43.39656	-45.72696	7.83065	2.42613	-5.26451	6.60831	6.96318	-4.99621
0.9C0	1.12163	44.00829	-46.60927	7.76528	2.31048	-5.36609	6.65416	7.04743	-5.06664
1.CC0	1.13460	44.69591	-47.48596	7.71005	2.19776	-5.46702	6.71004	7.12891	-5.14581
1.2C0	1.15997	46.26492	-49.24837	7.62543	1.98464	-5.66993	6.84677	7.28831	-5.32645
1.4C0	1.18537	48.03571	-51.04372	7.56818	1.79098	-5.87663	7.00901	7.44791	-5.53032
1.6C0	1.21129	49.94810	-52.87766	7.53113	1.61768	-6.08777	7.18913	7.61077	-5.75049
1.8C0	1.23789	51.95375	-54.74509	7.50873	1.46394	-6.30276	7.38134	7.77792	-5.98140
2.CC0	1.26517	54.01576	-56.63683	7.49683	1.32813	-6.52056	7.58142	7.94932	-6.21879
2.5C0	1.33569	59.25500	-61.41096	7.49508	1.05467	-7.07020	8.09775	8.39240	-6.82199
3.CC0	1.40806	64.43611	-66.15659	7.51321	0.85376	-7.61656	8.61701	8.84710	-7.41848
3.5C0	1.48076	69.45203	-70.80132	7.53825	0.70392	-8.15130	9.12658	9.30389	-7.99596
4.CC0	1.5528C	74.26636	-75.30968	7.56449	0.59011	-8.67035	9.62134	9.75654	-8.55023
4.5C0	1.6236C	78.87465	-79.66922	7.58952	0.50205	-9.17226	10.09959	10.20140	-9.08078
5.CC0	1.69286	83.28558	-83.87939	7.61244	0.43269	-9.65697	10.56127	10.63655	-9.58861
5.5C0	1.76043	87.51321	-87.94362	7.63302	0.37717	-10.12488	11.00703	11.06112	-10.07533
6.CC0	1.82628	91.57266	-91.86906	7.65135	0.33207	-10.57682	11.43782	11.47485	-10.54269

TM(2) MODE T/LAMBDA_O = 0.3000

ER1 = 1.000 -J* 0.0 MUR1 = 1.000 -J* 0.0

ER2 = 2.000 -J* 0.0 MUR2 = 1.000 -J* 0.0

ER2PP	L_RATIC	ATTEN.-Z	ATTEN.-X	REAL(U)	AIMAG(U)	REAL(V)	AIMAG(V)	REAL(KZ)	AIMAG(KZ)
0.C	1.03562	17.43095	-30.69537	6.66913	1.95802	-3.53394	3.69511	6.50697	-2.00681
0.2C0	1.0886C	19.43225	-35.27737	6.35387	1.78701	-4.06146	3.76768	6.83986	-2.23722
0.3C0	1.11288	20.47858	-37.38666	6.20633	1.70217	-4.30430	3.83012	6.99244	-2.35768
0.4C0	1.1355C	21.56987	-39.36528	6.06959	1.61820	-4.53210	3.90933	7.13459	-2.48332
0.5C0	1.15653	22.70987	-41.21860	5.94527	1.53561	-4.74547	4.00365	7.26668	-2.61457
0.6C0	1.17611	23.89799	-42.95796	5.83399	1.45498	-4.94572	4.11099	7.38974	-2.75136
0.7C0	1.19448	25.13069	-44.59749	5.73556	1.37685	-5.13448	4.22913	7.50513	-2.89328
0.8C0	1.21184	26.40251	-46.15189	5.64928	1.30170	-5.31343	4.35594	7.61423	-3.03970
0.9C0	1.22842	27.70709	-47.63428	5.57416	1.22989	-5.48410	4.48951	7.71839	-3.18990
1.CC0	1.24439	29.03790	-49.05614	5.50908	1.16167	-5.64780	4.62816	7.81874	-3.34311
1.2C0	1.27509	31.75299	-51.75514	5.40451	1.03637	-5.95853	4.91531	8.01163	-3.65570
1.4C0	1.30481	34.50311	-54.30484	5.32726	0.92575	-6.25208	5.20891	8.19838	-3.97232
1.6C0	1.33406	37.25375	-56.74086	5.27052	0.82884	-6.53253	5.50340	8.38217	-4.28900
1.8C0	1.36312	39.98019	-59.08598	5.22905	0.74429	-6.80253	5.79527	8.56471	-4.60289
2.CC0	1.39209	42.66565	-61.35452	5.19890	0.67060	-7.06370	6.08247	8.74678	-4.91206
2.5C0	1.46438	49.14018	-66.74867	5.15576	0.52487	-7.68473	6.77371	9.20094	-5.65747
3.CC0	1.53617	55.23225	-71.81290	5.13870	0.42001	-8.26777	7.42349	9.65204	-6.35885
3.5C0	1.60699	60.94688	-76.60074	5.13419	0.34303	-8.81899	8.03362	10.09701	-7.01677
4.CC0	1.67646	66.31583	-81.14899	5.13568	0.28532	-9.34262	8.60808	10.53349	-7.63489
4.5C0	1.74436	71.37694	-85.48524	5.13993	0.24113	-9.84185	9.15126	10.96013	-8.21758
5.CC0	1.81060	76.16667	-89.63570	5.14532	0.20663	-10.31969	9.66687	11.37632	-8.76901
5.5C0	1.87516	80.71730	-93.61821	5.15101	0.17923	-10.77820	10.15835	11.78195	-9.29292
6.CC0	1.93806	85.05666	-97.44986	5.15661	0.15712	-11.21933	10.62847	12.17719	-9.79251

TM(2) MODE   T/LAMBDA_0 =   0.4000

ER1 =   1.000 -J*   0.0   MUR1 =   1.000 -J*   0.0

ER2 =   2.000 -J*   0.0   MUR2 =   1.000 -J*   0.0

ER2PP	L_RATIC	ATTEN.-Z	ATTEN.-X	REAL(U)	AIMAG(U)	REAL(V)	AIMAG(V)	REAL(KZ)	AIMAG(KZ)
0.0	1.09332	4.88136	-26.12112	5.70442	0.67677	-3.00731	1.28373	6.86951	-0.56199
0.2C0	1.17787	8.84068	-36.33553	5.07154	0.70686	-4.18328	1.80066	7.40080	-1.01782
0.3C0	1.20409	10.89383	-39.38864	4.88122	0.73075	-4.53479	2.09242	7.56555	-1.25420
0.4C0	1.22588	12.84245	-41.87564	4.72871	0.73862	-4.82111	2.36218	7.70245	-1.47854
0.5C0	1.2449C	14.71170	-44.00983	4.60234	0.73415	-5.06682	2.61473	7.82196	-1.69375
0.6C0	1.26206	16.52248	-45.90411	4.49599	0.72078	-5.28491	2.85418	7.92974	-1.90222
0.7C0	1.27791	18.28932	-47.62680	4.40583	0.70123	-5.48324	3.08338	8.02937	-2.10564
0.8C0	1.29286	20.02162	-49.22241	4.32910	0.67762	-5.66694	3.30421	8.12331	-2.30508
0.9C0	1.30719	21.72523	-50.72141	4.26367	0.65154	-5.83952	3.51796	8.21331	-2.50121
1.CC0	1.321C9	23.40347	-52.14520	4.20779	0.62415	-6.00344	3.72544	8.30065	-2.69443
1.2C0	1.34817	26.69008	-54.82462	4.11915	0.56861	-6.31192	4.12381	8.47082	-3.07281
1.4C0	1.37487	29.88641	-57.34030	4.05414	0.51523	-6.60155	4.50253	8.63859	-3.44080
1.6C0	1.40156	32.99197	-59.73682	4.00631	0.46591	-6.87746	4.86361	8.80629	-3.79834
1.8C0	1.4284C	36.00565	-62.04004	3.97103	0.42134	-7.14262	5.20869	8.97490	-4.14530
2.CC0	1.45542	38.92740	-64.26588	3.94496	0.38153	-7.39888	5.53914	9.14467	-4.48168
2.5C0	1.52361	45.84041	-69.55309	3.90587	0.30076	-8.00760	6.30935	9.57310	-5.27757
3.CC0	1.59205	52.23436	-74.51321	3.88797	0.24138	-8.57865	7.01230	10.00316	-6.01370
3.5C0	1.66002	58.17087	-79.20137	3.88050	0.19733	-9.11840	7.66064	10.43022	-6.69717
4.CC0	1.7270C	63.71150	-83.65579	3.87825	0.16413	-9.63123	8.26406	10.85108	-7.33506
4.5C0	1.7927C	68.91103	-87.90453	3.87863	0.13864	-10.12038	8.83007	11.26390	-7.93368
5.CC0	1.85698	73.81581	-91.97433	3.88029	0.11872	-10.58894	9.36418	11.66774	-8.49836
5.5C0	1.91977	78.46439	-95.88148	3.88253	0.10290	-11.03876	9.87114	12.06226	-9.03355
6.CC0	1.98107	82.88884	-99.64337	3.88499	0.09013	-11.47187	10.35439	12.44746	-9.54293

TM(2) MODE T/LAMBDA_0 = 0.4900

ER1 = 1.000 -J* 0.0 MUR1 = 1.000 -J* 0.0

ER2 = 2.000 -J* 0.0 MUR2 = 1.000 -J* 0.0

ER2PP	L_RATIO	ATTEN.-Z	ATTEN.-X	REAL(U)	AIMAG(U)	REAL(V)	AIMAG(V)	REAL(KZ)	AIMAG(KZ)
0.0	1.26229	-0.00000	-42.03964	4.00660	-0.00000	-4.83999	-0.00000	7.93120	0.00000
0.200	1.27350	5.30509	-43.53851	3.91927	0.23967	-5.01256	0.97499	8.00166	-0.61077
0.300	1.28386	7.67488	-44.89418	3.84237	0.31388	-5.16863	1.37905	8.06673	-0.88360
0.400	1.29507	9.88113	-46.33141	3.76405	0.36164	-5.33410	1.73542	8.13717	-1.13761
0.500	1.30651	11.96531	-47.76534	3.69026	0.38990	-5.49919	2.05638	8.20905	-1.37756
0.600	1.31796	13.95871	-49.16646	3.62324	0.40420	-5.66050	2.35103	8.28100	-1.60706
0.700	1.32938	15.88277	-50.52765	3.56357	0.40862	-5.81721	2.62559	8.35274	-1.82857
0.800	1.34079	17.75168	-51.84999	3.51109	0.40613	-5.96945	2.88423	8.42442	-2.04374
0.900	1.35222	19.57481	-53.13730	3.46525	0.39889	-6.11766	3.12988	8.49628	-2.25363
1.000	1.36373	21.35825	-54.39346	3.42540	0.38846	-6.26228	3.36456	8.56859	-2.45896
1.200	1.38709	24.82039	-56.82704	3.36099	0.36226	-6.54246	3.80661	8.71535	-2.85755
1.400	1.41102	28.15622	-59.17294	3.31285	0.33334	-6.81254	4.21858	8.86572	-3.24160
1.600	1.43556	31.37442	-61.44582	3.27693	0.30462	-7.07421	4.60559	9.01990	-3.61211
1.800	1.46067	34.48042	-63.65443	3.25012	0.27753	-7.32849	4.97135	9.17764	-3.96971
2.000	1.48625	37.47894	-65.80492	3.23009	0.25265	-7.57607	5.31864	9.33840	-4.31492
2.500	1.55167	44.53690	-70.95432	3.19947	0.20076	-8.16892	6.11956	9.74945	-5.12750
3.000	1.61806	51.03294	-75.81653	3.18486	0.16174	-8.72870	6.84321	10.16660	-5.87539
3.500	1.68439	57.04622	-80.42854	3.17826	0.13247	-9.25968	7.50654	10.58336	-6.56769
4.000	1.75001	62.64757	-84.82079	3.17574	0.11027	-9.76536	8.12125	10.99567	-7.21257
4.500	1.81455	67.89699	-89.01541	3.17532	0.09318	-10.24828	8.69629	11.40118	-7.81693
5.000	1.87782	72.84392	-93.03772	3.17597	0.07980	-10.71136	9.23777	11.79869	-8.38647
5.500	1.93972	77.52914	-96.90421	3.17715	0.06915	-11.15651	9.75081	12.18763	-8.92587
6.000	2.00024	81.98579	-100.62846	3.17856	0.06056	-11.58528	10.23945	12.56786	-9.43896

(See Section 4.3 for an Explanation of the Roots for ER2PP=0)

VITA

Jerry Kent Sutton

Candidate for the Degree of

Master of Science

Thesis: THE EFFECT OF LOSSES UPON THE PROPAGATION OF SURFACE AND LEAKY WAVES OVER A GROUNDED DIELECTRIC SLAB

Major Field: Engineering

Biographical:

Personal Data: Born at Jefferson Barracks Army Post, Missouri, October 27, 1944, the son of Vivian E. and Ruth H. Sutton.

Education: Graduated from Bolton High School, Alexandria, Louisiana, in 1962; received the Bachelor of Science degree in Electrical Engineering from the Louisiana Polytechnic Institute in January, 1967; completed requirements for the Master of Science degree in June, 1969.

Professional Experience: Employed by the Department of Electrical Engineering of Kansas State University as a graduate assistant during the spring of 1967 and as an instructor from September, 1967 to June, 1968; employed by Collins Radio Company, Dallas, Texas, during the summer of 1967 and since August, 1968.

Honorary Organizations: Member of Phi Kappa Phi, Tau Beta Pi, and Eta Kappa Nu.

THE EFFECT OF LOSSES UPON THE PROPAGATION OF SURFACE AND LEAKY WAVES OVER A GROUNDED DIELECTRIC SLAB

by

JERRY KENT SUTTON

B. S., Louisiana Polytechnic Institute, 1967

AN ABSTRACT OF A MASTER'S THESIS

submitted in partial fulfillment of the

requirements for the degree

MASTER OF SCIENCE

Department of Electrical Engineering

KANSAS STATE UNIVERSITY
Manhattan, Kansas

1969

ABSTRACT

The purpose of this research is to examine the effect of losses upon the propagation of surface waves and leaky waves over an infinitely wide, planar, electrically thick dielectric slab coated onto the surface of a perfect conductor.

A transcendental equation having complex coefficients in the general case is solved in order to obtain the propagation constants. A computer program has been written to perform this task. This program relies upon the numerical techniques of linear iteration and steepest descent.

The quantities of interest are the attenuation in directions parallel and normal to the surface of the slab, the guide wavelength, and the angle at which the wave enters or leaves the slab. The results of the computer analysis indicate that for a surface wave mode there is an abrupt transition in the behavior of each of these quantities occurring at a particular slab thickness. In the attenuation parallel to the slab, this transition is from decreasing attenuation at high losses for a thin slab to increasing attenuation at high losses for a thick slab. Furthermore, it is found that, for sufficiently high losses, odd-numbered TM modes exhibit the behavior of a surface wave though such modes describe physically unreal waves in the lossless case.